PICES Scientific Report No. 15
2000

PICES-GLOBEC INTERNATIONAL PROGRAM ON CLIMATE CHANGE AND CARRYING CAPACITY

REPORT OF THE 1999 MONITOR AND REX WORKSHOPS, AND THE 2000 MODEL WORKSHOP ON LOWER TROPHIC LEVEL MODELLING

Edited by

Bernard A. Megrey (MODEL), Bruce A. Taft (MONITOR) and
William T. Peterson (REX)

September 2000
Secretariat / Publisher
North Pacific Marine Science Organization (PICES)
c/o Institute of Ocean Sciences, P.O. Box 6000, Sidney, B.C., Canada. V8L 4B2
E-mail: pices@ios.bc.ca Home Page: http://pices.ios.bc.ca

TABLE OF CONTENTS

EXECUTIVE SUMMARY

This volume summarizes the results of workshops organized by the PICES-GLOBEC Climate Change and Carrying Capacity Program held just prior to the Eighth Annual Meeting in Vladivostok, Russia, in October 1999. In addition, a very successful modelling workshop was subsequently convened in Nemuro, Japan, the following January.

One of the most important goals is to integrate the results of national GLOBEC and related programs in order to review and promote a better understanding of how climate change affects the ecosystems of the North Pacific Ocean. PICES plays a key role in this regard, because it serves as the forum where diverse scientists can come together, presenting their own recent findings, and learning about progress in other regions around the Pacific Rim. With the rapid changes in climate occurring in the 1990s, PICES has played a crucial role in organizing meetings where scientists can meet to compare recent findings and exchange views on what seems to be happening in the North Pacific.

The MONITOR Task Team first met in 1998 in Fairbanks. Since that initial meeting a number of initiatives to improve monitoring of the North Pacific Ocean have been successfully implemented. As this report indicates, large-scale plankton monitoring has begun with the deployment of a Hardy Continuous Plankton Recorder in the year 2000. The Hardy recorder was developed in the 1920s and 1930s, so it is hardly a modern electronic instrument. However, it marks the first time that large scale plankton monitoring of the North Pacific has begun, and it is expected that the data so collected will provide badly needed information on the spatial scale of the plankton of the North Pacific–essential information if a more extensive monitoring program is to be put in place in future. Most of the remainder of the MONITOR Task Team meeting was devoted to an extensive review and discussion of international efforts in GOOS (Global Ocean Observing System), which will serve as a framework for questions about how to get oceanographic data into a useable form in a timely manner. The data from these new initiatives will form the basis for the monitoring systems of the future.

The REX Task Team held a workshop to review the population dynamics of herring and euphausiids around the Pacific Rim. Typical of small pelagic animals, large changes in the abundance of these key members of coastal ecosystems are observed over time, and interesting data on the changes in feeding success and overwinter energy depletion were reported. An interesting development within the North Pacific are the reports on longer-term fluctuations in herring abundance, which will no doubt serve to provide a better perspective on the short-term fluctuations evident when only data from modern fisheries is examined. A number of interesting relationships were also noted between the abundance of herring and euphausiids from around the Pacific Rim.

Finally, the MODEL Task Team met to discuss developments during the past year and to make the final plans for an intensive workshop scheduled for Nemuro, Japan, in January 2000. The extensive report from that meeting is included here, and describes the results of a substantial effort by many members of the PICES modelling community to develop a consensus on the essential elements of an ecosystem model for the North Pacific Ocean; their progress in doing so will provide an essential stepping stone towards a better understanding of what aspects of the ecosystem are most important to measure and monitor in the future.

In conclusion, the many scientific threads within PICES are progressing well, and there is excellent reason to believe that in the near future, we will be able to weave these threads together and to produce

new understanding that will be beyond what would be possible from the efforts of either individual scientists or individual specialities. As its name suggests, PICES' "Four Seas" Program (Climate Change and Carrying Capacity) has an ambitious goal. The hard work by the many individuals at the Task Team meetings (plus the dedication of the members of the PICES Secretariat to quietly ensure that that work is done as promised!) has led PICES very far in the first eight years of its existence. I am very proud to be a part of this group, and am privileged to have had the opportunity to work with such a diverse group of talented and interesting people. There are many challenges on the horizon for PICES. I feel confident that the networks of people and ideas being nurtured within PICES will provide the nucleus for addressing them in the North Pacific– both those that we can foresee, and those that we have yet to discover.

David W. Welch

Co-Chairman, CCCC Program

MODEL TASK TEAM WORKSHOP REPORT

Final Report of the International Workshop to Develop a Prototype Lower Trophic Level Ecosystem Model for Comparison of Different Marine Ecosystems in the North Pacific

David L. Eslinger, NOAA Coastal Services Centre. 2234 South Hobson Avenue, Charleston, SC 29407, U.S.A. E-mail: dave.eslinger@noaa.gov

Makoto B. Kashiwai, Fisheries Oceanography Division, Hokkaido National Fisheries Research Institute. Kushiro Hoddaido 085-0802, Japan. E-mail: kashiwai@hnf.affrc.go.jp

Michio J. Kishi, Faculty of Fisheries, Hokkaido University. Hokkaido, Hakodate 041, Japan. E-mail: kishi@salmon.fish.hokudai.ac.jp

Bernard A. Megrey, National Marine Fisheries Service, Alaska Fisheries Science Centre. 7600 Sand Point Way NE, Seattle, WA 98115-0070, U.S.A. E-mail: bern_megrey@noaa.gov

Daniel M. Ware, Pacific Biological Station. 3190 Hammond Bay Road, Nanaimo, B.C. V9R 5K6, Canada. E-mail: ware_mrc@island.net

Francisco E. Werner, Marine Sciences Department, University of North Carolina. Chapel Hill, NC 27599-3300, U.S.A. E-mail: cisco@marine.unc.edu

Summary

The NEMURO workshop made several significant achievements:

1. Assembled an international team of marine biologists and physical oceanographers who collectively achieved a consensus on the structure and function of a PICES CCCC prototype lower trophic level ecosystem model for the North Pacific Ocean, and named it "*NEMURO*";
2. Developed executable computer simulation models and preliminary outputs. Models developed included:
   a) *NEMURO*/FORTRAN Box Model
   b) *NEMURO*/1-D Yamanaka Model
   c) *NEMURO*/1-D Kishi Model
   d) *NEMURO*/MATLAB Box Model;
3. Constructed physical forcing data files and parameter sets for three locations in the North Pacific, station A7 on the A-line off southeast of Hokkaido (41.5ºN, 145.5°E), Ocean Station P (50°N, 145°W), and the Eastern Bering Sea (57.5°N, 175°W);
4. Through an extensive dialog between modelers and plankton biologists, conducted a comprehensive review of NEMURO process equations and their parameter values for the three distinct geographic regions;
5. Developed post-processing software to analyze model output in tabular and graphic formats;
6. Carefully considered the benefit including a microbial food web loop in NEMURO and designed a preliminary strategy for conducting comparative model experiments;
7. Identified leaders and members of model experiment teams, a subgroup of the Model Task Team members and meeting participants, who will be active in conducting future model experiments;
8. Initiated development of comparison protocols;
9. Made recommendations for future lower trophic level modeling activities.

The significance of these achievements will ultimately be evaluated by how well the CCCC Program effectively utilizes and embraces these models as a basis of future modeling activity.

1.0 Introduction

The North Pacific Marine Science Organization (PICES) organizes and promotes an international science program on Climate Change and Carrying Capacity (CCCC) in the temperate and subarctic regions of the North Pacific Ocean. Ecosystem modeling is one of five key research activities defined by the CCCC Implementation Panel. The PICES CCCC MODEL Task Team is given the role to encourage, facilitate and coordinate modeling activities within the member nations with respect to the goals and objectives of the PICES-CCCC Program. At the 1996 Nemuro Workshop on Modeling there was no support for efforts to standardize models or model approaches within the CCCC Program, believing that diversity in assumptions and techniques lead to faster advances in the North Pacific region. However, at the Lower Trophic Level Model Workshop, held in Fairbanks, October 1998, the participants agreed that: i) Models with different state variables and mathematical formulations would be impossible to compare, and ii) comparison protocols are necessary to tackle the problem. Thus, the MODEL Task Team recommended to the CCCC Implementation Panel to convene a workshop on the development of a prototype model and comparison protocols. The recommendation was approved by the CCCC-IP, Science Board, and finally by Governing Council.

2.0 Goals and Objectives of the Workshop

The goals of the workshop were to:

1. Select a lower trophic level model of the marine ecosystem as a PICES prototype;

2. Select a suite of model comparison protocols with which to examine differences and similarities in model dynamics;

3. Demonstrate the applicability of the prototype model by comparing lower trophic ecosystem dynamics among different regional study sites in the CCCC Program;

4. Compare the prototype model with other models;

5. Identify information gaps and the necessary process studies and monitoring activities to fill the gaps;

6. Discuss how to best link lower trophic level (LTL) marine ecosystem models to higher trophic level (HTL) marine ecosystem models, regional circulation models, and how to best incorporate these unified models into JGOFS models and the PICES CCCC Program.

3.0 Organizing Committee, Sponsors, Venue and Participants

Drs. Michio J. Kishi, Makoto B. Kashiwai, Bernard A. Megrey and Daniel M. Ware organized the meeting. Dr. Bernard Megrey served as workshop chairman. The Japan International Science and Technology Exchange Center (JISTEC), PICES, and the city of Nemuro provided financial support and access to excellent meeting rooms in the City Hall. The Nemuro Support Committee supplied local logistical support.

The venue was set at the Multi Purpose Hall, a large octagon shaped room, in the Nemuro City Cultural Center. The hall had four personal computers forming a local network which included a server workstation, laser and color printers, and another one personal computer connected to the Internet. These computers were allocated to four work areas for use by individual workgroups. A classroom style table was arranged in the center of the room for the plenary

session. A set of LCD projectors and screens and AC power outlets for participants' laptop computers were available. These were arranged in each work area to make group work more effective.

Twenty-nine scientists from China, Korea, Russia, Japan, Canada, and the United States (Fig. 1) met in Nemuro, Japan, between January 30-February 4, 2000, to participate in a modeling workshop focused on developing a lower trophic level model of the marine ecosystem. Out of the total, 15 scientists arrived with their own laptop computers, ready to get down to the business of building a numerical NPZ (nutrients, phytoplankton-zooplankton) model, estimate the models parameters, select a suite of model comparison protocols, compare the model to validation data sets, and to perform regional comparisons.

Participants (Appendix 1) consisted of plankton scientists, modelers, and individuals with knowledge about key data sets about each selected region and lower trophic level modeling activity in that region.

4.0 Workshop Schedule

January 30

1830-1930 **Opening Ceremony**

January 31

0930-1730 **1st Session**: Opening Plenary Session
- Opening of Workshop
- General introduction
- Model Comparison Protocols
- Linking LTL model to HTL model
- Introduction of Prototype Model
- Inventory of available data and selection of Study Sites
- Discussion on Prototype Model
- Discussion on Microbial Loop
- Model Comparison Protocols
- Workplan for development of Prototype Model

1900-2030 **Welcome Reception** (Hosted by Nemuro Supporting Committee)

February 1

0930-1230 **2nd Session**: Work Group Session

1330-1730 **3rd Session**: Plenary Session
- Introduction of 1-D Yamanaka Model
- Introduction of FORTRAN Box Model
- Review of Forcing File Preparation
- Alternative Formulations for Primary Production

February 2

0930-1730 **4th Session**: Work Group Session

February 3

0930-1200 **5th Session**: Summary Plenary Session
- Reports from Working Groups
- Workplan for remaining tasks
- Discussion of Workshop Report
- Discussion of Workshop Recommendations

1200-1230 **Closing Plenary Session**
- Closing remarks by conveners
- Speech by Vice-Chairman of Nemuro Supporting Committee

1330- **Workshop Excursion**
(Draft report writing by conveners)

1500-1700 **Nemuro Public Session** for citizens of Nemuro

1830-2000 **Farewell Party** (Co-sponsored by JISTEC and Nemuro)

5.0 Workshop Activity

After an opening ceremony and a welcome party held the day before, the participants convened at the venue to start the four day workshop.

1st Session

On the first day, the workshop officially opened with a welcome to all who had endured a long journey, cold weather, and a powerful snow storm to come to Nemuro.

In the morning session, Dr. Megrey began by providing a general introduction to the activities of the PICES CCCC MODEL Task Team and some background information on decisions made at past Task Team meetings. Since many in the audience had not been involved in the deliberations of the MODEL Task Team, the introduction was designed to give the participants a better sense of how we got to the Nemuro workshop.

This was followed by a presentation by Dr. Makoto Kashiwai on model comparison protocols. Starting from a brief review of reasons for comparison, Dr. Kashiwai discussed the requirements of the model. In order for model results to be comparable, the basic underlying model should have the following items in common:

- The currency of the model and its units of measurement
- The time step
- Spatial dimensions and size segmentation
- Time series of driving factors
- Functional ecological groups (i.e. state variables)
- Mathematical description of biological processes and a definition of parameters and starting values

A model imitating observed phenomena is nothing but a scientific toy. A model can be a scientific tool only when it can output necessary comparison factors and indexes of ecosystem structure and performance. After pointing out these views, Dr. Kashiwai reviewed basic analyses resulting in graphic, diagrammatic, and/or index representation of the structure and performance of an ecosystem:

- Methods to graphically or schematically represent the structure and function of an ecosystem model
- Seasonal patterns of biomass for ecosystem components
- Seasonal patterns of production for ecosystem components
- Annual biomass balance and its seasonal pattern
- Production and its allocation to primary production, or 'ecological efficiency'
- Representation of the dynamic performance of an ecosystem model through sensitivity analysis
- Methods of performing a sensitivity analysis
- Carrying capacity dynamics described by P/B to B relationships
- Dynamic response to ecosystem interactions by interaction coefficient matrices based on ecological niche theory.

Dr. Francisco Werner presented logistical, practical, and theoretical issues related to linking lower trophic marine ecosystem models to higher trophic level models. Based on the modeling and field activities presently underway in the Northwest Atlantic (Georges Bank) Program, Dr. Werner discussed various approaches to linking lower trophic models with higher trophic levels. It was pointed out that the approaches in the NW Atlantic program have not included a detailed description of the population dynamics of the nutrient-phytoplankton-zooplankton (NPZ) system. Rather, the approach has been one where climatological maps of existing decade-long observations of the lower trophic levels have been used as a baseline for setting quantitative levels of these components of the food web. Coupled with realistic 3-D circulation fields and individual-based models of zooplankton, successful studies establishing spatial and temporal links between the zooplanktonic populations in waters neighboring Georges Bank

and their (behaviorally modified) transport onto the Bank were described. Similarly, using adjoint methods (for mathematical inversion), studies were discussed that enabled the inference of the spatial dependence of certain vital rates (e.g., mortality) that would otherwise be difficult to determine in the field. In turn, these results have been coupled with individual-based models of larval fish to determine the (vertically integrated, seasonal and monthly) optimum growth zones of cod and haddock early life stages on Georges Bank. This has allowed the examination of fundamental ecological theories of match-mismatch versus member-vagrant in the regulation of marine populations. Finally, with the recent completion of the 5-year intensive field program, data of unprecedented detail in space, time and species will be coupled to circulation models to determine the links between the larval fish and the NPZ system on shorter time scales (weekly) and in full three-dimensional space.

Dr. Megrey then had a discussion on what models, data sets, parameters, and validation data were brought to the meeting by participants. The core parts of his presentation can be found in the Introduction, Goals, and Objectives sections of this report.

The afternoon session focused primarily on a presentation by Dr. Michio J. Kishi and the current status of the prototype model as originally developed by Dr. Kishi. The state variables, process equations representing system fluxes, parameter needs and outputs were discussed in detail. A long discussion developed regarding whether the model correctly represented the marine ecosystem and could reproduce the dynamic features of lower trophic level production in the selected study areas. Consequently, one more state variable representing predatory zooplankton and the connecting process equations were added to the proposed prototype. After considerable discussion, the group of 29 scientists collectively agreed to accept this model as the PICES prototype lower trophic level marine ecosystem model (Fig. 2).

This significant occasion was followed by a presentation by Dr. Dan Ware on the importance of including a microbial food web in the marine ecosystem lower trophic level model. Details of his presentation are partly reproduced in the Microbial Food Web Team Report (below).

The afternoon ended with a selection of model comparison locations. Regions selected for comparison included station A7 on the A-line off the east side of Hokkaido (41.30°N, 145.30°E), Ocean Station P (50°N, 145°W), and the Eastern Bering Sea (57.5°N, 175°W) (Fig. 3).

A summary of changes needed to complete the prototype model was discussed, the development of a flow diagram for data processing was presented (Fig. 4), and followed by a discussion of potential topics for breakout groups. This list included

- Biological review of the model parameters
- Microbial food web formulation
- Forcing file preparation and coding of new model segments
- Post-processing and plotting programming

2nd Session

The second day was taken up primarily with the teams beginning to deal with their specific tasks. The workshop split into four teams, each addressing a specific task (Appendix 2).

The first team concerned itself with the preparation of the forcing files for the three geographic locations as well as coding of the test models. The second team had the responsibility of reviewing the appropriateness of all biological process equations and reviewing the suitability of individual parameter values. This team also generated a list of parameter values for each geographic location and supplied, where possible, a reference and a plausible possible range of values (Table 4). The third team prepared the software for post-processing the model output (reformatting of output data files and defining standardized figures for

graphical presentation of model output). The fourth team concerned itself with the development of a microbial food web formulation and a strategy to incorporate the microbial food web submodel into the existing prototype model.

Fig. 1 Nemuro Workshop participants. Left to right, bottom row: *Tomonori Azumaya, Yukimasa Ishida, Kosei Komatsu, Makoto B. Kashiwai, Michio J. Kishi, Yuri I. Zuenko, Daji Huang, Hiroaki Saito, Katsumi Yokouchi*. Top row: *Hyun-chul Kim, Hitoshi Iizumi, Gennady A. Kantakov, Francisco E. Werner, Sukyung Kang, Vladim V. Navrotsky, Atsushi Tsuda, Daniel M. Ware, Bernard A. Megrey, David L. Eslinger, Vladimir I. Zvalinsky, Jing Zhang, Naoki Yoshie, Yasuhiro Yamanaka, Masahiko Fujii, Maki Noguchi, Lan S. Smith*.

3rd Session

On the afternoon of the second day, there was a presentation by Dr. Yasuhiro Yamanaka on the structure of the 1-D bio-physical coupled model and by Mr. Naoki Yoshie and Mr. Masahiko Fujii on the status of the Box Model. Also on the afternoon of the second day, we reviewed preparation of the forcing files for stations A7, Station P and Bering Sea and Dr. Vladimir Zvalinsky gave a presentation on alternative formulations for the primary production process.

4th Session

On the morning of the third day the teams continued their deliberations. In the afternoon of the third day, the output from model comparisons were generated for the three regional areas and some provisional analysis were begun.

5th Session

At the last session on the fourth day we had a summary plenary session where we heard reports from each team, discussed the work plan for

remaining tasks, then discussed the workshop report and workshop recommendations. The results of these discussions are in the Recommendations section.

Closing Plenary Session

The participants received closing remarks from the vice-chairman of the Nemuro Supporting Committee where appreciation was extended to have helped bring into being such a productive workshop. These feelings were amplified during the Sayonara Party, which was full of warm hospitality by the people of Nemuro city.

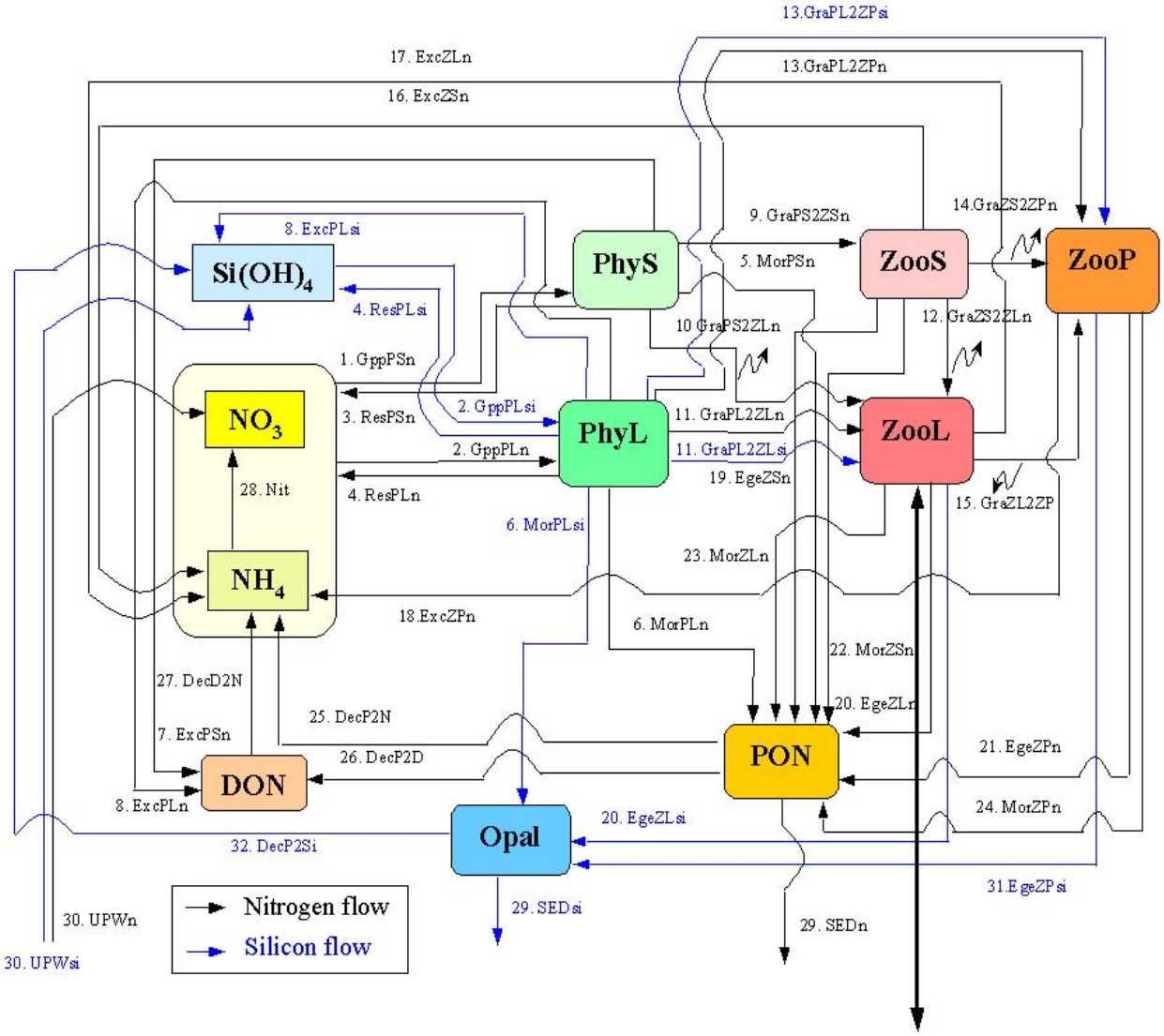

Fig. 2 *NEMURO*, a PICES CCCC prototype lower trophic level marine ecosystem model of the North Pacific Ocean. The dark arrow indicates diel vertical migration by large Zooplankton (ZooL).

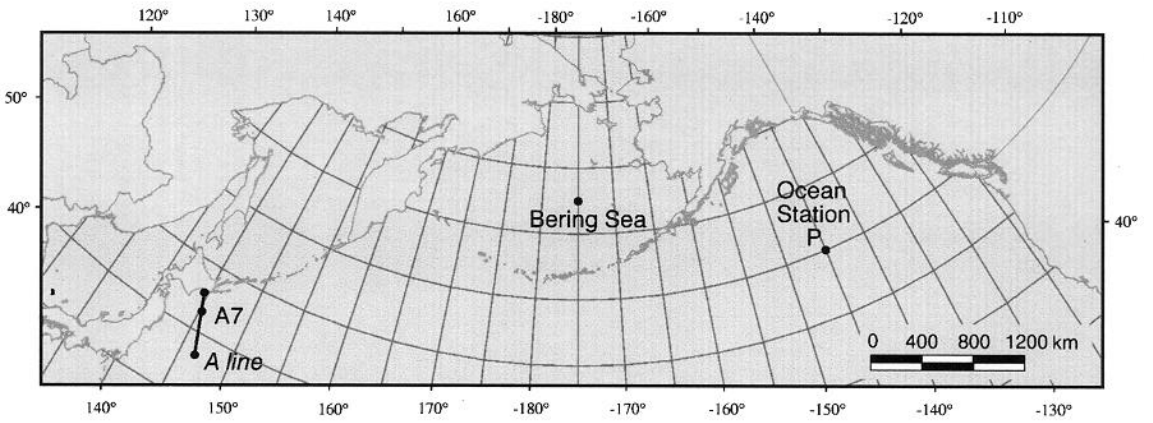

Fig. 3 Map of the North Pacific showing areas where model comparisons were performed.

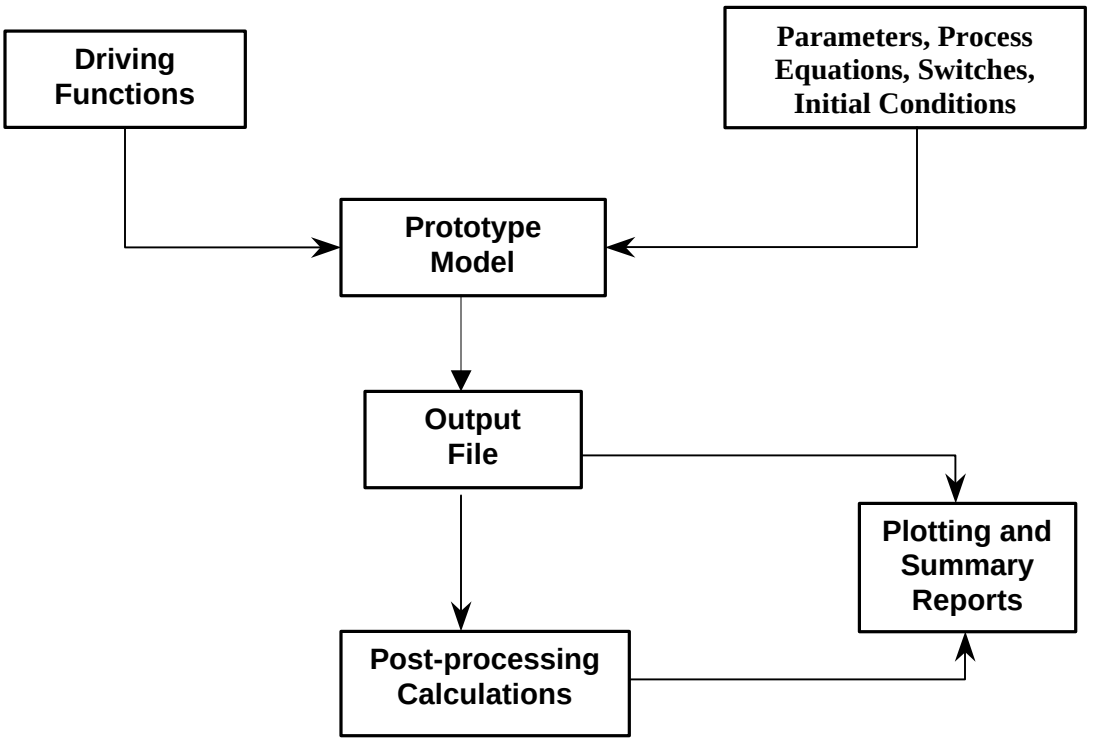

Fig. 4 Flow diagram of data processing steps used at the Modeling Workshop.

6.0 Model Description

Nota bene

We use several forms of nomenclature in this document to reference model parameters, state variables, biomass concentrations, and ecological functional groups. These are summarized below.

NOMENCLATURE

Description	Functional Groups	Biomass Concentration (Nitrogen Units)	Biomass Concentration (Silicon Units)
Small Phytoplankton	PhyS, PS	PhySn	PhySi
Large Phytoplankton	PhyL, PL	PhyLn	PhyLi
Small Zooplankton	ZooS, ZS	ZooSn	ZooSi
Large Zooplankton	ZooL, ZL	ZooLn	ZooLi
Predatory Zooplankton	ZooP, ZP	ZooPn	ZooPi
Nitrate concentration	NO3		
Ammonium concentration	NH4		
Particulate Organic Nitrogen concentration	PON		
Dissolved Organic Nitrogen concentration	DON		
Silicate concentration	Si(OH)4		
Particulate Organic Silica concentration	Opal		

Five different but related models were examined at the workshop.

- The PICES CCCC prototype lower trophic level marine ecosystem model named "*NEMURO*" (see below): a conceptual model representing the minimum trophic structure and biological relationships between and among all the marine ecosystem components thought to be essential in describing ecosystem dynamics in the North Pacific (Fig. 2).
- The "*NEMURO*/FORTRAN Box" Model: a FORTRAN computer program to solve the coupled set of differential equations making up *NEMURO* and the graphing software needed to examine model output.
- The "*NEMURO*/1-D Kishi" Model: The *NEMURO* model coupled with a 1-D ocean physics model. The physical model runs prior to *NEMURO*, and provides the necessary physical forcing required by *NEMURO*.
- The "*NEMURO*/1-D Yamanaka" Model: Similar to the 1-D Kishi model except that the ocean physics model and *NEMURO* are calculated simultaneously in one FORTRAN computer program.
- The "*NEMURO*/MATLAB Box" Model: a MATLAB® version of *NEMURO*.

In a friendly competition among meeting participants, the prototype model was named *NEMURO* (North Pacific Ecosystem Model for Understanding Regional Oceanography). The winning name was a joint effort with contributions coming from Drs. Vadim V. Navrotsky (Russia), Bernard A. Megrey (U.S.A.), and Lan S. Smith (Japan).

6.1 NEMURO Prototype Model

The *NEMURO* NPZ marine ecosystem model consists of the conceptual model, a set of coupled differential equations and process equations, and a table of parameter values and initial starting conditions. *NEMURO,* which is made up of 11 state variables each represented by a box compartment, is shown schematically in Figure 2. The state variables (and state variable names) are Nitrate (NO_3), Ammonium (NH_4), Small Phytoplankton Biomass (PhyS), Large Phytoplankton Biomass (PhyL), Small Zooplankton Biomass (ZooS), Large Zooplankton Biomass (ZooL), Predatory Zooplankton Biomass (ZooP), Particulate Organic Nitrogen (PON),

Dissolved Organic Nitrogen (DON), Particulate Organic Silicate (Opal), and Silicate Concentration ($Si(OH)_4$). Fluxes between and among the state variables (represented in Fig 2 with arrows) represent the fluxes between the model compartments in both nitrogen (black arrows) and silicon (blue arrows) units. The unit of currency for the model is expressed in units of nitrogen.

The formulation of the fluxes between the model compartments is given by a set of 14 coupled ordinary differential equations (Table 2).

Although parameter tuning is an important task for the future work, *NEMURO* is useful for use in regional comparisons of the eastern and western North Pacific by comparing results to changing the values of parameters. It is important to realize that regional comparisons cannot be made if the model is different with respect to:

- the physical model in which the ecological model is embedded,
- the number of ecological compartments,
- the equations representing each physiological process, and
- the parameter values.

During the drafting of this report, the conveners found that there were differences in the definition of important parameters used in traditional stand-alone lower trophic and higher trophic and/or population dynamics models. One is the relation-ship between assimilation coefficient (a), growth efficiency (b), egestion, and excretion. The traditional stand-alone lower trophic level models, including *NEMURO* use the following formulations:

Excretion: $ExcZ = (a - b) * GraPZ$,
Egestion: $EgeZ = (1.0 - a) * GraPZ$

where GraPZ is the grazing rate of zooplankton on phytoplankton. While the usual ecology textbook definitions of the above equations are:

Excretion: $ExcZ = (a\ (1.0 - b)) * GraPZ$,
Egestion: $EgeZ = (1.0 - a) * GraPZ$.

Another is the mortality coefficient (MorZ) which is related to biomass or the square of biomass:

$MorZ = Mor*\exp(K*Temp)*Z^2$
(traditional stand-alone LTL model), or
$MorZ = Mor*\exp(K*Temp)*Z$,

where, Mor is the mortality rate, K is the temperature coefficient, and Z is the biomass of zooplankton.

Without predation by carnivores, the model needs mortality related to biomass squared to avoid burst increases of zooplankton biomass and to stabilize the model dynamics. However, this is a mathematical trick that has nothing to do with biological theory. This may cause the linking of the lower trophic level model to higher trophic level models. This subject should be considered at the next workshop when discussing the linkage between lower trophic level ecosystem models and higher trophic level ecosystem models.

6.2 NEMURO/FORTRAN Box Model

This model is a FORTRAN computer program built to solve the coupled set of differential equations making up *NEMURO* and the graphing software needed to examine model output.

The process equations, which describe individual submodel processes (i.e. photosynthesis, grazing), are be presented in Table 2, parameter values for the three geographic areas are given in Table 1 and further details of the *NEMURO*/FORTRAN Box Model can be found in Appendix 3.3.

In Figure 5 the time-dependent features of each compartment solved by the *NEMURO*/ FORTRAN Box Model are shown. Panel A shows model dynamics for station A7 and Panel B shows dynamics for Station P (see Table 1 for simulation parameters). These results, however, are only preliminary because the parameters used are based on experiments, and are not yet tuned. Tuning of the parameters should be continued.

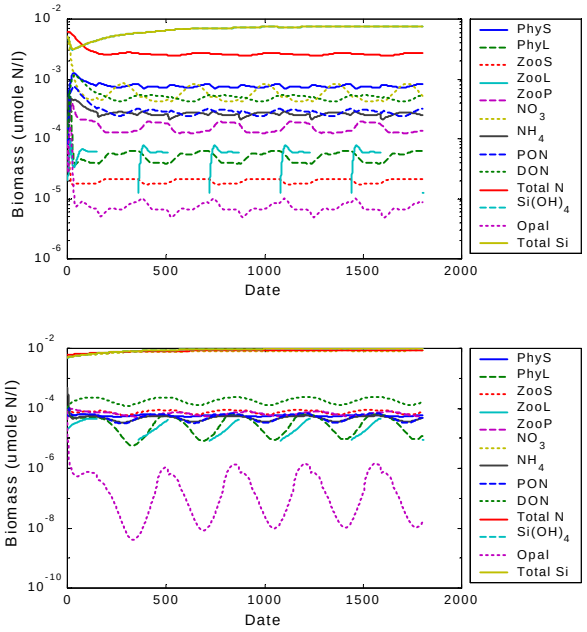

Fig. 5 *NEMURO*/FORTRAN Box model output showing the time-dependent dynamics of the state variables for two locations, station A7 (top panel) and Station P (lower panel). See Table 1 for simulation parameters and Table 2 for model equations.

6.3 NEMURO/1-D Kishi Model

The *NEMURO*/1-D Kishi Model is the *NEMURO* model coupled with a 1-D ocean physics model. The physical model runs prior to *NEMURO*, and provides the necessary physical forcing required by *NEMURO*.

Instructions for downloading the 1-D Kishi Model are given in Appendix 4, and further details about the model can be found in Appendix 3.2.

6.4. NEMURO/1-D Yamanaka Model

The *NEMURO*/1-D Yamanaka Model is similar to the 1-D Kishi model except that the ocean physics model and *NEMURO* are calculated simultaneously in one FORTRAN computer program. Biological process equations used are given in Table 2, parameter values for the three regions are described in Table 1, and further details about the model can be found in Appendix 3.

In the physical model, the water column is split into 50 layers with 20 layers above 100 m. The mixed layer process is the Mellor-Yamada level 2. Outputs from the physical model are temperature, salinity, diffusion coefficient for tracers, diffusion coefficient for momentum and turbulent energy through time and by depth.

Biological and physical results of applying the 1-D Yamanaka model to the three regions, presented as time-depth plots, are given for station A7 (Fig. 6), station P (Fig. 7), and the eastern Bering Sea station (Fig. 8). Note that the vertical axis is described by log scale and 0 of horizontal axis starts on September 1st.

It can be seen that large zooplankton immigrate into the domain of the model (i.e., shallow euphotic zone) from the zone deeper than 300 m. After large zooplankton increases, ZooLn (biomass of large zooplankton described by nitrogen) increases dramatically from large zooplankton grazing on large phytoplankton and small zooplankton. Large phytoplankton and small zooplankton decrease when large zooplankton abundance is high. Predatory zooplankton increases from grazing large zooplankton when large zooplankton densities are adequate for feding. The fluctuation of large phytoplankton follows one month after that of small phytoplankton. As to the biomass of plankton, the largest one is small phytoplankton, followed by predatory zooplankton and small zooplankton. This box model was run under the constant temperature and light without annual oscillation.

6.5. NEMURO/MATLAB

NEMURO/MATLAB is a MATLAB® version of *NEMURO*. The *MATLAB* scripts making up *NEMURO*/MATLAB are a convenient modeling framework in that MATLAB includes numerical integration routines as well as integrated plotting functions. The MATLAB scripts can be found in Appendix 5 and 6, the differential and process

equations are described in Table 3, parameter values for the base run are found in Table 4, and instructions for running the scripts are in Appendix 7.

It is important to note that the parameters and units in the *NEMURO*/MATLAB model are in different units compared to the *NEMURO*/ FORTAN Box model. For example, concentrations are in units of millimoles/m^3, lengths are in meters, time values (i.e. rates) are in units of days. Concentrations in the *NEMURO*/FORTRAN Box model are in moles/m^3. Therefore, close attention must be paid to the decimal place when converting constants, rates or comparing parameter values in Tables 1 and 4.

In preparing *NEMURO*/MATLAB changes were made to *NEMURO*, which required adding an additional 4 state variables. Thus *NEMURO* is an 11 state variable model and *NEMURO*/MATLAB is a 15 state variable model. The change was done primarily to conserve mass in *NEMURO* and does not alter system dynamics. Changes relative to 11 state variable *NEMURO*/ FORTRAN Box model are listed below.

- Large phytoplankton may be grazed by small zooplankton. Therefore terms needed to be added to the *PhyLn* and *ZooSn* equations. See Process Equation 10-2 in Table 3.
- In the *NEMURO*/MATLAB simulations, natural mortality terms are first order, not second order. These change the mortality parameters in equations *PhySn*, *PhyLn*, *ZooSn*, *ZooLn*, *ZooPn* and the related detritus (*PON*) term. Second order terms are retained in the model, but are commented out. See Process Equations 4, 5 in Table 3 for formulations.
- State variables related to silicon dynamics are simplified. Most of the 11-state variable model silicon equations either have rates equal to zero (as they should) or are simply the nitrogen dynamics with all terms multiplied by the Silicon:Nitrogen (Si:N) ratio. These three redundant equations are eliminated to make the model run faster. The silicon uptake equation uses the nitrate growth parameters multiplied by the large phytoplankton Si:N ratio. This is the same as in the *NEMURO*/FORTRAN Box model formulation, but uses fewer parameters, again, to speed things up for running on a PC.
- Four new state variables are added for the calculation of total Nitrogen (i.e., to conserve mass): *DeepNO3, DeepPON, DeepSi*, and *DeepOpal*. These are the nitrogen and silicon pools located below the model domain. They are the source of the upwelled nitrate/silicon and the recipient for the sinking detritus. They don't affect the dynamics, but are needed to conserve mass.
- Light limitation is parameterized differently. Instead of assuming some optimum light intensity and calculating light at the model depth, in the *NEMURO*/MATLAB model, light limitation is incorporated by a simple seasonally varying efficiency. In the model it ranged between 0.2 and 0.8. A diurnal component was also be added. See Process Equation 1 in Table 3.
- The *NEMURO*/MATLAB model was run with and without remineralization of particulate silicon (opal). The runs presented have no surface remineralization, i.e. $DecSi = 0$.

Preliminary results, presented in Figures 9 and 10, are from a "base" model run using the Station P parameters given in Table 4. This parameter set produced a fairly stable model with all populations persisting throughout the twenty-year model run (Fig. 9). Phytoplankton and zooplankton populations exhibited small seasonal variations, but no very large variations. There was a brief spring bloom of large phytoplankton, which was quickly grazed down by large zooplankton. This model is fairly similar to what might be expected at Station P in the North Pacific. However, the large phytoplankton (diatom) bloom, is generally not observed. However, given that this is a box model with no vertical migration of zooplankton and no iron

limitation, it was felt that this "base case" would serve to examine the behavior of the *NEMURO*/MATLAB model. Details of the "base case" run for years 4 through 6 are shown in Figure 10 for the plankton and nitrogen and silicon fields respectively.

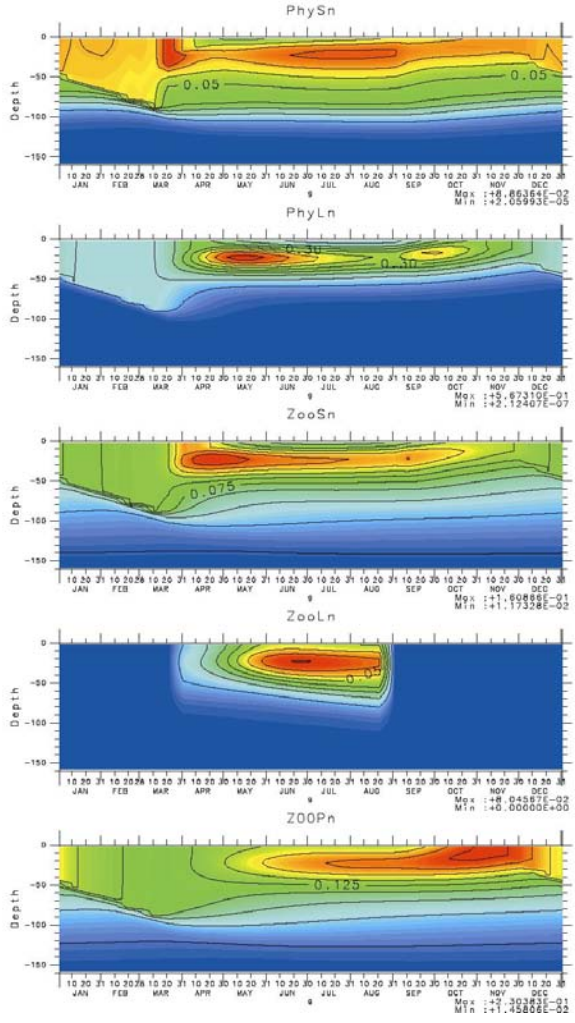

Fig. 6 Biological state variables output from applying the *NEMURO*/1-D Yamanaka model to station A7 using daily physical forcing data files and plotted against time and depth. Shown are small phytoplankton (PhySn), large phyto-plankton (PhyLn), small zooplankton (ZooSn), large zooplankton (ZooLn), and predatory zooplankton (ZooPn) biomass concentrations. All biological state variables are plotted as biomass concentration expressed in nitrogen units (*mmol*N/*l*).

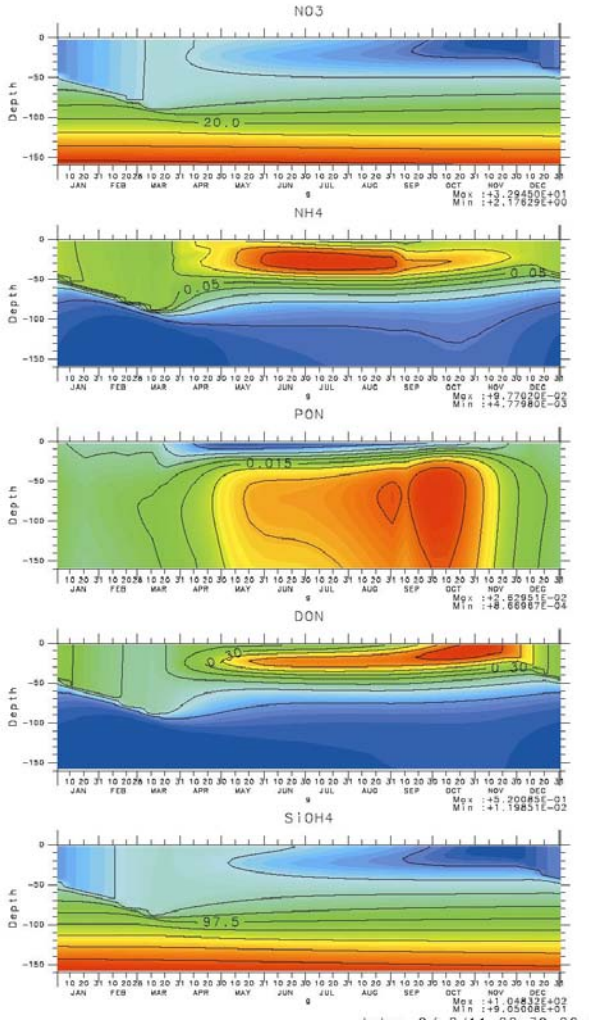

Fig. 6 (continued) Shown are nitrate (NO_3), ammonia (NH_4), particulate organic nitrogen concentration (PON), dissolved organic nitrogen concentration (DON), expressed in nitrogen units (*mmol*N/*l*) Also plotted is silicate concentration (SiOH4) in silicon units (*mmol*Si/*l*)

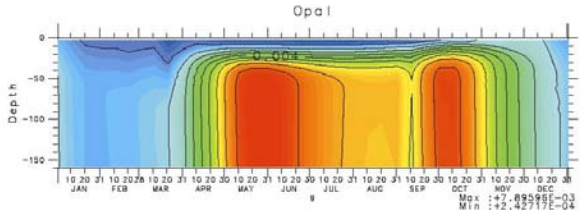

Fig. 6 (continued) Shown is Particulate Organic Silica concentration (Opal) in silicon units (*mmol*Si/*l*).

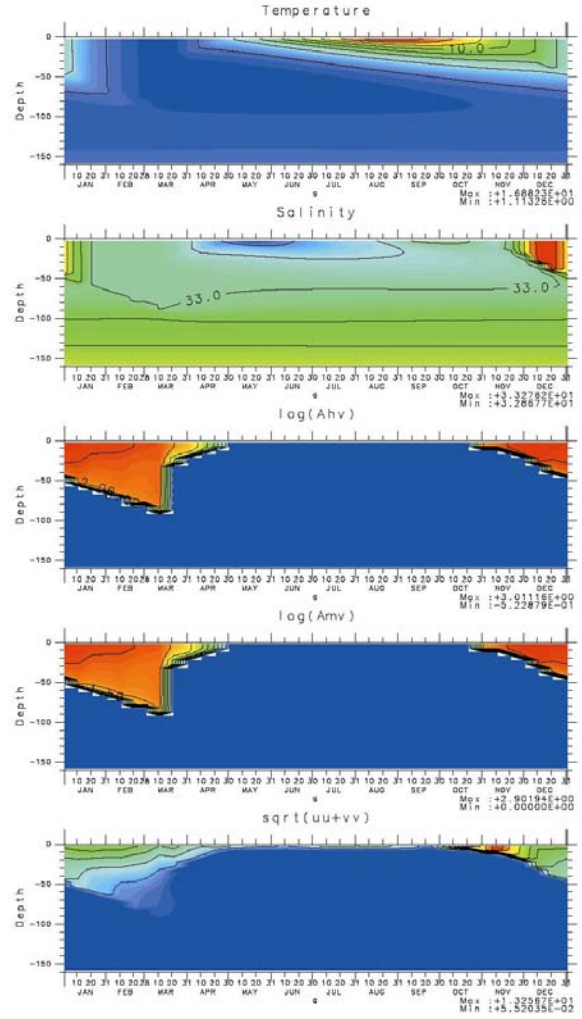

Fig. 6 (continued) Physical state variables output. Shown are temperature (°C), salinity (ppt), diffusion coefficient for tracers (log Ahv), diffusion coefficient for momentum (log Amv), and turbulent energy (sqrt(*uu*+*vv*)) plotted against time and depth.

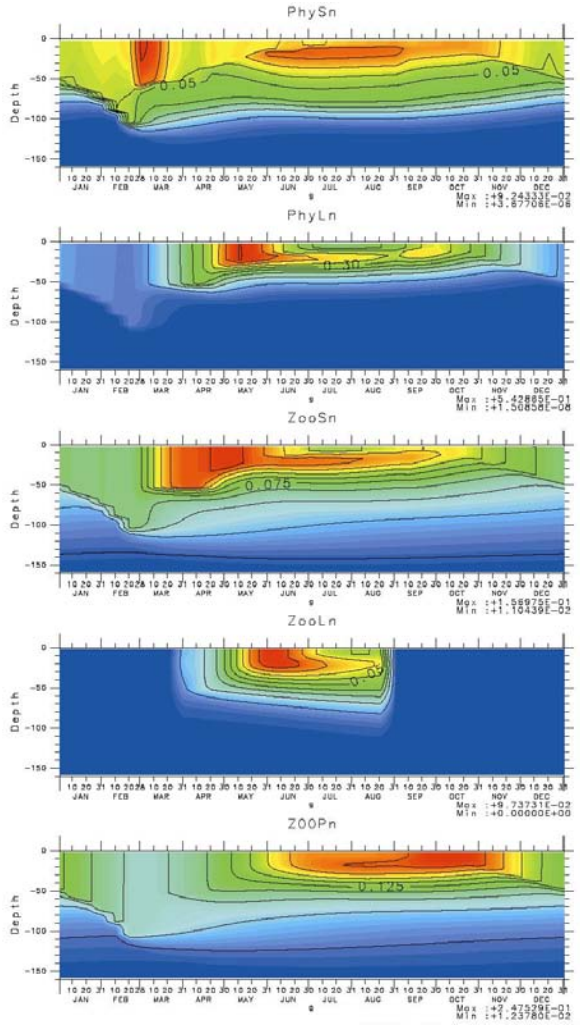

Fig. 7 Biological state variables output from applying the *NEMURO*/1-D Yamanaka model to station P using daily physical forcing data files and plotted against time and depth. Shown are small phytoplankton (PhySn), large phyto-plankton (PhyLn), small zooplankton (ZooSn), large zooplankton (ZooLn), and predatory zooplankton (ZooPn) biomass concentrations. All biological state variables are plotted as biomass concentration expressed in nitrogen units (*mmol*N/*l*).

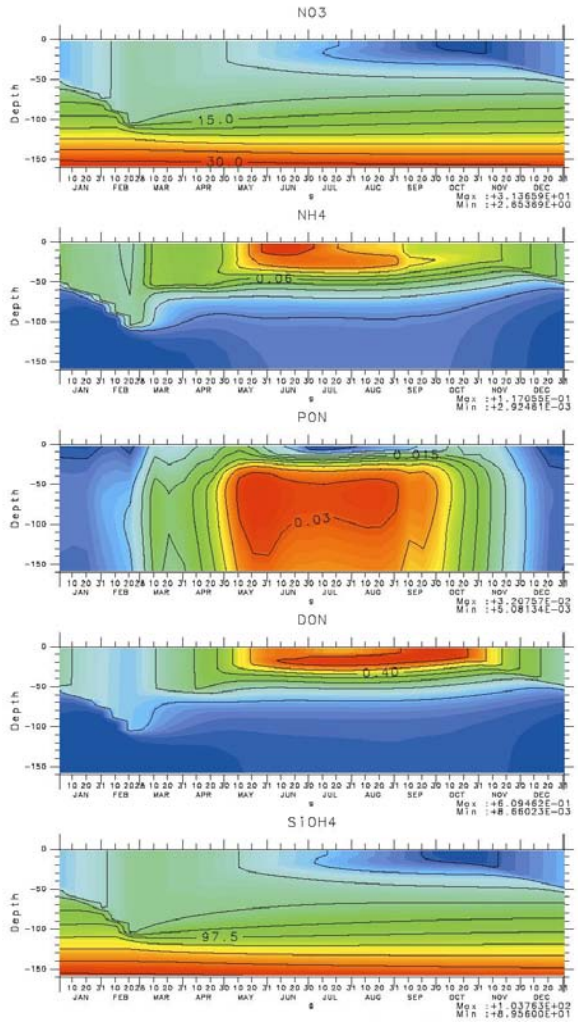

Fig. 7 (continued) Biological state variables output from applying the *NEMURO*/1-D Yamanaka model to station P using daily physical forcing data files and plotted against time and depth. Shown are nitrate (NO_3), ammonia (NH_4), particulate organic nitrogen concentration (PON), dissolved organic nitrogen concentration (DON), expressed in nitrogen units (*mmol*N/*l*). Also plotted is silicate concentration (SiOH4) in silicon units (*mmol*Si/*l*).

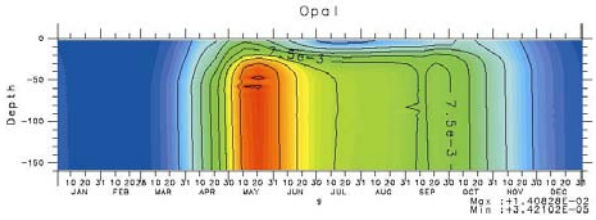

Figure 7 (continued) Shown is Particulate Organic Silica concentration (Opal) in silicon units (*mmol*Si/*l*).

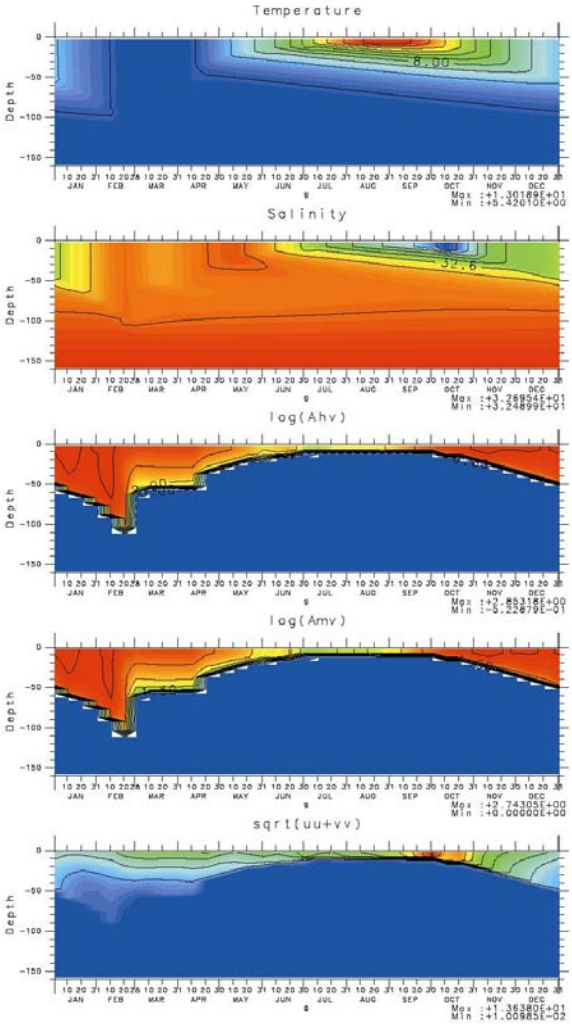

Fig. 7 (**continued**) Physical state variables output. Shown are temperature (°C), salinity (ppt), diffusion coefficient for tracers (log Ahv), diffusion coefficient for momentum (log Amv), and turbulent energy (sqrt(uu+vv)) plotted against time and depth plotted against time and depth.

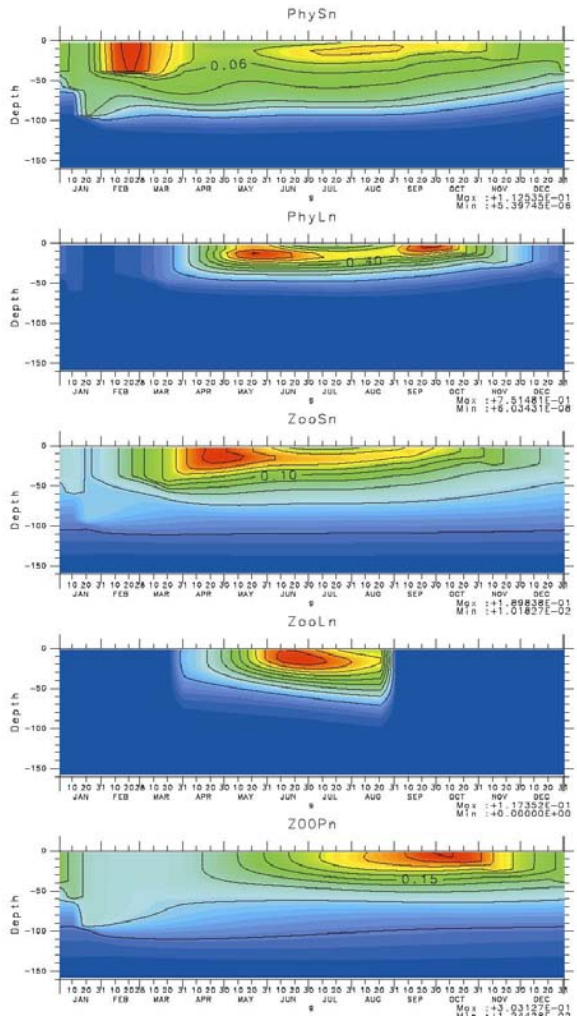

Fig. 8 Biological state variables output from applying the *NEMURO*/1-D Yamanaka model to station Bering Sea using daily physical forcing data files and plotted against time and depth. Shown are small phytoplankton (PhySn), large phytoplankton (PhyLn), small zooplankton (ZooSn), large zooplankton (ZooLn), and predatory zooplankton (ZooPn) biomass concentrations. All biological state variables are plotted as biomass concentration expressed in nitrogen units (*mmol*N/*l*).

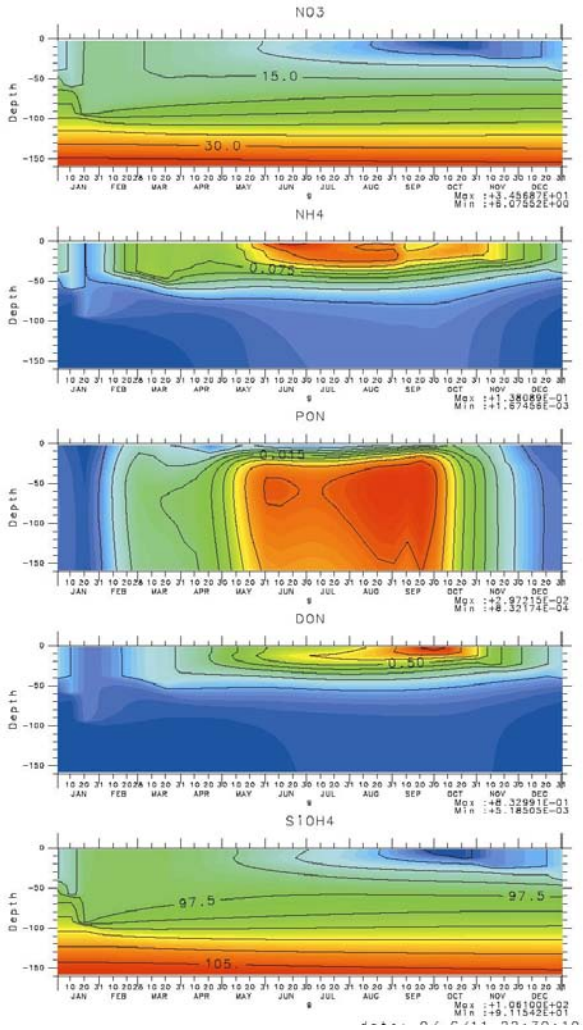

Fig. 8 (**continued**) Shown are nitrate (NO_3), ammonia (NH_4), particulate organic nitrogen concentration (PON), dissolved organic nitrogen concentration (DON), expressed in nitrogen units (*mmol*N/*l*). Also plotted is silicate concentration (SiOH4) in silicon units (*mmol*Si/*l*).

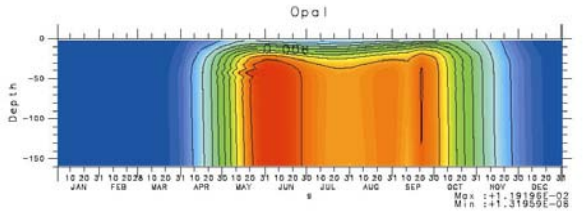

Fig. 8 (**continued**) Shown is Particulate Organic Silica concentration (Opal) in silicon units (*mmol*Si/*l*).

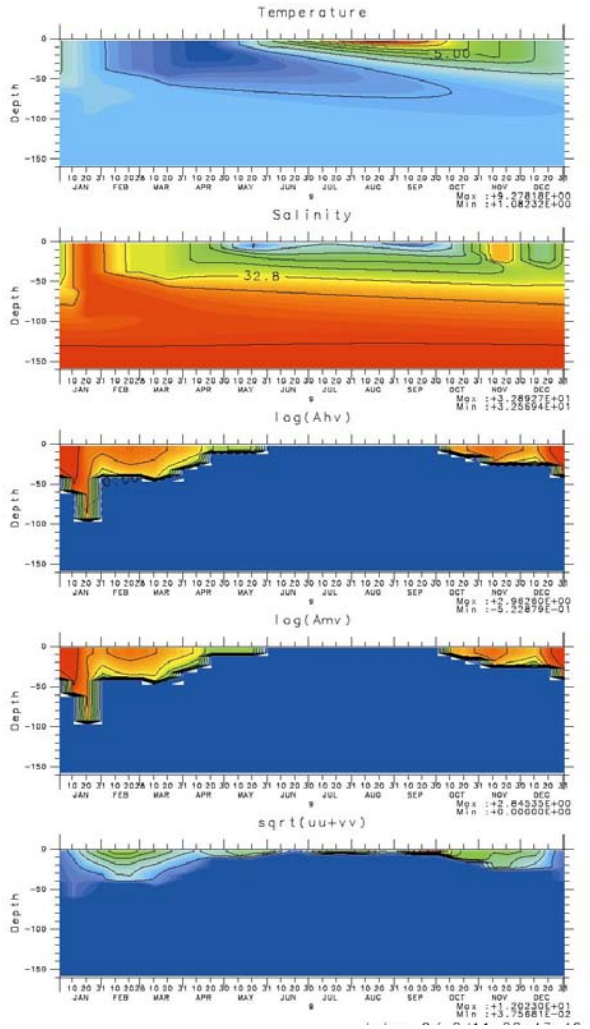

Fig. 8 (**continued**) Physical state variables output. Shown are temperature (°C), salinity (ppt), diffusion coefficient for tracers (log Ahv), diffusion coefficient for momentum (log Amv), and turbulent energy (sqrt($uu+vv$)) plotted against time and depth plotted against time and depth.

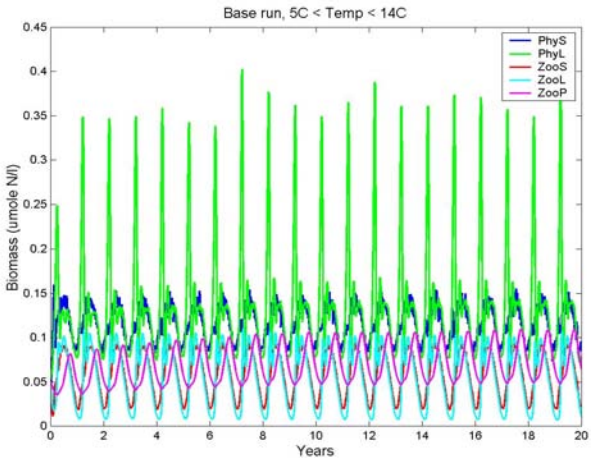

Fig. 9 Base twenty-year run of the *NEMURO*/MATLAB Box model for Station P. Shown are biomass dynamics of Small Phytoplankton (PhyS), Large Phytoplankton (PhyL), Small Zooplankton (ZooS), Large Zooplankton (ZooL), and Predatory Zooplankton (ZooP).

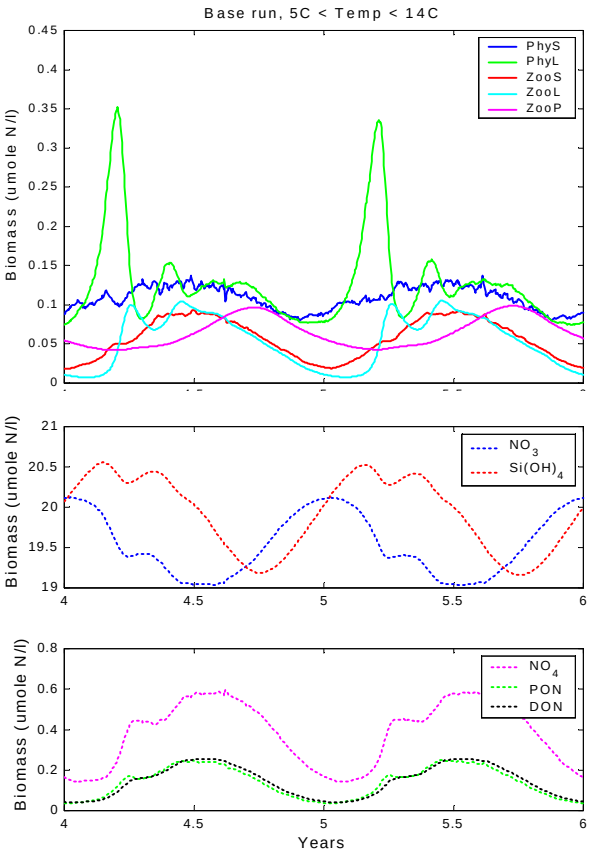

Fig. 10 Details of plankton fields for years 4 through 6 of the *NEMURO*/MATLAB Box model 20-year base run for Station P.

7.0 Model Comparison Measures

The participants discussed the possible outputs from the model. For adequate model comparison, the minimum requirements from the model are as follows:

- Time trace of state variables
- P/B ratio
- Proportion of production by trophic functional groups
- Ecotrophic coefficient (%Primary Production available to ZL & ZP)
- Total biomass (ZS+ZL+ZP) production
- Si/NO3 integrated over the whole water column
- Si production/N production integrated over the whole water column
- Evaluation of conservation of mass

However, during the workshop, there was not enough time to change the model code to add the above variables. Thus only the time-dependent features of each compartment were discussed.

8.0 Team Groups' Reports

8.1 Biological Parameter Team Report

Discussions were held over three days to review the suitability of the biological process equations formulations, determine the appropriate parameter values for three distinct physical locations, provide references and parameter ranges where possible, and to examine different formulations for several of the biological equations. The general form of the equations was endorsed, but there were a few minor changes. The most important was the suggestion to replace the Steele (1962) formulation of the photosynthesis light curve

$$P = P_{\max} \frac{I}{I_{opt}} e^{\left(1-\frac{I}{I_{opt}}\right)} \qquad (1)$$

with the Platt et al. (1980) formulation:

$$P = P_{\max}(1-e^{\left[-\frac{a*I}{P}\right]})e^{\left[-\frac{b*I}{P}\right]} \qquad (2)$$

where

P= Photosynthetic rate
P_{max} = maximum photosynthetic rate
á= light attenuation with depth
â= self shading light inhibition
I= light intensity (W/m^2)
I_{opt}= optimum light intensity (W/m^2)

This change was made because the Steele formulation uses only one parameter to describe both the increase in photosynthesis with light at low light levels and the decrease in photosynthesis with light at high light levels. Using only one parameter produces a photosynthesis light relationship with excessive light inhibition (Fig. 11).

Another major discussion and effort went into the formulation of a grazing selectivity equation for the new predatory zooplankton component. The formulation agreed upon (proposed by Dr. Kishi) used an approach similar to the ammonium inhibition formulation to account for the fact that the diet of predatory zooplankton consists of three prey groups and the grazing equation needed to take into consideration prey preferences (assumed to be proportional to abundance):

$$\begin{aligned} GrZP = \; & GR_{max}(R_{PL}\,(1-\exp^{-ëpl(P*plp-PL)})\exp^{Øplp(ZS+ZL)} \\ & + R_{ZS}\,(1-\exp^{-ëzs(P*pzs-ZS)})e^{Øzsp(ZL)} \\ & + R_{ZL}\,(1-\exp^{-ëzl(P*pzl-ZL)})\,) \end{aligned} \qquad (3)$$

A test suite of parameter values for three locations: Ocean Station P, Station 7 on the A line south of Hokkaido (A7), and a Bering Sea basin location, were compiled. Station P values were used as a base case. References, comments and appropriate ranges were provided whenever possible. Some parameters were estimated and were noted as needing additional research and

sensitivity analyses performed on them. In particular, all the parameters related to processes required to describe the dynamics of the ZP state variable were unknown.

8.2 Microbial Food Web Team Report

The PICES *NEMURO* simulation model partitions the plankton into five state variables: small phytoplankton, large phytoplankton, small zooplankton, large zooplankton, and predatory zooplankton. The task of the working group was to describe what functional groups of organisms were represented by these five components, to develop a simple parameterization of the microbial food web for inclusion in the model, and to suggest possible additions that could be included in future generations of the model.

Why is the Microbial Food-web Important?

The classical food web concept that many of us were taught assumed that the primary production in marine ecosystems was grazed primarily by herbivorous mesozooplankton, which in turn supported a food-web of higher trophic level predators. However, studies over the last decade have revealed the importance of the microbial food-web in aquatic ecosytems, and have shown that it can have a significant impact on the amount of primary production that is actually available to the mesozooplankton, and hence to higher trophic levels (Moloney and Field, 1991). For example, in low nutrient ecosystems, or during periods of low nutrient availability, a relatively high percentage of the gross primary production ends up as dissolved organic matter that is utilized by bacteria. The bacteria in turn are grazed by heterotrophic nanoflagellates, which in turn are eaten by ciliates and other microzooplankton. Since the microzooplankton are an important food source for the mesozooplankton, this group of organisms links the microbial food web to the classical food-web. Cushing (1989) noted that the classical food-web transfers most energy during the spring and autumn blooms in temperate waters (under weakly stratified conditions), but that the microbial food-web dominates the strongly stratified (oligotrophic) waters of the temperate summer. Permanently well-mixed coastal zones in the temperate seas presumably could be dominated by either the classical food web or the microbial food web, depending on the trophic status of the area.

It has been estimated that 10 to 50% of the primary production passes through the bacterioplankton (McManus and Peterson 1988), and that very little of the resulting bacterial production is available to the mesozooplankton. For example, in the NE subactic Pacific Ocean, Rivkin et al. (1999) estimate that only about 3% to 12% of the bacterial carbon production is transferred to copepods. Consequently, in this ecosystem a large proportion of the primary production is respired by the microbial food web in the surface layer, rather than being exported to higher trophic level predators, or the deep-sea.

Structure of the Plankton Community

It is imperative that the model user has a clear understanding of the components of the plankton which are represented by each state variable, and the "hidden" interactions that can occur between the components within some state variables. Figure 12 indicates that the small phytoplankton (PS) group implicitly contains the autotrophic picoplankton (0.2-2 microns equivalent spherical diameter (ESD) in size), and autotrophic nanoflagellates (2-20 microns ESD). The large phytoplankton group (PL) contains the netphytoplankton (20-200 microns ESD), which are primarily diatoms. The small zooplankton (ZS) group contains the heterotrophic flagellates (2-20 microns ESD), and the microzooplankton (20-200 microns ESD). The large zooplankton (ZL) group consists of copepods and euphausiids, which are primarily (but not exclusively) herbivores. The predatory zooplankton, like amphipods and chaetognaths, are represented by the state variable, ZP. The predatory zooplankton and large herbivorous zooplankton form the interface between the lower trophic levels and the higher trophic levels, which will be added to future generations of the model.

Trophic Interactions

Figure 12 indicates that picophytoplankton are primarily eaten by heterotrophic flagellates, while the microzooplankton are assumed to graze primarily on nanophytoplankton. An important "hidden" feeding interaction occurs within the ZS compartment, since microzooplankton will also consume heterotrophic flagellates. Similarly, within the ZL compartment euphausiids will consume copepods, under some circumstances.

Note that the functional importance of bacteria is captured implicitly in *NEMURO* in the decomposition process, which is assumed to occur "instantaneously". Bacteria do not appear explicitly in the model, because very little bacterial production passes through the microbial loop to the large herbivorous and predatory zooplankton, which form the link to the higher trophic levels.

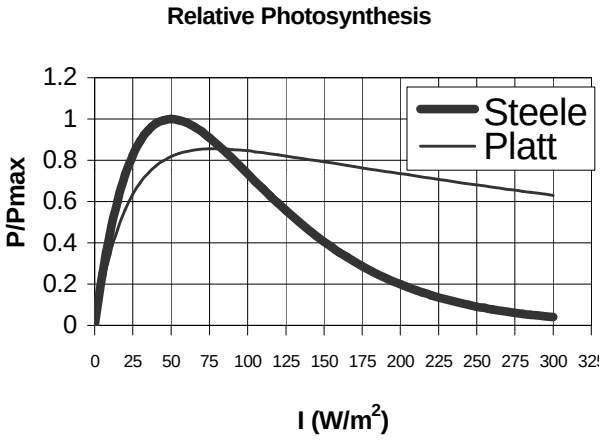

Fig. 11 Comparison of the light-photosynthesis relationship using the Platt (1980) two parameter and the one parameter Steel (1962) formulation.

To anticipate future requirements, the model has a switch, which allows the user to enable microzooplankton to consume netphytoplankton. Normally this switch will not be activated, because it is not a primary pathway of energy flow.

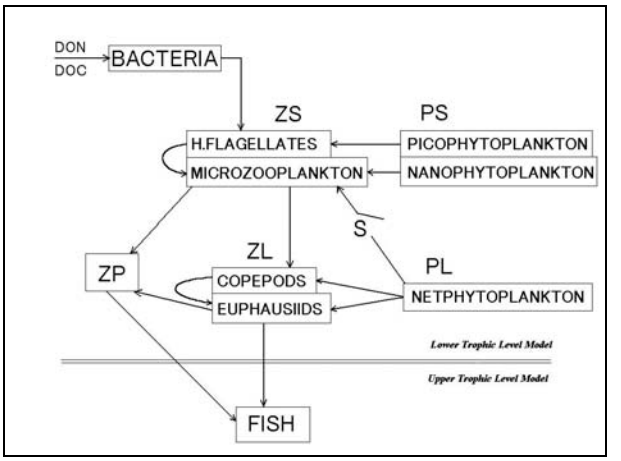

Fig. 12 Proposed microbial food web submodel with a suggestion for linking lower trophic level (LTL) models to higher trophic level (HTL) models. Compartments above the double line belong to the LTL model while the fish compartment, falling below the doubel line, belongs to the HTL model.

Representing the Microbial Food Web

In natural communities, diatoms and dinoflagellates are able to take rapid advantage of nitrate availability, whereas the smaller phytoplankton are more adapted to survive in nutrient poor, oligotrophic environments. Diatoms and dinoflagellates tend to be the main contributors to new production, while cyanobacteria, prochlorophytes and small autotrophic flagellates are believed to be most likely involved in systems dominated by regenerated production. In oligotrophic regions of the oceans and in some coastal upwelling regions, picophytoplankton can contribute up to 80% of the total autotrophic biomass and primary production.

In response to changes in nitrate availability, temperature and grazing pressure, there is an implicit shift in the size structure of the microbes within the small phytoplankton and small zooplankton compartments in the model, which has important energetic implications. For example, when nanoplankton dominate the small phytoplankton (PS) component it requires one

trophic step to convert nanoplankton production into microzooplankton production, with a growth efficiency of 0.3 (Fig. 12). At the other extreme, when picoplankton dominate the PS, then two trophic steps are required to convert picoplankton production into microzooplankton production, with an efficiency of 0.3^2 (or 0.09). The resulting growth efficiency is much lower in this case because picophytoplankton are primarily consumed by heterotrophic flagellates, which in turn, are eaten by microzooplankton. Accordingly, the length of the microbial food chain will vary dynamically between a value of 1 and a maximum of 2, in response to changes in physical forcing, nutrient availability, and grazing mortality. The working group discussed how these "hidden" changes in the length of the microbial food chain and, their impact on the growth efficiency of the ZS could be parameterized with a minimal increase in model complexity.

Field studies have shown that the large phytoplankton are dominant when there is an abundant supply of silicate and nitrate (a high f-ratio). Conversely, the smaller phytoplankton become dominant when the concentrations of nitrite and silicate are depleted, and the ammonium concentration increases. Accordingly, when the proportion of small phytoplankton (i.e. PS/[PS+PL]) changes in the model, we assume that a similar change occurs in the relative proportion of picoplankton in the PS compartment (i.e. pico/[pico + nano]). The resulting change this causes in the length of the microbial food chain (m = fractional number of trophic steps between PS and ZS), and in the PZ growth efficiency ($\hat{a}_{ZS}$) can be represented by:

$$m = \left[1 + a\left(\frac{PS}{PS + PL}\right)\right]$$

$$b_{ZS} = 0.3^{[1+m]} \qquad (4)$$

where, α = maximum ratio of picoplankton/total phytoplankton biomass in the study area. Observed values of α vary between 0.2 to 0.8; lower values are typical in coastal ecosystems and larger values in oceanic systems. The simple formulation summarized in equation 4 causes the growth efficiency to vary between 0.11 when picophytoplankton dominate the PS biomass, and 0.3 when nanophytoplankton dominate. In *NEMURO*, changes in the growth efficiency affect the excretion rate, and hence the productivity of the small zooplankton.

Future Steps

The sensitivity of the model output to "the band-aid solution" proposed in equation 4 needs to be fully tested. If the productivity of the large zooplankton is particularly sensitive to equation 4, then a better formulation of the ZS growth efficiency equation should be developed and tested. Clearly, it is important that the model estimate the production of large zooplankton, as accurately as possible because this functional group of organisms often forms the primary link to higher trophic levels, which will eventually be added to the model. In ecosystems where autotrophic picoplankton are particularly important, the microbial food web could be simulated better by creating separate picoplankton, nanophytoplankton, heterotrophic flagellates and microzooplankton groups. However, this increase in realism comes at an expense, since it would increase the model complexity by two state variables and several process equations.

In the current formulation of the model the team noted that the production of large zooplankton will be somewhat overestimated because euphausiids can also eat copepods (Fig. 12). Hence the ZL growth efficiency will be somewhat less than the fixed value of 0.3 assumed in the model. If this interaction is considered to be important, the ZL growth efficiency should also be transformed into a variable.

8.3 Post Processing & Plotting Software Team

The post-processing team's efforts focused on taking the output of Yamanaka's preliminary 1-D

coupled physics and foodweb model and post-processing it for display by MATLAB. Four cases were processed:

1. Station P Climatological Conditions
2. Bering Sea Climatological Conditions
3. Station A7 Climatological Conditions
4. Station A7 for 1990

and presented at the workshop. *It should be stressed that all these cases are preliminary and should be considered only representative of the type of analyses and inter-comparisons that could be possible once the Yamanaka model is fully tested.*

All files generated by the team are available via the web at ***http://www.OPNML.unc.edu/Personnel/few/Nemuro.html***. Web-postings for each of the 4 cases above have 14 files associated with them. We list below only the names of the files related to the A7 1990 case; the remaining 3 cases have identical formats, with only the file names changing slightly:

1. *YThist.dat*: 1-D Yamanaka Model Foodweb Output (ASCII text format)

2. *ztlabel.f*: Order of output foodweb variables from Yamanaka Model (ASCII text format)

3. *Bio2mat.f*: Fortran code for translation of foodweb model output into MATLAB format (ASCII text format) (Appendix 8)
   Input file: *YThist.dat* (ASCII text format)
   NOTE: The example code in Appendix 8 uses the Bering Sea data set as the input data set.
   Output file:*YThist_mat.dat* (ASCII text format)

4. *YThist_mat.dat*: output from *Bio2mat.f* formatted for input to MATLAB (ASCII text format)

5. *matlab.A7bio*: MATLAB code for generating plots of model foodweb results (ASCII text format) (Appendix 9)
   Input file: YThist_mat.dat

6. *YPhist.dat*: 1-D Yamanaka Model Physics Output (ASCII text format)

7. *zplabel.f*: Order of output physical variables from Yamanaka Model (ASCII text format)

8. *Phys2mat.f*: Fortran code for translation of physics model output into MATLAB format (ASCII text format) (Appendix 10)
   Input file: *YPhist.dat* (ASCII text format)
   NOTE: The example code in Appendix 10 uses the Bering Sea data set as the input data set.
   Output file: *YPhist_mat.dat* (ASCII text format)

9. *YPhist_mat.dat*: output from *Phys2mat.f* formatted for input to MATLAB (ASCII text format)

10. *matlab.A7phys*: MATLAB code for model (physics) plotting (text format) (Appendix 11)
    Input file: *YPhist_mat.dat*

11. *A7phys.jpg*: Plot of physical variables - T, S, Vertical Eddy Viscosity (jpeg format)

12. *A7bio1.jpg*: Plot of foodweb variables - PSn, ZSn, PLn, ZLn (jpeg format)

13. *A7bio2.jpg*: Plot of foodweb variables - ZPn, PLs, ZLs, ZPs (jpeg format)

14. *A7bio3.jpg*: Plot of foodweb variables - NO3, NH4, PON, DON, SiO (jpeg format)

8.4. Model Coding & Forcing File Team Report

The model coding team consisted of four subgroups. The first was lead by Prof. Yamanaka. They worked on coding the *NEMURO*/1-D Yamanaka Model. The second, lead by Dr. Kishi, worked on coding the *NEMURO*/1-D Kishi Model. The third, lead by Dr. Fujii, worked on coding the *NEMURO*/ FORTRAN Box Model. The fourth, lead by Dr. Dave Eslinger, engaged in coding of *NEMURO*/MATLAB Box Model.

The specifications of these models are described in the section on Model Descriptions and in Appendix 3.

The following forcing files were assembled;

1. Climatological forcing file (monthly averages) for Station A7;
2. Climatological forcing file (monthly averages) for Station P;
3. Climatological forcing file (monthly averages) for Eastern Bering Sea; and
4. Daily forcing file (daily averages) for Station A7 for the year 1990.

9.0 Model Experiments and Model Comparisons

Several model comparison experiments were designed during the workshop. For those planned experiments, three factors were varied: which model was used, which geographical location and corresponding set of biological parameters were used, and which physical forcing scenario was used. The details of the experiments and their objectives are described below.

Experiment 1

Objective: To compare the *NEMURO*/FORTRAN Box model with simpler physical forcing (biology but minimal physics) to the fully forced *NEMURO*/1-D Yamanaka NPZ bio-physical model. Both models used the same biological state variables, parameters and process equations.

Configuration: The *NEMURO*/FORTRAN Box Model configured to station A7 was compared to the *NEMURO*/1-D Yamanaka model configured to station A7. The *NEMURO*/FORTRAN Box model was forced with sea surface temperature and solar radiation, while the *NEMURO*/1-D Yamanaka model was forced with daily average values from station A7.

Experiment 2

Objective: To observe differences in model behavior due to differences in temporal resolution of the physical forcing data while holding the biological model information set constant.

Configuration: The *NEMURO*/1-D Yamanaka model with the biological model configured for station A7. This model was run with A7 physical forcing data on two temporal scales, daily averages and monthly averages.

Experiment 3

Objective: To compare the same bio-physical marine ecosystem model to two widely separated locations in the North Pacific using separate biological data and physical forcing data. This run provided an west (A7)-east (Station P) North Pacific comparison in model dynamics.

Configuration: The *NEMURO*/1-D Yamanaka model configured for specific geographic locations. This model was run with biological data and climatological physical forcing data (monthly averages) from station A7 and compared to a *NEMURO*/1-D Yamanaka model run with the Ocean Station P biological and climatological physical forcing data (monthly averages).

Experiment 4

Objective: To compare the same bio-physical marine ecosystem model to two widely separated locations in the North Pacific using separate biological data and physical forcing data. This run provided model dynamics for a western Pacific open ocean station (A7) to an enclosed sea North Pacific station (Bering Sea).

Configuration: The *NEMURO*/1-D Yamanaka model configured for specific geographic

locations. This model was run with biological data and climatological physical forcing data (monthly averages) from station A7 and compared to a *NEMURO*/1-D Yamanaka model run with the Bering Sea biological and climatological physical forcing data (monthly averages).

Experiment 5

Objective: To compare the same bio-physical marine ecosystem model to two widely separated locations in the North Pacific using separate biological data and physical forcing data. This run provided model dynamics for an eastern Pacific open ocean station (Ocean Station P) to an enclosed sea North Pacific station (Bering Sea).

Configuration: The *NEMURO*/1-D Yamanaka model configured for specific geographic locations. This model was run with biological data and climatological physical forcing data (monthly averages) from Ocean Station P and compared to a *NEMURO*/1-D Yamanaka model run with the Bering Sea biological and climatological physical forcing data (monthly averages).

Experiment 6

Objective: To compare the sensitivity of the biological processes equations to different physical forcing scenarios.

Configuration: The *NEMURO*/1-D Yamanaka model configured for station A7. This experiment was run with biological data from station A7 and climatological physical forcing data from station A7 and Ocean Station P.

Experiment 7

Objective: To compare the sensitivity of model's biological parameters to the same physical forcing scenario.

Configuration: The *NEMURO*/1-D Yamanaka model configured for station A7. This experiment was run with biological data from station A7 and Ocean Station P and climatological physical forcing data from station A7.

10.0 Recommendations

Results of the MODEL TASK TEAM work accomplished at the workshop results in several recommendations:

- Perform a sensitivity/stability analysis on *NEMURO*, and proceed to compare the structure and performance, and dynamic characteristics of the model.

- Test the sensitivity of production of small and large zooplankton, P/B ratio, and ecological efficiency to inclusion of the "Band-Aid" microbial food web. If model output is sensitive then implement a more complete description of the microbial food web.

- Develop a way to measure when a change in model output is "significant". The metric should consider time, space, and some absolute values of parameters.

- Future work should be coordinated by the MODEL Task Team Co-Chairmen and encouraged to present results at next annual meeting of PICES. Cooperation and coordination with other CCCC Task Teams is very important.

- Issues related to model management need to be addressed so as to better control the increasing number of different versions of a model, including process equations, parameter files, physical forcing data files, and post-processing programs. We propose to examine the ICES/GLOBEC experience to obtain guidance as to how best to proceed.

- Develop "*NEMURO*/Stella" Box Model using the Stella software package.
- Make progress on making an executable version of the prototype model available on the WWW.
- Develop a means of staying in contact to continue unfinished work.
- Develop a project home page.

11.0 Achievements and Future Steps

The achievements of the Workshop can be listed as follows:

1. Developed the prototype model, *NEMURO*
2. Developed executable models and preliminary outputs for
   2-1. *NEMURO*/FORTRAN Box Model
   2-2. *NEMURO*/1-D Yamanaka Model
   2-3. *NEMURO*/1-D Kishi Model
   2-4. *NEMURO*/MATLAB Model
3. Assembled forcing data files and parameter sets
   3-1. Daily Forcing/Sta. A/Sta. P
   3-2. Climatological Forcing/Sta. A/Sta. P /Bering Sea
   3-3. Parameter Sets/Sta. A/Sta. P/Bering Sea
4. Reviewed biological parameters and process equations
5. Developed tools for post analysis viewing of model output
6. Considered the microbial food web model and developed an implementation plan
7. Identified model experiment teams
   Compared to the goals and objectives of the workshop, the following activities must be undertaken:
   - Link with high trophic level model
     The model needs to include fishes, marine mammal, marine birds, and also micro-nekton.
   - Perform basic model validation studies
     Develop model validation protocols.
     Compare physical factors with direct observations.
     Compare model biomass predictions with direct observations.
   - Identify scientific questions for comparison
     Communication and cooperation with the REX and BASS Task Teams is needed
   - Perform listed experiments.
     It is important to identify a leader for each experiment and to encourage team activities. Dr. Kishi will contact participants of the Nemuro workshop by e-mail and will give a concrete task to each participant. The results of each team should be presented at the MODEL workshop at PICES IX in Hakodate.

12.0 Acknowledgements

This workshop was proposed and convened by PICES, more precisely the PICES/CCCC-IP/MODEL Task Team. On behalf of the workshop participants, the co-conveners would like to express sincere thanks for giving us a timely and valuable opportunity to participate in the development of a lower trophic level marine ecosystem model common among component programs of PICES GLOBEC Program. The Japan International Science and Technology Exchange Center, charged by Japan Science and Technology Agency for execution of the international workshop by Japan Science and Technology Promotion and Coordination Fund,

contributed the major part of financial support for this workshop. We note this valuable support, for without it, the workshop would have been very small. Nemuro was selected as the venue due in large part to the invitation from Nemuro Supporting Committee. The conveners, on behalf of all who attended the workshop, express their very deep appreciation for the warm welcome and perfect support arranged and given by Nemuro Supporting Committee, their staff, and the people of Nemuro city.

13.0 References

Cushing, D.H. 1989. A difference in structure between ecosystems in strongly stratified waters and those that are only weakly stratified. J. Plankton Res. 11:1-13.

Eppley, R.W. 1972. Temperature and phytoplankton growth in the sea. Fishery Bulletin, 70:1063-1085.

Eppley, R.W., R.W. Holmes,and J.D.H. Strickland. 1967. Sinking rates of marine phytoplankton measured with a fluorometer. J. Exp. Mar. Biol. Ecol. 1:191-208.

Fasham, M.J.R., Ducklow, H.W. and D.S. McKelvie. 1990. A nitrogen-based model of plankton dynamics in the oceanic mixed layer. Journal of Marine Research 48:591-639.

Hansen, P.J., P.K. Bjornsen and B.W. Hansen. 1997. Zooplankton grazing and growht: Scaling within the 2-2,000-um body size range. Limnology and Oceanography 42:687-704.

Harrison, W.G. 1980. Nutrient regeneration and primary production in the sea. In: Primary Productivity in the Sea, P. G. Falkowski, editor, Plenum Press, New York, pp 433-460.

Kishi, M. and H. Motono. 1999. An ecosystem model with zooplankton vertical migration focused on Oyashio region. Journal of Oceanography. (submitted)

Lomas, M.W., and P.M. Glibert. 1999. Temperature regulation of nitrate uptake: A novel hypothesis about nitrate uptake and reduction in cool-water diatoms. Limnology and Oceanography.

McManus, G.B. and W.T. Peterson. 1988. Bacterioplankton production in the nearshore zone during upwelling off central Chile. Mar. Ecol. Prog. Ser. 43:11-17.

Moloney, C.L. and J.G. Field. 1991. The size-based dynamics of plankton food webs. I. Description of a simulation model of carbon and nitrogen flows. J. Plank. Res. 13:1039-1092.

Magley, W.C. 1990. A phytoplankton-zooplankton model of the middle and outer Shelf domains of the southeast Bering Sea shelf during spring bloom conditions, Ph.D. dissertation, Florida State Univ., 293 p.

Nelson, D.M. and P. Treguer. 1992. Role of silicon as a limiting nutrient to Antarctic diatoms: evidence from kinetic studies in the Ross Sea ice-edge zone. Mar. Ecol. Prog. Ser. 80:255-264.

Niebauer, H.J., C.P. McRoy, and J.J. Goering. 1982a. April—June 1979, R/V T. G. Thompson cruise 138, legs 1--3, hydrographic (bottle) data. PROBES Data Report PDR 82-006, University of Alaska, Fairbanks, Alaska.

Niebauer, H.J., C.P. McRoy, and J.J. Goering. 1982b. March—June 1980, R/V T. G. Thompson cruise 149, legs 1--4, hydrographic (bottle) data. PROBES Data Report PDR 82-008, University of Alaska, Fairbanks, Alaska.

Niebauer, H.J., C.P. McRoy, and J.J. Goering. 1982c. April—July 1981 R/V T. G. Thompson cruise 159, legs 1-4, hydrographic (bottle) data. PROBES Data Report PDR 82-012, University of Alaska, Fairbanks, Alaska.

Niebauer, H.J., C.P. McRoy, and J.J. Goering. 1982d. Mixed layer depth calculations for 1978--1981, standard PROBES station

listings and silicate productivity addendum. PROBES Data Report PDR 82-013, University of Alaska, Fairbanks, Alaska.

Niebauer, J.H., C.P. McRoy, and J.J. Goering. 1982e. 1978—1980 R/V T. G. Thompson cruises TT131, TT138 and TT149 chlorophyll a data (addendum). PROBES Data Report PDR 82-010, University of Alaska, Fairbanks, Alaska.

Paasche, E. 1973. Silicon and the ecology of marine plankton diatoms. II. Silicate uptake kinetics I five diatom species. Marine biology 19:262-269.

Parsons, T.R., M. Takahashi, and B. Hargrave. 1984. Biological Oceanographic Processes (3rd Ed.). Pergamon Press, Oxford, 330pp.

Platt, T., C. Gallegos, and W.G. Harrison. 1980. Photoinhibition of photosynthesis in natural assemblages of marine phytoplankton. J. Mar. Res. 38(5):687-701.

Rivkin, R.B., J.N. Putland, M.R. Anderson and D. Deibel. 1999. Microzooplankton bacterivory in the NE subarctic Pacific. Deep-Sea Research II 46:2578-2618.

Steel, J.H. 1962. Environmental control of photosynthesis in the sea. Limnol. Oceanogr. 7:137-150.

Steele, J.H. 1998. Incorporating the microbial loop in a simple plankton model. Proc. R. Soc. Lond. B, Vol. 265, No. 1407:1771-1777.

Wroblewski, J.S. 1977. A model of phytoplankton plume formation during variable Oregon upwelling. J. Marine Research, 35:357-393.

Table 1 *NEMURO*/FORTRAN Box Model parameters for three regions of the North Pacific. Columns 1 (Simulation parameter set A7) and 2 (Station P) were used to generate Figure 5.
Small-Phytoplankton: PhyS, Large-Phytoplankton: PhyL, Small-Zooplankton: ZooS, Large-Zooplankton: ZooL, Predatory Zooplankton: ZooP

Parameter	*Description*	Simulation Parameter set A7	Station P	A7	Bering
alpha1	Light extinction coefficient of sea water	3.500E-04	4.000E-04	Same as P	Same as A7
alpha2	Light extinction coefficient of Phytoplankton self shading	2.810E+02	6.000E+02	Same as P	Same as A7
Int0	Light intensity of sea surface	8.000E-02	Same as Sim	Same as P	Same as A7
IoptS	Light intensity of optimum phytosynthesis by PhyS	7.000E-02	Same as Sim	Same as P	?
IoptL	Light intensity of optimum phytosynthesis by PhyL	7.000E-02	Same as Sim	Same as P	?
VmaxS	Maximum rate of photoshynthesis at 0 °C by PhyS	1.000E+00	5.000E-01	6.000E-01	7.200E-01
KNO3S	Half saturation constant for NO3 by PhyS	3.000E-06	Same as Sim	Same as P	6.000E-07
KNH4S	Half saturation constant for NH4 by PhyS	1.000E-06	1.000E-07	Same as P	6.000E-07
PusaiS	Ammonium inhibition coefficient by PhyS	1.500E+06	1.300E+06	Same as P	1.400E+06
KGppS	Temperature coefficient for photosynthesis by PhyS	6.930E-02	Same as Sim	Same as P	Same as A7
VmaxL	Maximum rate of photoshynthesis at 0 °C by PhyL	1.000E+00	2.000E-01	8.500E-01	1.100E+00
KNO3L	Half saturation constant for NO3 by PhyL	3.000E-06	Same as Sim	Same as P	2.500E-06
KNH4L	Half saturation constant for NH4 by PhyL	1.000E-06	1.300E-06	Same as P	2.500E-06
KSiL	Half saturation constant for Si(OH)4 by PhyL	3.000E-06	Same as Sim	Same as P	Same as A7
PusaiL	Ammonium inhibition coefficient by PhyL	1.500E+06	2.700E+06	Same as P	1.400E+06
KGppL	Temperature coefficient for photosynthesis by PhyL	6.930E-02	Same as Sim	Same as P	Same as A7
ResPS0	Respiration rate at 0 °C by PhyS	3.000E-02	Same as Sim	Same as P	Same as A7
KResPS	Temperature coefficient for respiration by PhyS	5.190E-02	6.930E-02	Same as P	Same as A7
ResPL0	Respiration rate at 0 °C by PhyL	3.000E-02	4.250E-02	Same as P	5.000E-02
KResPL	Temperature coefficient for respiration by PhyL	5.190E-02	6.930E-02	Same as P	Same as A7

Table 1 (Continued) *NEMURO*/FORTRAN Box Model parameters for three regions of the North Pacific. Columns 1 (Simulation parameter set A7) and 2 (Station P) were used to generate Figure 5.

Parameter	*Description*	Simulation Parameter set A7	Station P	A7	Bering
MorPS0	Mortality rate of PhyS at 0 °C	5.850E+04	5.000E+04	Same as P	Same as A7
KMorPS	Temperature coefficient for PhyS Mortality	6.930E-02	Same as Sim	Same as P	Same as A7
MorPL0	Mortality rate of PhyL at 0 °C	5.850E+04	5.000E+04	Same as P	Same as A7
KMorPL	Temperature coefficient for PhyL Mortality	6.930E-02	Same as Sim	Same as P	Same as A7
GammaS	Ratio of extracellular excretion to photosynthesis of PhyS	1.350E-01	Same as Sim	Same as P	Same as A7
GammaL	Ratio of extracellular excretion to photosynthesis of PhyL	1.350E-01	Same as Sim	Same as P	Same as A7
GRmaxSps	Maximum rate of grazing at 0 °C by PhyS to ZooS	4.000E-01	4.000E+00	1.000E+00	3.120E-01
GRmaxSpl	Maximum rate of grazing at 0 °C by PhyL to ZooS	0.000E+00	Same as Sim	2.000E-01	1.200E-01
KGraS	Temperature coefficient for grazing by ZooS	6.930E-02	Same as Sim	Same as P	Same as A7
LamS	ZooS Ivlev constant	1.400E+06	1.500E+06	Same as P	Same as A7
PS2ZSstar	Threshold value for grazing by ZooS	4.300E-08	4.000E-08	Same as P	Same as A7
GRmaxLps	Maximum rate of grazing at 0 °C by PhyS to ZooL	4.000E-01	1.000E-01	5.000E-02	2.160E-01
GRmaxLpl	Maximum rate of grazing at 0 °C by PhyL to ZooL	4.000E-01	2.000E-01	4.000E-01	2.160E-01
GRmaxLzs	Maximum rate of predation at 0 °C by ZooS to ZooL	4.000E-01	2.000E-01	1.000E-01	0.000E+00
KGraL	Temperature coefficient for grazing by ZooL	6.930E-02	Same as Sim	Same as P	Same as A7
LamL	ZooL Ivlev constant	1.400E+06	1.500E+06	Same as P	Same as A7
PL2ZLstar	Threshold value for grazing PhyL to ZooL	1.433E-08	4.000E-08	Same as P	Same as A7
PS2ZLstar	Threshold value for grazing PhyS to ZooL	1.433E-08	4.000E-08	Same as P	Same as A7
ZS2ZLstar	Threshold value for predation ZooS to ZooL	1.433E-08	4.000E-08	Same as P	Same as A7

Table 1 (continued) *NEMURO*/FORTRAN Box Model parameters for three regions of the North Pacific. Columns 1 (Simulation parameter set A7) and 2 (Station P) were used to generate Figure 5.

Parameter	*Description*	Simulation Parameter set A7	Station P	A7	Bering
GRmaxPpl	Maximum rate of grazing at 0 °C by PhyL to ZooP	4.000E-01	1.000E-01	Same as P	Same as A7
GRmaxPzs	Maximum rate of predation at 0 °C by ZooS to ZooP	4.000E-01	2.000E-01	Same as P	Same as A7
GRmaxPzl	Maximum rate of predation at 0 °C by ZooL to ZooP	4.000E-01	2.000E-01	Same as P	Same as A7
KGraP	Temperature coefficient for predation by ZooP	6.930E-02	Same as Sim	Same as P	Same as A7
LamP	ZooP Ivlev constant	1.400E+06	1.500E+06	Same as P	Same as A7
PL2ZPstar	Threshold value for grazing PhyL to ZooP	1.433E-08	4.000E-08	Same as P	Same as A7
ZS2ZPstar	Threshold value for predation ZooS to ZooP	1.433E-08	4.000E-08	Same as P	Same as A7
ZL2ZPstar	Threshold value for predation ZooL to ZooP	1.433E-08	4.000E-08	Same as P	Same as A7
PusaiPL	Grazing inhibition coefficient PhyL to ZooP	4.605E+06	Same as Sim	Same as P	Same as A7
PusaiZS	Grazing inhibition coefficient ZooS to ZooP	3.010E+06	Same as Sim	Same as P	Same as A7
AlphaZS	Assimilation efficiency of ZooS	7.000E-01	Same as Sim	Same as P	Same as A7
BetaZS	Growth efficiency of ZooS	3.000E-01	Same as Sim	Same as P	Same as A7
AlphaZL	Assimilation efficiency of ZooL	7.000E-01	Same as Sim	Same as P	Same as A7
BetaZL	Growth efficiency of ZooL	3.000E-01	Same as Sim	Same as P	Same as A7
AlphaZP	Assimilation efficiency of ZooP	7.000E-01	Same as Sim	Same as P	Same as A7
BetaZP	Growth efficiency of ZooP	3.000E-01	Same as Sim	Same as P	Same as A7
MorZS0	Mortality rate of ZooS at 0 °C	5.850E+04	5.000E+04	Same as P	Same as A7
KMorZS	Temperature coefficient for ZooS mortality	6.930E-02	Same as Sim	Same as P	Same as A7
MorZL0	Mortality rate of ZooL at 0 °C	5.850E+04	5.000E+04	Same as P	Same as A7
KMorZL	Temperature coefficient for ZooL mortality	6.930E-02	Same as Sim	Same as P	Same as A7
MorZP0	Mortality rate of ZooP at 0 °C	5.850E+04	5.000E+04	Same as P	Same as A7
KMorZP	Temperature coefficient for ZooP mortality	6.930E-02	Same as Sim	Same as P	Same as A7

Table 1 (continued) *NEMURO*/FORTRAN Box Model parameters for three regions of the North Pacific. Columns 1 (Simulation parameter set A7) and 2 (Station P) were used to generate Figure 5.

Parameter	*Description*	Simulation Parameter set A7	Station P	A7	Bering
VP2N0	Remineralization rate at 0 °C (PON-NH4)	5.000E-02	2.200E-02	Same as P	Same as A7
KP2N	Temp. coefficient for Remineralization (PON-NH4)	6.930E-02	3.000E-02	Same as P	Same as A7
VP2D0	Decomposition rate at 0 °C (PON-DON)	5.000E-02	2.200E-02	Same as P	Same as A7
KP2D	Temp. coefficient for decomposition (PON-DON)	6.930E-02	3.000E-02	Same as P	Same as A7
VD2N0	Remineralization rate at 0 °C (DON-NH4)	5.000E-02	2.200E-02	Same as P	Same as A7
KD2N	Temp. coefficient for Remineralization (DON-NH4)	6.930E-02	3.000E-02	Same as P	Same as A7
VO2S0	Remineralization rate at 0 °C (Opal-Si(OH)4)	5.000E-03	5.000E-03	Same as P	Same as A7
KO2S	Temp. coefficient for Remineralization (Opal-Si(OH)4)	6.930E-02	6.930E-02	Same as P	Same as A7
Nit0	Nitrification rate at 0 °C	3.000E-02	1.000E-01	Same as P	Same as A7
Knit	Temp. coefficient for Nitrification	6.930E-02	Same as Sim	Same as P	Same as A7
RSiNPL	Si/N Ratio of PhyL	1.000E+00	Same as Sim	Same as P	Same as A7
RCN	C/N Ratio	6.625E+00	Same as Sim	Same as P	Same as A7
setVP	Sinking rate of PON	5.000E+01	Same as Sim	Same as P	Same as A7
setVO	Sinking rate of Opal	1.000E+02	Same as Sim	Same as P	Same as A7
setVC	Sinking rate of CaCO3	1.000E+02	Same as Sim	Same as P	Same as A7

Table 1 (continued) *NEMURO*/FORTRAN Box Model parameters for three regions of the North Pacific. Columns 1 (Simulation parameter set A7) and 2 (Station P) were used to generate Figure 5.

Parameter	*Description*	Simulation Parameter set A7	Station P	A7	Bering
Box, model parameters					
Vsedn	Sinking rate of PON	1.000E+03	Same as Sim		
Vsedsi	Sinking rate of Opal	1.000E+04	Same as Sim		
TMP	Water temperature	1.300E+01	Same as Sim		
Lzmax	Depth of euphotic layer	1.000E+04	Same as Sim		
ExUP	Exchange coefficient	3.000E-03	Same as Sim		
NO3D	Conc. of Nitrate at under euphotic layer	1.000E-05	Same as Sim		
SiOH4D	Conc. of Silicate at under euphotic layer	1.000E-05	Same as Sim		

Table 2 *NEMURO*/FORTRAN Box Model Equations for an 11 state variable model differential equations. Process equations are indexed to flux arrows in Figure 2.

Nitrogen

$$\frac{dPhySn}{dt} = GppPSn - ResPSn - MorPSn - ExcPSn - GraPS2ZSn - GraPS2ZLn$$

$$\frac{dPhyLn}{dt} = GppPLn - ResPLn - MorPLn - ExcPLn - GraPL2ZLn - GraPL2ZPn$$

$$\frac{dZooSn}{dt} = GraPS2ZSn - GraZS2ZLn - GraZS2ZPn - MorZSn - ExcZSn - EgeZSn$$

$$\frac{dZooLn}{dt} = GraPS2ZLn + GraPL2ZLn + GraZS2ZLn - GraZL2ZPn - MorZLn - ExcZLn - EgeZLn$$

$$\frac{dZooPn}{dt} = GraPL2ZPn + GraZS2ZPn + GraZL2ZPn - MorZPn - ExcZPn - EgeZPn$$

$$\frac{dNO_3}{dt} = -(GppPSn - ResPSn)RnewS - (GppPLn - ResPLn)RnewL + Nit + UPWn$$

$$\frac{dNH_4}{dt} = -(GppPSn - ResPSn)(1 - RnewS) - (GppPLn - ResPLn)(1 - RnewL) - Nit + DecP2Nn + DecD2Nn + ExcZSn + ExcZLn + ExcZPn$$

$$\frac{dPON}{dt} = MorPSn + MorPLn + MorZSn + MorZLn + MorZPn + EgeZSn + EgeZLn + EgeZPn - DecP2Nn - DecP2Dn - SEDn$$

$$\frac{dDON}{dt} = ExcPSn + ExcPLn + DecP2Dn - DecD2Nn$$

Silicon

$$\frac{dPhyLsi}{dt} = GppPLsi - ResPLsi - MorPLsi - ExcPLi - GraPL2ZLsi - GraPL2ZPsi$$

$$\frac{dZooLsi}{dt} = GraPL2ZLsi - EgeZLsi$$

$$\frac{dZooPsi}{dt} = GraPL2ZPsi - EgeZPsi$$

$$\frac{dSi(OH)_4}{dt} = -GppPLsi + ResPLsi + ExcPLsi + UPWsi + DecP2Si$$

$$\frac{dOpal}{dt} = MorPLsi + EgeZLsi + EgeZPsi - SEDsi - DecP2Si$$

$$\frac{dOpal}{dt} = MorPLsi + EgeZLsi + EgeZPsi - SEDsi - DecP2Si$$

PhySn:	Small-Phytoplankton Biomass	(ìmolN/l)
PhyLn:	Large-Phytoplankton Biomass	(ìmolN/l)
ZooSn:	Small-Zooplankton Biomass	(ìmolN/l)
ZooLn:	Large-Zooplankton Biomass	(ìmolN/l)
ZooPn:	Predator-Zooplankton Biomass	(ìmolN/l)
NO3:	Nitrate concentration	(ìmolN/l)
NH4:	Ammonium concentration	(ìmolN/l)
PON:	Particulate Organic Nitrogen concentration	(ìmolN/l)
DON:	Dissolved Organic Nitrogen concentration	(ìmolN/l)
PhyLsi:	Large-Phytoplankton Biomass	(ìmolSi/l)
ZooLsi:	Large-Zooplankton Biomass	(ìmolSi/l)=0
ZooPsi:	Predator-Zooplankton Biomass	(ìmolSi/l)=0
Si(OH)4:	Silicate concentration	(ìmolSi/l)
Opal:	Particulate Organic Silica concentration	(ìmolSi/l)

Process Equations

Nitrogen

1. ***GppPSn*:** Gross Primary Production rate of Small-Phytoplankton (ìmolN/l/day)

$$GppPSn = V\max S * \left(\frac{NO_3}{NO_3 + K_{NO3S}} \exp(-Ø_S * NH_4) + \frac{NH_4}{NH_4 + K_{NH4S}} \right) * \exp(kGpp_S * TMP) * \int_{-H}^{0} \frac{I}{I_{optS}} \exp\left(1 - \frac{I}{I_{optS}}\right) dz * PhySn$$

$$I = I_0 \exp(-k|Z|)$$

$$k = a_1 + a_2(PhySn + PhyLn)$$

***RnewS*:** f-ratio of Small-Phytoplankton (No dimension)

$$RnewS = \frac{\frac{NO_3}{NO_3 + K_{NO3S}} \exp(-Ø_S * NH_4)}{\frac{NO_3}{NO_3 + K_{NO3S}} \exp(-Ø_S * NH_4) + \frac{NH_4}{NH_4 + K_{NH4S}}}$$

2. ***GppPLn*:** Gross Primary Production rate of Large-Phytoplankton (ìmolN/l/day)

$$GppPLn = V\max L * \min\ \frac{NO_3}{NO_3 + K_{NO3L}}\exp(-\ _L * NH_4) + \frac{NH_4}{NH_4 + K_{NH4L}}, \frac{Si(OH)_4}{Si(OH)_4 + K_{SiL}} / (Si/N)_{pl}$$

$$* \exp(kGpp_L * TMP) * \int_{-H}^{0} \frac{I}{I_{optL}} \exp\left(1 - \frac{I}{I_{optL}}\right) dz * PhyLn$$

$$I = I_0 \exp(-k|Z|)$$

$$k = a_1 + a_2(PhySn + PhyLn)$$

RnewL: f-ratio of Large-Phytoplankton (No dimension)

$$RnewL = \frac{\frac{NO_3}{NO_3 + K_{NO3L}}\exp(-\Psi_L * NH_4)}{\frac{NO_3}{NO_3 + K_{NO3L}}\exp(-\Psi_L * NH_4) + \frac{NH_4}{NH_4 + K_{NH4L}}}$$

3. ***ResPSn*:** Respiration rate of small-phytoplankton (ìmolN/l/day)
   ResPSn = Res_{PS0} * exp(K_{ResPS} * TMP) * PhySn

4. ***ResPLn*:** Respiration rate of large-phytoplankton (ìmolN/l/day)
   $ResPLn = Res_{PL0} * exp(K_{ResPL} * TMP) * PhyLn$

5. ***MorPSn*:** Mortality rate of small-phytoplankton (ìmolN/l/day)
   $MorPSn = Mor_{PS0} * exp(K_{MorPS} * TMP) * PhySn^2$

6. ***MorPLn*:** Mortality rate of large-phytoplankton (ìmolN/l/day)
   $MorPLn = Mor_{PL0} * exp(K_{MorPL} * TMP) * PhyLn^2$

7. ***ExcPSn*:** Extracellular Excretion rate of small-phytoplankton (ìmolN/l/day)
   ExcPSn = GammaS * GppPSn

8. ***ExcPLn*:** Extracellular Excretion rate of large-phytoplankton (ìmolN/l/day)
   ExcPLn = GammaL * GppPLn

9. ***GraPS2ZSn*:** Grazing rate of small-phytoplankton to small-zooplankton (ìmolN/l/day)

$$GraPS2ZSn = \text{Max}\left[0, GR\max S * \exp(k_{GraS} * TMP) * \left\{1 - \exp(\ _S * (PS2ZS^* - PhySn))\right\} * ZooSn\right]$$

$$GraPS2ZLn = \text{Max}\left[0, GR\max L_{ps} * \exp(k_{GraL} * TMP) * \left\{1 - \exp(\ _L * (PS2ZL^* - PhySn))\right\} * ZooLn\right]$$

10. ***GraPS2ZLn*:** Grazing rate of small-phytoplankton to large-zooplankton (ìmolN/l/day)

11. ***GraPL2ZLn*:** Grazing rate of large-phytoplankton to large-zooplankton (ìmolN/l/day)

$$GraPL2ZLn = \text{Max}\left[0, GR\max L_{pl} * \exp(k_{GraL}T) * \left\{1 - \exp(\ _L(PL2ZL^* - PhyLn))\right\} * ZooLn\right]$$

12. ***GraZS2ZLn*:** Grazing rate of small-zooplankton to large-zooplankton (ìmolN/l/day)

$$GraZS2ZLn = \text{Max}\left[0, GR\max L_{zs} * \exp(k_{GraL}T) * \left\{1 - \exp(\ _L(ZS2ZL^* - ZooSn))\right\} * ZooLn\right]$$

13. ***GraPL2ZPn*:** Grazing rate of large-phytoplankton to predator-zooplankton (ìmolN/l/day)

$$GraPL2ZPn = \mathrm{Max}\begin{bmatrix} 0, GR\max P_{pl} * \exp(k_{GraP} * TMP) * \{1 - \exp(\ddot{e}_P * (PL2ZP^* - PhyLn))\} \\ * \exp(-Ø_{PL} * (ZooLn + ZooSn)) * ZooPn \end{bmatrix}$$

14. ***GraZS2ZPn*:** Grazing rate of small-zooplankton to predator-zooplankton (ìmolN/l/day)

$$GraZS2ZPn = \mathrm{Max}\begin{bmatrix} 0, GR\max P_{zs} * \exp(k_{GraP} * TMP) * \{1 - \exp(\ddot{e}_P (ZS2ZP^* - ZooSn))\} \\ * \exp(-Ø_{ZS} * ZooLn) * ZooPn \end{bmatrix}$$

15. ***GraZL2ZPn*:** Grazing rate of large-zooplankton to predator-zooplankton (ìmolN/l/day)

$$GraZL2ZPn = \mathrm{Max}\left[0, GR\max P_{zl} * \exp(k_{GraP} * TMP) * \{1 - \exp(\ _P(ZL2ZP^* - ZooLn))\} * ZooPn\right]$$

***BetaZS* :** Growth efficiency of small-zooplankton (No dimension)

$Beta_{ZS} = 0.3 \wedge (1 + PhySn / (PhySn + PhyLn))$

16. ***ExcZSn*:** Excretion rate of small-zooplankton (ìmolN/l/day)

$ExcZSn = (Alpha_{ZS} - Beta_{ZS}) * GraPS2ZSn$

17. ***ExcZLn*:** Excretion rate of large-zooplankton (ìmolN/l/day)

$ExcZLn = (Alpha_{ZL} - Beta_{ZL}) * (GraPL2ZLn + GraZS2ZLn + GraPS2ZLn)$

18. ***ExcZPn*:** Excretion rate of predator-zooplankton (ìmolN/l/day)

$ExcZPn = (Alpha_{ZP} - Beta_{ZP}) * (GraPL2ZPn + GraZS2ZPn + GraZL2ZPn)$

19. ***EgeZSn*:** Egestion rate of small-zooplankton (ìmolN/l/day)

$EgeZSn = (1.0 - Alpha_{ZS}) * GraPS2ZSn$

20. ***EgeZLn*:** Egestion rate of large-zooplankton (ìmolN/l/day)

$EgeZLn = (1.0 - Alpha_{ZL}) * (GraPL2ZLn + GraZS2ZLn + GraPS2ZLn)$

21. ***EgeZPn*:** Egestion rate of predator-zooplankton (ìmolN/l/day)

$EgeZPn = (1.0 - Alpha_{ZP}) * (GraPL2ZPn + GraZS2ZPn + GraZL2ZPn)$

22. ***MorZSn*:** Mortality rate of small-zooplankton (ìmolN/l/day)

$MorZSn = Mor_{ZS0} * exp(K_{MorZS} * TMP) * ZooSn^2$

23. ***MorZLn*:** Mortality rate of large-zooplankton (ìmolN/l/day)

$MorZLn = Mor_{ZL0} * \exp(K_{MorZL} * TMP) * ZooLn^2$

24. ***MorZPn*:** Mortality rate of predator -zooplankton (ìmolN/l/day)

$MorZPn = Mor_{ZP0} * \exp(K_{MorZP} * TMP) * ZooPn^2$

25. ***DecP2N*:** Decomposition rate from PON to NH_4 (ìmolN/l/day)

$DecP2N = VP2N_0 * exp(K_{P2N} * TMP) * PON$

26. ***DecP2D*:** Decomposition rate from PON to DON (ìmolN/l/day)

$DecP2D = VP2D_0 * exp(K_{P2D} * TMP) * PON$

27. ***DecD2N*:** Decomposition rate from DON to NH_4 (ìmolN/l/day)
    *DecD2N = $VD2N_0$ * exp(K_{D2N} * TMP) * DON*

28. ***Nit:*** Nitrification rate (ìmolN/l/day)
    *Nit = Nit_0 * exp(K_{Nit} * TMP) * NH4*

29. ***SEDn:*** Sedimentation rate of PON (ìmolN/l/day)
    SEDn = Vsedn / H * PON

30. ***UPWn:*** Upwelling rate of NO_3 (ìmolN/l/day)
    *UPWn = ExUP * (NO3D - NO3)*

Silicon

2. ***GppPLsi:*** Gross Primary Production rate of large-phytoplankton (ìmolSi/l/day)
    *GppPLsi = GppPLn * RSiNPL*

4. ***ResPLsi:*** Respiration rate of large-phytoplankton (ìmolSi/l/day)
    *ResPLsi = ResPLn * RSiNPL*

6. ***MorPLsi:*** Mortality rate of large-phytoplankton (ìmolSi/l/day)
    *MorPLsi = MorPLn * RSiNPL*

8. ***ExcPLsi:*** Extracellular Excretion rate of large-phytoplankton (ìmolSi/l/day)
    *ExcPLsi = ExcPLn * RSiNPL*

11. ***GraPL2Zlsi:*** Grazing rate of large-phytoplankton to large-zooplankton (ìmolSi/l/day)
    *GraPL2ZLsi = GraPL2ZLn * RSiNPL*

13. ***GraPL2ZPsi:*** Grazing rate of large-phytoplankton to predator-zooplankton (ìmolSi/l/day)
    *GraPL2ZLsi = GraPL2ZLn * RSiNPL*

20. ***EgeZLsi:*** Egestion rate of large-zooplankton (ìmolSi/l/day)
    EgeZLsi = GraPL2ZLsi

29. ***SEDsi:*** Sedimentation rate of Opal (ìmolSi/l/day)
    *SEDsi = Vsedsi / H * Opal*

30. ***UPWsi:*** Upwelling rate of Si(OH)4 (ìmolSi/l/day)
    *UPWsi = ExUP * (SiOH4D - SiOH4)*

31. ***EgeZPsi:*** Egestion rate of predator-zooplankton (ìmolSi/l/day)
    EgeZPsi = GraPL2Zpsi

32. ***DecP2Si*:** Decomposition rate from Opal to $Si(OH)_4$ (ìmolSi/l/day)
    *DecP2Si = $VP2Si_0$ * exp(K_{P2Si} * TMP) * Opal*

Table 3 NEMURO/MATLAB 15 Compartment Box model equations.

Differential Equations

Nitrogen

$$\frac{dPhySn}{dt} = GppPSn - ResPSn - MorPSn - ExcPSn - GraPS2ZSn - GraPS2ZLn$$

$$\frac{dPhyLn}{dt} = GppPLn - ResPLn - MorPLn - ExcPLn - GraPL2ZSn - GraPL2ZLn - GraPL2ZPn$$

$$\frac{dZooSn}{dt} = GraPS2ZSn + GraPL2ZSn - GraZS2ZLn - GraZS2ZPn - MorZSn - ExcZSn - EgeZSn$$

$$\frac{dZooLn}{dt} = GraPS2ZLn + GraPL2ZLn + GraZS2ZLn - GraZL2ZPn - MorZLn - ExcZLn - EgeZLn$$

$$\frac{dZooPn}{dt} = GraPL2ZPn + GraZS2ZPn + GraZL2ZPn - MorZPn - ExcZPn - EgeZPn$$

$$\frac{dNO_3}{dt} = -(GppPSn - ResPSn)RnewS - (GppPLn - ResPLn)RnewL + Nit + UPWn$$

$$\frac{dNH_4}{dt} = -(GppPSn - ResPSn)(1 - RnewS) - (GppPLn - ResPLn)(1 - RnewL) - Nit + DecP2Nn + DecD2Nn + ExcZSn + ExcZLn + ExcZPn$$

$$\frac{dPON}{dt} = MorPSn + MorPLn + MorZSn + MorZLn + EgeZSn + EgeZLn - DecP2Nn - DecP2Dn - SEDn$$

$$\frac{dDON}{dt} = ExcPSn + ExcPLn + DecP2Dn - DecD2Nn$$

$$\frac{dDeepNO_3}{dt} = -UPWn$$

$$\frac{dDeepPON}{dt} = SEDn$$

Silicon

$$\frac{dSiOH_4}{dt} = \left(-GppPLn + ResPLn + ExcPLn\right) \quad RSiNPL + UPWsi + DecP2Si$$

$$\frac{dOpal}{dt} = \left(MorPLn + EgeZLn\right) \quad RSiNPL - SEDsi - DecP2Si$$

$$\frac{dDeepSiOH_4}{dt} = -UPWsi$$

$$\frac{dDeepOpal}{dt} = SEDsi$$

PhySn:	Small-Phytoplankton Biomass	(mmolN/l)
PhyLn:	Large-Phytoplankton Biomass	(mmolN/l)
ZooSn:	Small-Zooplankton Biomass	(mmolN/l)
ZooLn:	Large-Zooplankton Biomass	(mmolN/l)
ZooPn:	Predator-Zooplankton Biomass	(mmolN/l)
NO3:	Nitrate concentration	(mmolN/l)
NH4:	Ammonium concentration	(mmolN/l)
PON:	Particulate Organic Nitrogen concentration	(mmolN/l)
DON:	Dissolved Organic Nitrogen concentration	(mmolN/l)
DeepNO3:	Nitrate concentration	(mmolN/l)
DeepPON:	Particulate Organic Nitrogen concentration	(mmolN/l)
SiOH4:	Silicate concentration	(mmolSi/l)
Opal:	Particulate Organic Silica concentration	(mmolSi/l)
DeepSiOH4:	Silicate concentration	(mmolSi/l)
DeepOpal:	Particulate Organic Silica concentration	(mmolSi/l)

Equations of Each Process

Nitrogen

1. ***GppPSn*** **:** Gross Primary Production rate of Small-Phytoplankton (mmolN/l/day)

$$GppPSn = V\max S * \frac{NO_3}{NO_3 + K_{NO3S}} \exp(-\ _S * NH_4) + \frac{NH_4}{NH_4 + K_{NH4S}} * \exp(kGpp_S * TMP) * PhySn$$

TMP: Water temperature (Celcius)

LIGHT: Relative photosynthetic efficiency (unitless). Ranges seasonally from 0.2 to 0.8, decreases due to light limitation. Use second formulation to include diurnal variability.

$$LIGHT = 0.2 + 0.6\left(0.5(1 - \cos(2pt / 365))\right)$$

For diurnal variability:

$$LIGHT = \left[0.2 + 0.6\left(0.5(1 - \cos(2pt / 365))\right)\right] \quad \max\left(0, \cos(2pt)\right)$$

RnewS**:** f-ratio of Small-Phytoplankton (Non-dimensional)

$$RnewS = \frac{\frac{NO_3}{NO_3 + K_{NO3S}} \exp(-\Psi_S * NH_4)}{\frac{NO_3}{NO_3 + K_{NO3S}} \exp(-\Psi_S * NH_4) + \frac{NH_4}{NH_4 + K_{NH4S}}}$$

2. ***GppPLn* :** Gross Primary Production rate of Large-Phytoplankton (mmolN/l/day)

$$GppPLn = V\max L * \min\left(\frac{NO_3}{NO_3 + K_{NO3L}}\exp(-\Psi_L * NH_4) + \frac{NH_4}{NH_4 + K_{NH4L}}, \frac{Si(OH)_4}{Si(OH)_4 + K_{SiL}}\right) / \left(Si/N\right)_{pl} * \exp(kGpp_L * TMP) * LIGHT$$

RnewL: f-ratio of Large-Phytoplankton (Non-dimensional

$$RnewL = \frac{\frac{NO_3}{NO_3 + K_{NO3L}}\exp(-\Psi_L * NH_4)}{\frac{NO_3}{NO_3 + K_{NO3L}}\exp(-\Psi_L * NH_4) + \frac{NH_4}{NH_4 + K_{NH4L}}}$$

3. ***ResPSn*:** Respiration rate of small-phytoplankton (mmolN/l/day)
   ResPSn = Res_{PS0} * exp(K_{ResPS} * TMP) * PhySn

4. ***ResPLn*:** Respiration rate of large-phytoplankton (mmolN/l/day)
   $ResPLn = Res_{PL0} * exp(K_{ResPL} * TMP) * PhyLn$

5. ***MorPSn*:** Mortality rate of small-phytoplankton (mmolN/l/day)
   $MorPSn = Mor_{PS0} * exp(K_{MorPS} * TMP) * PhySn^2$ First order mortality
   $MorPSn = Mor_{PS0} * exp(K_{MorPS} * TMP) * PhySn^2$ Second order mortality, **not used.**

6. ***MorPLn*:** Mortality rate of large-phytoplankton (mmolN/l/day)
   $MorPLn = Mor_{PL0} * exp(K_{MorPL} * TMP) * PhyLn$ First order mortality
   $MorPLn = Mor_{PL0} * exp(K_{MorPL} * TMP) * PhyLn^2$ Second order mortality, **not used.**

7. ***ExcPSn*:** Extracellular Excretion rate of small-phytoplankton (mmolN/l/day)
   ExcPSn = GammaS * GppPSn

8. ***ExcPLn*:** Extracellular Excretion rate of large-phytoplankton (mmolN/l/day)
   ExcPLn = GammaL * GppPLn

9. ***GraPS2ZSn*:** Grazing rate of small-phytoplankton to small-zooplankton (mmolN/l/day)

$$GraPS2ZSn = \text{Max}\left[0, GR\max S * \exp(k_{GraS} * TMP) * \left\{1 - \exp(\ _S * (PS2ZS^* - PhySn))\right\} * ZooSn\right]$$

9-2. ***GraPS2ZLn*:** Grazing rate of small-phytoplankton to large-zooplankton (mmolN/l/day)

$$GraPS2ZLn = \text{Max}\left[0, GR\max L_{ps} * \exp(k_{GraL} * TMP) * \left\{1 - \exp(\ _L * (PS2ZL^* - PhySn))\right\} * ZooLn\right]$$

$$GraPL2ZLn = \text{Max}\left[0, GR\max L_{pl} * \exp(k_{GraL} T) * \left\{1 - \exp(\ _L (PL2ZL^* - PhyLn))\right\} * ZooLn\right]$$

10. ***GraPL2ZLn*:** Grazing rate of large-phytoplankton to large-zooplankton (mmolN/l/day)

10-2. ***GraPL2ZSn*:** Grazing rate of large-phytoplankton to small-zooplankton (mmolN/l/day)

$$GraPL2ZSn = \text{Max}\left[0, GR\max S_{pl} * \exp(k_{GraS} T) * \left\{1 - \exp(\ _L (PL2ZS^* - PhyLn))\right\} * ZooSn\right]$$

11. ***GraZS2ZLn*:** Grazing rate of small-zooplankton to large-zooplankton (mmolN/l/day)

$$GraZS2ZLn = \mathrm{Max}\left[0, GR\max L_{zs} * \exp(k_{GraL}T) * \left\{1 - \exp(\ {}_{L}(ZS2ZL^{*} - ZooSn))\ \right\} * ZooLn\right]$$

11-2. ***GraPL2ZPn*:** Grazing rate of large-phytoplankton to predator-zooplankton (mmolN/l/day)

$$GraPL2ZPn = \mathrm{Max}\left[\begin{matrix} 0, GR\max P_{pl} * \exp(k_{GraP} * TMP) * \left\{1 - \exp(\ddot{e}_{P} * (PL2ZP^{*} - PhyLn))\right\} \\ * \exp(\ -\emptyset_{PL} * (ZooLn + ZooSn)\ ) * ZooPn \end{matrix}\right]$$

11-3. ***GraZS2ZPn*:** Grazing rate of small-zooplankton to predator-zooplankton (mmolN/l/day)

$$GraZS2ZPn = \mathrm{Max}\left[\begin{matrix} 0, GR\max P_{zs} * \exp(k_{GraP} * TMP) * \left\{1 - \exp(\ddot{e}_{P}(ZS2ZP^{*} - ZooSn))\right\} \\ * \exp(\ -\emptyset_{ZS} * ZooLn\ ) * ZooPn \end{matrix}\right]$$

11-4. ***GraZL2ZPn*:** Grazing rate of large-zooplankton to predator-zooplankton (mmolN/l/day)

$$GraZL2ZPn = \mathrm{Max}\left[0, GR\max P_{zl} * \exp(k_{GraP} * TMP) * \left\{1 - \exp(\ {}_{P}(ZL2ZP^{*} - ZooLn))\right\} * ZooPn\right]$$

***BetaZS* :** Growth efficiency of small-zooplankton (Nodim)
$Beta_{ZS} = 0.3\ \hat{}\ (\ 1 + PhySn\ /\ (\ PhySn + PhyLn\ )\ )$

12. ***ExcZSn*:** Excretion rate of small-zooplankton (mmolN/l/day)
ExcZSn = ($Alpha_{ZS}$ - $Beta_{ZS}$) * GraPS2ZSn

13. ***ExcZLn*:** Excretion rate of large-zooplankton (mmolN/l/day)
$ExcZLn = (\ Alpha_{ZL} - Beta_{ZL})\ *\ (\ GraPL2ZLn + GraZS2ZLn + GraPS2ZLn\ )$

13-2. ***ExcZPn*:** Excretion rate of predator-zooplankton (mmolN/l/day)
$ExcZPn = (\ Alpha_{ZP} - Beta_{ZP}\ )\ *\ (\ GraPL2ZPn + GraZS2ZPn + GraZL2ZPn\ )$

14. ***EgeZSn*:** Egestion rate of small-zooplankton (mmolN/l/day)
EgeZSn = (1.0 - $Alpha_{ZS}$) * GraPS2ZSn

15. ***EgeZLn*:** Egestion rate of large-zooplankton (mmolN/l/day)
$EgeZLn = (\ 1.0 - Alpha_{ZL})\ *\ (\ GraPL2ZLn + GraZS2ZLn + GraPS2ZLn\ )$

15-2. ***EgeZPn*:** Egestion rate of predator-zooplankton (mmolN/l/day)
$EgeZPn = (\ 1.0 - Alpha_{ZP}\ )\ *\ (\ GraPL2ZPn + GraZS2ZPn + GraZL2ZPn\ )$

16. ***MorZSn*:** Mortality rate of small-zooplankton (mmolN/l/day)
$MorZSn = Mor_{ZS0} * exp(\ K_{MorZS} * TMP\ ) * ZooSn^{2}$

17. ***MorZLn*:** Mortality rate of large-zooplankton (mmolN/l/day)
MorZLn = Mor_{ZL0} * exp(K_{MorZL} * TMP) * $ZooLn^{2}$

17-2. ***MorZPn*:** Mortality rate of predator -zooplankton (mmolN/l/day)
MorZPn = Mor_{ZP0} * exp(K_{MorZP} * TMP) *$ZooPn^{2}$

18. ***DecP2N*:** Decomposition rate from PON to NH_4 (mmolN/l/day)
$DecP2N = VP2N_{0} * exp(\ K_{P2N} * TMP\ ) * PON$

19. ***DecP2D*:** Decomposition rate from PON to DON (mmolN/l/day)
    $DecP2D = VP2D_0 * exp(K_{P2D} * TMP) * PON$

20. ***DecD2N*:** Decomposition rate from DON to NH_4 (mmolN/l/day)
    $DecD2N = VD2N_0 * exp(K_{D2N} * TMP) * DON$

21. ***Nit:*** Nitrification rate (mmolN/l/day)
    $Nit = Nit_0 * exp(K_{Nit} * TMP) * NH4$

22. ***SEDn:*** Sedimentation rate of PON (mmolN/l/day)
    SEDn = Vsedn / H * PON

23. ***UPWn:*** Upwelling rate of NO_3 (mmolN/l/day)
    *UPWn = ExUP * (NO3D - NO3)*

Silicon

22. ***SEDSi:*** Sedimentation rate of Opal (mmolSi/l/day)
    *SEDSi = Vsedsi / H * Opal*

23. ***UPWSi:*** Upwelling rate of Si(OH)4 (mmolSi/l/day)
    *UPWSi = ExUP * (SiOH4D - SiOH4)*

25. ***DecP2Si*:** Decomposition rate from Opal to $Si(OH)_4$ (mmolSi/l/day)
    $DecP2Si = VP2Si_0 * exp(K_{P2Si} * TMP) * Opal$

Table 4 *NEMURO*/MATLAB parameter values for 3 geographic regions of the North Pacific.

			Station P			A(7)			Bering		
		Unit	**Value**	**Remark**	**Range**	**Value**	**Remark**	**Range**	**Value**	**Remark**	**Range**
V_{maxS}	Small Phytoplankton Maximum Photosynthetic Rate at 0 ºC	1/day	1.000		0.3 - 1	0.6	0.6 Vmax*e^(ksT)<2.0 0.85 (Eppely's 1977)	0.3 - 0.85	0.72	Epply, 77	
Ψ_S	Small Phytoplankton Ammonium Inhibition Coefficient	l/ìmol	1.300	1.3 Lomas&Gilbert, 1996; 1.4 Wroblewski, 1977		Same as P			1.4	Wroblewski	
K_{no3S}	Small Phytoplankton Half Saturation Constant for nitrate	ìmol/l	3.000	4.21 Parsons et al., 1984	1-5?	Same as P			0.6	PROBES data	
K_{nh4S}	Small Phytoplankton Half Saturation Constant for ammonium	ìmol/l	0.100	1.3 Parsons et al. 1984 0.05 ref Saito?	0.05 - 1.3	Same as P			0.6	PROBES data	
K_{SiS}	Small Phytoplankton Half Saturation Constant for silicate	ìmol/l	0.000	No Si uptake		Same as P			Same as A(7)		
κ_S	Small Phytoplankton Temperature Coefficient for Photosynthetic Rate	1/deg. C	0.069	Q10 = 2.0	1.5<Q10<2.5 ?	Same as P			Same as A(7)		
I_{optS}	Small Phytoplankton Optimum Light Intensity	ly/min	0.070	20-500 uE/m2/s Ref Saito?		Same as P			?	3.25 with Platt et all formulation	
V_{maxL}	Large Phytoplankton Maximum Photosynthetic Rate at 0 ºC	1/day	1.000		0.3 - 1	0.85	0.6 Vmax*e^(ksT)<2.0 0.85 (Eppely's 1977); 0.5 @ ?T, MF,1989	0.3 - 0.85	1.1	PROBES data	
Ψ_L	Large Phytoplankton Ammonium Inhibition Coefficient	l/ìmol	2.700	2.7 Lomas&Gilbert, 1996; 1.4 Wroblewski, 1977		Same as P			1.4	Wroblewski	

Table 4 (continued) *NEMURO*/MATLAB parameter values for 3 geographic regions of the North Pacific.

			Station P			A(7)			Bering		
		Unit	**Value**	**Remark**	**Range**	**Value**	**Remark**	**Range**	**Value**	**Remark**	**Range**
K_{no3L}	Large Phytoplankton Half Saturation Constant for nitrate	ìmol/l	3.000	3.8 MF, 1991, 0.4 - 5.1 Parsons et al.	.4 - 5.1	Same as P			2.5	Epply et al., 1969	
K_{nh4L}	Large Phytoplankton Half Saturation Constant for ammonium	ìmol/l	1.300	1.3, .5-9.4, Parsons et al., 2,5 Epply et al., 1969	.5 - 9.4	Same as P			2.5	PROBES data	
K_{SiL}	Large Phytoplankton Half Saturation Constant for silicate	ìmol/l	3.000	0.8-3.7 Paasche, 1973 1.1 - 4.6 Nelson and Treguer, 1992		Same as P			Same as A(7)		
κ_L	Large Phytoplankton Temperature Coefficient for Photosynthetic Rate	1/deg. C	0.069	Q10 = 2.0		Same as P			Same as A(7)		
I_{optL}	Large Phytoplankton Optimum Light Intensity	ly/min	0.070	20-500 uE/m2/s Ref Saito?		Same as P			?	3.25 with Platt et all formulation	
α_1	Light Dissipation Coefficient of Sea Water	1/m	0.040	Gives 1% light at 115m		Same as P			Same as A(7)		
α_2	Self Shading Coefficient	l/ìmolN m	0.060	0.281 ref		Same as P			Same as A(7)		
R_{0S}	Small Phytoplankton Respiration Rate at 0 °C	1/day	0.030	3% of Vmax		Same as P			Same as A(7)		
κ_{RS}	Small Phytoplankton Temperature Coefficient for Respiration	1/deg. C	0.069	Q10 = 2.0		Same as P			Same as A(7)		
R_{0L}	Large Phytoplankton Respiration Rate at 0 °C	1/day	0.090	3% of Vmax		Same as P			0.05	0.07 @ ~8C, PROBES	

Table 4 (continued) *NEMURO*/MATLAB parameter values for 3 geographic regions of the North Pacific.

			Station P			A(7)			Bering		
		Unit	**Value**	**Remark**	**Range**	**Value**	**Remark**	**Range**	**Value**	**Remark**	**Range**
κ_{RL}	Large Phytoplankton Temperature Coefficient for Respiration	1/deg. C	0.069	Q10 = 2.0		Same as P			Same as A(7)		
$G_{RmaxSps}$	Small Zooplankton Maximum Grazing Rate on PS at 0 ºC	1/day	3.000	Nanoflagellates & Ciliates, Hansen et al., 1997		1	Ciliates & Pseudocalanus, Hansen et al., 1997		0.312	Pseudocalanus	
$G_{RmaxSpl}$	Small Zooplankton Maximum Grazing Rate on PL at 0 ºC	1/day	0.000	not at Station P		0.2			0.12	Pseudocalanus	
κ_{gZS}	Small Zooplankton Temperature Coefficient for Grazing	1/deg. C	0.069	Q10 = 2.0		Same as P			Same as A(7)		
λ_S	Small Zooplankton Ivlev Constant	l/ìmolN	1.500	Magley,1990		Same as P			Same as A(7)		
ZS^*	Small Zooplankton Threshold Value for Grazing	ìmolN/l	0.040	Fasham et al., 1990		Same as P			Same as A(7)		
GR_{maxLps}	Large Zooplankton Maximum Grazing Rate on PS at 0 ºC	1/day	0.200			0.05			0.216	Neocalanus/Calanus spp	
GR_{maxLpl}	Large Zooplankton Maximum Grazing Rate on PL at 0 ºC	1/day	1.000			0.4	GrmaxL*e^kgT < 0.9, @ 20C		0.216		
GR_{maxLzs}	Large Zooplankton Maximum Grazing Rate on ZS at 0 ºC	1/day	0.400			0.1			0		
k_{gZL}	Large Zooplankton Temperature Coefficient for Grazing	1/deg. C	0.069	Q10 = 2.0		Same as P			Same as A(7)		

Table 4 (continued) *NEMURO*/MATLAB parameter values for 3 geographic regions of the North Pacific.

			Station P			**A(7)**			**Bering**		
		Unit	**Value**	**Remark**	**Range**	**Value**	**Remark**	**Range**	**Value**	**Remark**	**Range**
λL	Large Zooplankton Ivlev Constant	l/ìmolN	1.500			Same as P			Same as A(7)		
ZL^*	Large Zooplankton Threshold Value for Grazing	ìmolN/l	0.040			Same as P			Same as A(7)		
M_{PS0}	Small Phytoplankton Mortality Rate at 0 ^oC	l/ìmolN day	0.005			Same as P			Same as A(7)		
κ_{MPS}	Temperature Coefficient for Small Phytoplankton Mortality	1/deg. C	0.069	Q10 = 2.0		Same as P			Same as A(7)		
M_{PL0}	Large Phytoplankton Mortality Rate at 0 ^oC	l/ìmolN day	0.005			Same as P			Same as A(7)		
κ_{MPL}	Temperature Coefficient for Large Phytoplankton Mortality	1/deg. C	0.069	Q10 = 2.0		Same as P			Same as A(7)		
M_{ZS0}	Small Zooplankton Mortality Rate at 0 ^oC	l/ìmolN day	0.050			Same as P			Same as A(7)		
κ_{MZS}	Temperature Coefficient for Small Zooplankton Mortality	1/deg. C	0.069	Q10 = 2.0		Same as P			Same as A(7)		
M_{ZL0}	Large Zooplankton Mortality Rate at 0 ^oC	l/µmolN day	0.025			Same as P			Same as A(7)		
κ_{MZL}	Temperature Coefficient for Large Zooplankton Mortality	1/deg. C	0.069	Q10 = 2.0		Same as P			Same as A(7)		
M_{ZP0}	Predatory Zooplankton Mortality Rate at 0 ^oC	l/µmolN day	0.004			Same as P			Same as A(7)		

Table 4 (continued) *NEMURO*/MATLAB parameter values for 3 geographic regions of the North Pacific.

			Station P			**A(7)**			**Bering**		
		Unit	**Value**	**Remark**	**Range**	**Value**	**Remark**	**Range**	**Value**	**Remark**	**Range**
κ_{MZP}	Temperature Coefficient for Predatory Zooplankton Mortality	1/deg. C	0.069	Q10 = 2.0		Same as P			Same as A(7)		
k_{N0}	Nitrification Rate at 0 ºC	1/day	0.030			Same as P			Same as A(7)		
κ_{NT}	Temperature Coefficient for Nitrification	1/deg. C	0.069	Q10 = 2.0		Same as P			Same as A(7)		
V_{PIN0}	Decomposition Rate at 0 ºC (PON=>NH4)	1/day	0.022	from Harrison, 1980 data		Same as P			Same as A(7)		
V_{PINT}	Temperature Coefficient for Decomposition (PON=>NH4)	1/deg. C	0.030	from Harrison, 1980 data		Same as P			Same as A(7)		
V_{PDN0}	Decomposition Rate at 0 ºC (PON=>DON)	0.05 /day	0.022	from Harrison, 1980 data		Same as P			Same as A(7)		
V_{PDNT}	Temperature Coefficient for Decomposition (PON DON)	1/deg. C	0.030	from Harrison, 1980 data		Same as P			Same as A(7)		
V_{DIN0}	Decomposition Rate at 0 ºC (DON=>PON)	1 /day	0.022	from Harrison, 1980 data		Same as P			Same as A(7)		
V_{DINT}	Temperature Coefficient for Decomposition (DON PON)	1/deg. C	0.030	from Harrison, 1980 data		Same as P			Same as A(7)		
V_{PISi0}	Decomposition Rate at 0 ºC (POSi=>Si(OH)4)	1 /day	0.005	Ref?		Same as P			Same as A(7)		

Table 4 (continued) *NEMURO*/MATLAB parameter values for 3 geographic regions of the North Pacific.

			Station P			**A(7)**			**Bering**		
		Unit	**Value**	**Remark**	**Range**	**Value**	**Remark**	**Range**	**Value**	**Remark**	**Range**
V_{PISiT}	Temperature Coefficient for Decomposition (POSi Si(OH)4)	1/deg. C	0.069	Q10 = 2.0		Same as P			Same as A(7)		
γ_S	Small Phytoplankton Ratio of Extracellular Excretion to Photosynthesis	fraction/day	0.010	Fasham et al., 1990		Same as P			Same as A(7)		
γ_L	Large Phytoplankton Ratio of Extracellular Excretion to Photosynthesis	fraction/day	0.010	Fasham et al., 1990		Same as P			Same as A(7)		
a_S	Assimilation Efficiency of Small Zooplankton	unitless	0.700			Same as P			Same as A(7)		
b_S	Growth Efficiency of Small Zooplankton	unitless	0.300			Same as P			Same as A(7)		
a_L	Assimilation Efficiency of Large Zooplankton	unitless	0.700			Same as P			Same as A(7)		
b_L	Growth Efficiency of Large Zooplankton	unitless	0.300			Same as P			Same as A(7)		
$(Si/N)_{PS}$	Si : N Ratio of Small Phytoplankton	mole Si/mole N	0.000			Same as P			Same as A(7)		
$(Si/N)_{PL}$	Si : N Ratio of Large Phytoplankton	mole Si/mole N	1.000			Same as P			Same as A(7)		
$(Si/N)_{ZS}$	Si : N Ratio of Small Zooplankton	mole Si/mole N	0.000			Same as P			Same as A(7)		

Table 4 (Continued) *NEMURO*/MATLAB parameter values for 3 geographic regions of the North Pacific.

			Station P			**A(7)**			**Bering**		
		Unit	**Value**	**Remark**	**Range**	**Value**	**Remark**	**Range**	**Value**	**Remark**	**Range**
$(Si/N)_{ZL}$	Si : N Ratio of Large Zooplankton	mole Si/mole N	0.000			Same as P			Same as A(7)		
λ_{PL}	Large Phytoplankton Ivlev Constant by ZP	l/ìmolN	1.500			Same as P			Same as A(7)		
P_{PL}^{*}	Large Phytoplankton Threshold Value for Grazing by ZP	ìmolN/l	0.040			Same as P			Same as A(7)		
Ψ_{PL}	Constant of ZP grazing inhibition of large phyto by ZS and ZL	l/ìmolN	4.500			Same as P			Same as A(7)		
R_{PL}	Large Phytoplankton relative Grazing by ZP	ìmolN/l	0.200			Same as P			Same as A(7)		
λ_{ZS}	Small zooplankton Ivlev Constant by ZP	l/ìmolN	1.500			Same as P			Same as A(7)		
P_{ZS}^{*}	Small zooplankton Threshold Value for Grazing by ZP	ìmolN/l	0.040			Same as P			Same as A(7)		
Ψ_{ZS}	Constant of ZP Predation inhibition of Small Zooplankton by ZL	l/ìmolN	3.000			Same as P			Same as A(7)		
R_{ZS}	Small Zooplankton relative Grazing by ZP	ìmolN/l	0.400			Same as P			Same as A(7)		
λ_{ZL}	Large zooplankton Ivlev Constant by ZP	l/ìmolN	1.500			Same as P			Same as A(7)		
P_{ZL}^{*}	Large zooplankton Threshold Value for Grazing by ZP	ìmolN/l	0.040			Same as P			Same as A(7)		

Table 4 (continued) *NEMURO*/MATLAB parameter values for 3 geographic regions of the North Pacific.

			Station P			**A(7)**			**Bering**		
		Unit	**Value**	**Remark**	**Range**	**Value**	**Remark**	**Range**	**Value**	**Remark**	**Range**
R_{ZL}	Large Zooplankton relative Grazing by ZP	ìmolN/l	1.000			Same as P			Same as A(7)		
G_{RmaxZP}	Predatory Zooplankton Maximum Grazing Rate at 0 ºC	1/day	0.250			Same as P			Same as A(7)		
κ_{gZP}	Predatory Zooplankton Temperature Coefficient for Grazing	1/deg. C	0.069			Same as P			Same as A(7)		

Appendix 1 List of workshop participants.

Name	Country	Institute	Address	Phone	Fax	E-mail
Dr. HUANG, Daji	China	Laboratory of Ocean Dynamic Processes and Satellite Oceanography, Second Institute of Oceanography,	P. O. Box 1207, Hangzhou, Zhejiang. 310012 CHINA	86-571-807-6924 X2249	86-571-807-1539	globec@hz.col.com.cn
Prof. ZHANG, Jing	China	State Key Laboratory of Estuarine and Coastal Research, East China Normal University	3663 North Zhongshan Road, Shanghai. 200062 CHINA	86-21-6223-3009	86-21-6254-6441	jzhang@sklec.ecnu.edu.cn
Dr. ZUENKO Yury I.	Russia	Pacific Fisheries Research Center	Shevchenko Alley 4,Vladivostok. 690600 RUSSIA	7-4232-25-7451	7-4232-25-7783	root@tinro.marine.su
Mr. KANTAKOV Gennady A.	Russia	Sakhalin Research Institute of Fisheries and Oceanography	Komsomolskaya Street 196 Yuzhno-Sakhalinsk. PB 693016 RUSSIA	7-42422-56985	7-42422-56357	okhotsk@tinro.sakhalin.ru
Ms. KANG, Sukyung	Korea	Korea Ocean Research & Development Institute	Ansan P.O.Box 29 Seoul, 425-600 KOREA	82-345-400-6423	82-345-408-5825	kangsk@kordi.re.kr
Mr. KIM, Hyun-chul	Korea	Biological Division, Korea Ocean Research & Development Institute	Ansan P.O.Box 29 Seoul, 425-600 KOREA	82-345-400-6220	82-345-408-5934	kimhc@kordi.re.kr
Dr. MEGREY, Bernard A.	USA	National Marine Fisheries Service, Alaska Fisheries Science Center	7600 Sand Point Way N.E., Seattle, WA 98115-0070 USA	1-206-526-4147	1-206-526-6723	bmegrey@afsc.noaa.gov
Dr. WERNER, Francisco E.	USA	Department of Marine Science, University of North Carolina	University of North Carolina, Department of Marine Sciences, Chapel Hill, NC, 27599-3300 USA	1-919-962-0269	1-919-962-1254	cisco@marine.unc.edu
Dr. WARE, Daniel M.	Canada	Pacific Biological Station	3190 Hammond Bay Road Nanaimo, B.C. V9R 5K6 CANADA	1-250-756-7199	1-250-756-7053	WareD@pac.dfo-mpo.gc.ca
Dr. ESLINGER, David L.	USA	NOAA Coastal Services Center, NOAA/National Ocean Service	2234 South Hobson Ave. Charleston, SC, 29405-2413 USA	1-843-740-1270	1-843-740-1290	dave.eslinger@noaa.gov
Dr. ZVALINSKY Vladimir I.	Russia	Pacific Oceanological Institute	Baltiyskaya Street 43, Vladivostok 690041 RUSSIA	7-4232-31-4584	7-4232-31-4584	pacific@online.marine.su
Dr. NAVROTSKY Vadim V.	Russia	Pacific Oceanological Institute	Baltiyskaya Street 43, Vladivostok 690041 RUSSIA	7-4232-31-2568 (4306)	7-4232-31-2573 (4306)	navr@online.vladivostok.ru
Dr. KISHI, Michio J.	Japan	Hokkaido University	Minato-cho 3-1-1, Hakodate. 041-8611 JAPAN	81-138-40-8873	81-138-40-8873	kishi@salmon.fish.hokudai.ac.jp
Dr. KOMATSU, Kosei	Japan	National Research Institute of Fisheries Science	Fukuura 2-12-4, Kanazawa-ku, Yokohama. 236-8648 JAPAN	81-45-788-7648	81-45-788-5001	kosei@nrifs.affrc.go.jp
Dr. KASHIWAI, Makoto B.	Japan	Hokkaido National Fisheries Research Institute	Katsurakoi-116, Kushiro. 085-0802 JAPAN	81-154-91-9136	81-154-91-9355	kashiwai@hnf.affrc.go.jp
Dr. YAMANAKA, Yasuhiro	Japan	Graduate School of Environmental Earth Science, Hokkaido University	North 10, West 5 Kita-ku, Sapporo. 060-0810 JAPAN	81-11-706-2363	81-11-706-4865	galapen@ees.hokudai.ac.jp

Appendix 1 (continued) List of workshop participants.

Name	Country	Institute	Address	Phone	Fax	E-mail
Mr. YOSHIE, Naoki	Japan	Graduate School of Environmental Earth Science, Hokkaido University	North 10, West 5 Kita-ku, Sapporo. 060-0810 JAPAN	81-11-706-2246	81-11-706-2247	naoki@ees.hokudai.ac.jp
Mr. FUJII, Masahiko	Japan	Graduate School of Environmental Earth Science, Hokkaido University	North 10, West 5 Kita-ku, Sapporo. 060-0810 JAPAN	81-11-706-2299	81-11-706-4865	fujii@ees.hokudai.ac.jp
Dr. TSUDA, Atsushi	Japan	Hokkaido National Fisheries Research Institute	Katsurakoi-116, Kushiro. 085-0802 JAPAN	81-154-92-1723	81-154-91-9355	tsuda@hnf.affrc.go.jp
Dr. YAMAMURA, Orio	Japan	Hokkaido National Fisheries Research Institute	Katsurakoi-116, Kushiro. 085-0802 JAPAN	81-154-91-9136	81-154-91-9355	orioy@hnf.affrc.go.jp
Dr. AZUMAYA, Tomonori	Japan	Hokkaido National Fisheries Research Institute	Katsurakoi-116, Kushiro. 085-0802 JAPAN	81-154-91-9136	81-154-91-9355	azumaya@hnf.affrc.go.jp
Dr. ISHIDA, Yukimasa	Japan	Hokkaido National Fisheries Research Institute	Katsurakoi-116, Kushiro. 085-0802 JAPAN	81-154-91-9136	81-154-91-9355	ishiday@hnf.affrc.go.jp
Dr. SMITH, Lan S.	Japan	Frontier Research System for Global Change	Seavans, N, 7F, Shibaura-1-2-1, Minato-ku, Tokyo. 105-6791 JAPAN	81-3-5765-7129	81-3-5232-2440	lanimal@frontier.esto.or.jp
Ms. NOGUCHI, Maki	Japan	Frontier Research System for Global Change	Seavans, N, 7F, Shibaura-1-2-1, Minato-ku, Tokyo. 105-6791 JAPAN	81-3-5765-7137	81-3-5232-2440	macky@frontier.esto.or.jp
Dr. HASHIMOTO, Shinji	Japan	National Research Institute of Far Seas Fisheries	Orido-5-7-1, Simizu. 424-8633 JAPAN	81-543-36-6063	81-543-36-6063	hashi@enyo.affrc.go.jp
Dr. YOKOUCHI, Katsumi	Japan	Seikai National Fisheries Research Institute	Kokubu-cho-3-30, Nagasaki. 850-0951 JAPAN	81-95-833-2691	81-95-821-4494	yokouchi@snf.affrc.go.jp
Dr. SAITO, Hiroaki	Japan	Hokkaido National Fisheries Research Institute	Katsurakoi-116, Kushiro. 085-0802 JAPAN	81-154-91-9136	81-154-91-9355	hsaito@hnf.affrc.go.jp
Dr. IIZUMI, Hitoshi	Japan	Hokkaido National Fisheries Research Institute	Katsurakoi-116, Kushiro. 085-0802 JAPAN	81-154-91-9136	81-154-91-9355	hiizumi@hnf.affrc.go.jp
Dr. TADOKORO, Kazuaki	Japan	Ocean Resarch Institute, University of Tokyo	Minamidai-1-15-1, Shinjuku-ku, Tokyo. 164-8639 JAPAN	81-3-5351-6505	81-3-5351-6506	denden@ori.u-tokyo.ac.jp

Appendix 2 List of breakout teams.

Team 1. ***PREPARATION OF FORCING FILES AND CODING OF TEST MODEL***

1-D Yamanaka Model
Leader: Yasuhiro Yamanaka
Members: Naoki Yoshie, Lan Smith, Maki Noguchi,

1-D Kishi Model
Leader: Michio J. Kishi
Members: Tomonori Azumaya, Kosei Komatsu

NEMURO/FORTRAN Box Model
Leader: Masahiko Fujii

NEMURO/MATLAB Model
Leader: David L. Eslinger
Members: Francisco E. Werner

Team 2. ***BIOLOGICAL REVIEW OF PARAMETERS AND PROCESS EQUATIONS***

Leader: David L. Eslinger
Members: Yukimasa Ishida, Katsumi Yokouchi, Shinji Hashimoto, Daji Huang, Yury Zuenko, Vladim Navrotsky, Atsushi Tsuda, Hiroaki Saito, Orio Yamamura, Kazuaki Tadokoro, Vladimir Zvalinsky, Masahiko Fujii, Hitoshi Iizumi

Team 3. ***POST- PROCESSING SOFTWARE PREPARATION***

Leader: Francisco E. Werner,
Members: Hyun-chul Kim, Gennady Kantakov

Team 4. ***DEVELOPMENT OF MICROBIAL FOOD WEB FORMATION***

Leader: Daniel M. Ware
Members: Jing Zhang, Sukyung Kang, Vladimir Zvalinsky, Lan Smith, Kosei Komatsu, Tomonori Azumaya, Makoto Kashiwai

Appendix 3 Model descriptions.

3.1 NEMURO/1-D Yamanaka Model

1. **Name (version):**
   NEMURO/1-D Yamanaka Model
2. **Coding Language:**
   FORTRAN
3. **Model Type:**
   1-D model
4. **Hardware/Software Requirements:**

5. **Linkage between Physical Process model and Biological Process model:**
   Simultaneous interaction between the physical model and the biological model
6. **Structure of Physical Model:**
   Water column split into 50 layers with 20 layers above 100 m.
   Mixed layer process is the Mellor-Yamada level 2.
   Upwelling process is not incorporated.
7. **Structure of Biological Model**
   NEMURO Prototype Model
   Photosynthesis light curve: after Platt *et al* (1980)
   Excretion:(á – â)
   Zooplankton Mortality: relate to biomass squared
8. **Input data**
   Climatic forcing: monthly mean wind stress, solar radiation, SST, SSS from Levitus data sets, COADs
   Daily forcing:
9. **Parameter set**
   Calibrated for:
   Validated for:
10. **Output data**
    Physical Model: temperature, salinity, and vertical eddy diffusivity through time and by depth.
    Biological model: NO3, NH4, PON, DON, SiO, PSn, PLn, ZSn, ZLn, ZPn; PLs, ZLs, ZPs
11. **Source Code**
    Available from:
    Contact: Prof. YAMANAKA, Yasuhiro, Graduate School of Environmental Earth Science, Hokkaido University, galapen@ees.hokudai.ac.jp
12. **Remarks:**
    The model links biological processes and physical process at each time step. This will be an advantage when incorporating effects of biological production upon thermal process in the surface layer. On the other hand, it will not be easy to apply the physical model to another areas.

    Instructions for obtaining the physical forcing files can be found at http://pices.ios.bc.ca/model/.

3.2 NEMURO/1-D Kishi Model

1. **Name (version):**
   NEMURO/1-D Kishi Model

2. **Coding Language:**
   FORTRAN

3. **Model Type:**
   1-D

4. **Hardware/Software Requirements:**

5. **Linkage between Physical Process model and Biological Process model:**
   Physical model gives the forcing data set for the biological model

6. **Structure of Physical Model:**
   Water column split into 50 layers with 20 layers above 100 m.
   Mixed layer process is the Mellor Yamada level 2 (reference).
   Upwelling process is not incorporated.

7. **Structure of Biological Model**
   NEMURO Prototype Model
   Photosynthesis light curve: after Platt *et al* (1980)
   Excretion:(alpha – beta)
   Zooplankton Mortality: relate to squared biomass

8. **Input data**
   date / time / SST / SSS / Wind / Solar Radiation

9. **Parameter set**
   Calibrated for:
   Validated for:

10. **Output data**

11. **Source Code**
    Instructions for obtaining the 1-D Kishi model and the physical forcing files can be found at http://pices.ios.bc.ca/model/
    Available from: ftp coast3.fish.hokudai.ac.jp (see Appendix 4)

12. **Remarks:**
    The separated physical process sub-model and biological process sub-model will be advantageous when one wants to use another physical model scheme.

3.3 NEMURO / FORTRAN Box Model

1. **Name (version):**
   NEMURO/FORTRAN Box Model

2. **Coding Language:**
   FORTRAN

3. **Model Type:**
   1-Box model for surface production layer

4. **Hardware/Software Requirements:**

5. **Linkage between Physical Process model and Biological Process model:**
   Biological Model is driven by given forcing data

6. **Structure of Physical Model:**

7. **Structure of Biological Model:**
   NEMURO Prototype Model
   Photosynthesis light curve: after Platt *et al* (1980)
   Excretion: (á – â)
   Zooplankton Mortality: relate to biomass squared

8. **Input data:**

9. **Parameter set:**
   Calibrated for:
   Validated for:

10. **Output data:**
    Physical Model: temperature, salinity, and vertical eddy diffusivity through time and by depth.
    Biological model: NO3, NH4, PON, DON, SiO, PSn, PLn, ZSn, ZLn, ZPn; PLs, ZLs, ZPs

11. **Source Code:**
    Available from:
    Contact: Mr. FUJII, Masahiko, Graduate School of Environmental Earth Science, Hokkaido University, fujii@ees.hokudai.ac.jp

12. **Remarks:**
    This model was originally developed to test biological parameters and process equations prior to incorporating these into the *NEMURO*/1-D Yamanaka Model.

3.4 NEMURO/MATLAB Model

1. **Name (version):**
   NEMURO/MATLAB Model

2. **Coding Language:**
   MATLAB

3. **Model Type:**
   1-Box model for surface production layer

4. **Hardware/Software Requirements:**

5. **Linkage between Physical Process model and Biological Process model:**
   The biological model is driven by the given forcing data

6. **Structure of Physical Model:**

7. **Structure of Biological Model:**
   NEMURO Prototype Model
   Photosynthesis light curve: after Platt *et al* (1980)
   Excretion: alpha (1 – â)
   Zooplankton Mortality: related to biomass

8. **Input data:**

9. **Parameter set:**
   Calibrated for:
   Validated for:

10. **Output data:**
    Biological model: NO3, NH4, PON, DON, SiO, PSn, PLn, ZSn, ZLn, ZPn; PLs, ZLs, ZPs

11. **Source Code:**
    A listing of the MATLAB scripts for implementing *NEMURO* can be found in Appendicies 5 and 6. Copies of the MATLAB script can be obtained via FTP from; http://www.OPNML.unc.edu/ Personnel/few/Nemuro.html

    Contact: Dr. WERNER, Francisco E, Department of Marine Science, University of North Carolina, cisco@marine.unc.edu

12. **Remarks:**
    The MATLAB version of the *NEMURO* was developed during the Nemuro workshop. Following the workshop, work continued to refine the model.

Appendix 4 Instructions for obtaining and the code and data files for the *NEMURO*/1-D Kishi physical biological coupled model.

(1) How to ftp
   0. make a directory under your home directory named “one-dim-phy” and “one-dim-bio”
   1. cd one-dim-phy
   2. ftp > coast0.fish.hokudai.ac.jp
   3. User(coast)> pices
   4. password required for pices
      Password
      ftp> cd /one-dim-phy
   5. ftp> mget *
   6. ftp> lcd ../one-dim-bio
   7. ftp> cd /one-dim-bio
   8. ftp> mget *
   9. ftp> quit

(2) How to compile
   0. run physical model
   0.1 need input file of sst,sss, tau under ~/one-dim-phy/ /kushiro
      surfn41-1+10.csv : sst and sss for A7 with 10 times of 1991 data to get steady annual cycle
      tau418-1+10.csv : wind stress for A7
   0.2 output file from physical part will be created in the same directory (Not /kushiro) named “hout.dat”
      move it to ~/one-dim-bio/kushiro/ and rename to "phyn41-1-b+10.dat"
   1. run biological model
      PS, PL, ZL, ZL, NO3, NH4, PON, DON, SI, POSI .
      with ZL migration
         kno3 = 2.0, knh4 = 0.6, ksi = 3.0, grmax = 0.3, W = 3.6 m/yr
         need input file under ~one-dim-bio/kushiro/
         "phyn41-1-b+10.dat": (this is from physical model)
      "srad420-1+10.csv": solar radiation

(3) How to add your idea
   1. If you want to change input file (i.e., physical forcing), make your file following to “surfn41-1+10”, “tau418-1+10.csv” and "srad420-1+10.csv"
   2. If you want to change ecosystem model, you have to change “bioprc.f” but also all kinds of common, arguments.
   3. If you want to change only values of biological parameters, change in “param2.f”

(4) When you use and publish your papers
   Refer to the following papers
   1. Kawamiya,M., M.J.Kishi, Y.Yamanaka and N.Suginohara (1995). An ecological-physical coupled model applied to Station Papa. Journal of Oceanography, 51.655-664.
   2. Kawamiya,M., M.J.Kishi, Y.Yamanaka and N.Suginohara (1997). Obtaining reasonable results in different oceanic regimes with the same ecological physical coupled model. Journal of Oceanography. 53, 397-402.
   3. Kishi, M.J. and H. Motono (2000). Ecological-physical coupled model with vertical migration of zooplankton in Northwestern Pacific. Submitted to Journal of Oceanography.

(5) When is this ftp available for use?
   March 1st, 2000

Appendix 5 NEMURO Model Commands for MATLAB Implementation.

```
PSn0=0.1*50*17/(12*133);  % converts mg Chl/m^3 --> mmole N/l
PLn0=0.1*50*17/(12*133);  % converts mg Chl/m^3 --> mmole N/l
%ZSn0=0.15; % mmolN/m^3
%ZLn0=0.15; % mmolN/m^3
%ZPn0=0.11; % mmolN/m^3
ZSn0=0.05; % mmolN/m^3
ZLn0=0.05; % mmolN/m^3
ZPn0=0.05; % mmolN/m^3
NO30=20;
%NO30=5;       % Kishi numbers
%NH40=1;       % =0   in initial runs
%PON0=1;       % =0   in initial runs
%DON0=1;       % =0   in initial runs
NH40=0;
PON0=0;
DON0=0;
RSiNPL=1.;
%PLsi0=PLn0*RSiNPL;
%ZLsi0=1;  % =0   in initial runs
%ZPsi0=1;  % =0   in initial runs
%ZLsi0=0;
%ZPsi0=0;
% Initial conditions for new equations
NO3deep0=0;
PONdeep0=0;
Sideep0=0;
SiOH40=20;
%SiOH40=20;
%Op0=1;    % =0   in initial runs
Op0=0;
Opdeep0=0;

Nem0=[PSn0 PLn0 ZSn0 ZLn0 ZPn0 NO30 NH40...
     PON0 DON0 NO3deep0 PONdeep0 Sideep0 SiOH40 Op0 Opdeep0];
%      PON0 DON0 PLsi0 ZLsi0 ZPsi0 SiOH40 Op0];

t0=0;
tf=365*20;  % in days
%tf=365*2;    % in days
nsteps=12;
dt=1/nsteps;      % in days, i.e., nsteps=2 => hour time step
tspan=[t0:dt:tf];

[t,Nemuro]=ode45('Nemuro_base',tspan,Nem0);

%setup for plotting one obs/day
lt=length(t);
```

```
ty=t(1:nsteps:lt)/365;     % Pick a time every nsteps increments to plot.
                           % Since dt = 1/nsteps, this give 1/day plotting

ps=Nemuro(:,1);
pl=Nemuro(:,2);
zs=Nemuro(:,3);
zl=Nemuro(:,4);
zp=Nemuro(:,5);
no3=Nemuro(:,6);
nh4=Nemuro(:,7);
pon=Nemuro(:,8);
don=Nemuro(:,9);
DeepNO3=Nemuro(:,10);
DeepPON=Nemuro(:,11);
Deepsi=Nemuro(:,12);
si=Nemuro(:,13);
opal=Nemuro(:,14);
Deepopal=Nemuro(:,15);

figure(1)
plot(ty,ps(1:nsteps:lt),'b',ty,pl(1:nsteps:lt),'g',...
   ty,zs(1:nsteps:lt),'r',ty,zl(1:nsteps:lt),'c',...
   ty,zp(1:nsteps:lt),'m');
legend('ps','pl','zs','zl','zp');
title('Base run','FontSize',12);
xlabel('Years');
ylabel('Biomass (umole N/l)');
%axis([0 400 0 .8])

figure(2);
subplot(211);
plot(ty,no3(1:nsteps:lt),'b:',ty,si(1:nsteps:lt),'g:');
legend('no3','si');
title('Base run','FontSize',12);
ylabel('Nutrient conc (umole/l)');


subplot(212);
plot(ty,nh4(1:nsteps:lt),'r:',...
    ty,pon(1:nsteps:lt),'c:',ty,don(1:nsteps:lt),'m:');
legend('nh4','pon','don');
xlabel('Years');
ylabel('Nutrient conc (umole/l)');
```

Appendix 6 NEMURO 15 State Variable Model coded in MATLAB.

```
function xdot=Nemuro(t,x);

% Concentration are in units of millimoles/m^3
% Length are in meters
% Time values (i.e. rates)s are in units of days

RSiNPL=1;   % Si/N Ratio of Large Phytoplankton
H=100.00;   % layer depth in meters

% Light limitation parameters.  For this box model, there is a diurnal and an
%    annual light signal, calculated below.

% Small Phytoplankton Growth parameters.
VmaxS=1;
KNO3S=3.;
KNH4S=.1;
PsiS=1.3;
KGppS=0.0693;

% Large Phytoplankton Growth parameters.
VmaxL=1;
KNO3L=3;
KNH4L=1.3;
KSiL=3.;
PsiL=2.7;
KGppL=0.0693;

ResPS0=0.03;
KResPS=0.0519;
ResPL0=0.03;
KResPL=0.0519;

% Mortality parameters.
% Note bene: There are two sets of these, one for using the first-order
%   formulation and one for the sedcond order (quadratic) formulation.
%   Units and values differ.

%MorPS0=.05??;        % Second order, units are fraction biomass lost/day/unit biomass
MorPS0=.005;         % First order, units are fraction biomass lost/day.
KMorPS=0.0693;
%MorPL0=.05??;        % cond order, units are fraction biomass lost/day/unit biomass
MorPL0=.005;         % First order, units are fraction biomass lost/day.
KMorPL=0.0693;

GammaS=0.01;         % Extracellular excretion by small phyto
GammaL=0.01;         % Extracellular excretion by large phyto
```

```
%Small Zooplankton grazing parameters
GRmaxSps=3.0;        % Max grazing rate on small phytoplankton
                     % (as fraction small zoop biomass/day)
KGraSps=0.0693;
LamSps=1.5;
PS2ZSstar=4.0e-2;
GRmaxSpl=0.0;        % NEW!Max grazing rate on large phytoplankton
                     % (as fraction small zoop biomass/day)
KGraSpl=0.0693;      % NEW!
LamSpl=1.5;          % NEW!
PL2ZSstar=4.0e-2;    % NEW!

%Large Zooplankton grazing parameters
GRmaxLps=0.2;        % Max grazing rate on small phytoplankton
                     % (as fraction large zoop biomass/day)
GRmaxLpl=1.0;        % Max grazing rate on large phytoplankton
                     % (as fraction large zoop biomass/day)
GRmaxLzs=0.4;        % Max grazing rate on small zooplankton
                     % (as fraction large zoop biomass/day)
KGraL=0.0693;
LamL=1.5;
PL2ZLstar=4.e-2;
ZS2ZLstar=4.e-2;
PS2ZLstar=4.e-2;

%Predatory Zooplankton grazing parameters
GRmaxPpl=0.05;       % Max grazing rate on large phytoplankton
                     % (as fraction predatory body biomass/day)
GRmaxPzs=0.2;        % Max grazing rate on small zooplankton
                     % (as fraction predatory body biomass/day)
GRmaxPzl=0.25;       % Max grazing rate on large zooplankton
                     % (as fraction predatory body biomass/day)
KGraP=0.0693;
LamP=1.5;
PL2ZPstar=4.e-2;
ZS2ZPstar=4.e-2;
ZL2ZPstar=4.e-2;
PsiPL=4.5;
PsiZS=3.0;

AlphaZS=0.7;
BetaZS=0.3;
AlphaZL=0.7;
BetaZL=0.3;
AlphaZP=0.7;
BetaZP=0.3;

MorZS0=0.05;
KMorZS=0.0693;
MorZL0=0.025;
KMorZL=0.0693;
```

```
MorZP0=0.0035;
KMorZP=0.0693;

VP2N0=0.05;
KP2N=0.0693;
VP2D0=0.05;
KP2D=0.0693;
VD2N0=0.05;
KD2N=0.0693;
VP2Si0=0.05;          % new process
KP2Si=0.0693;         % new process

Nit0=0.03;            % Nitrification rate at 0 C.
Knit=0.0693;

Vsedn=1.0;            % PON sedimentation rate in meters/day
Vsedsi=10.0;          % Particulate Si sedimentation rate in meters/day
ExUP=0.003;           % Fraction of upper layer exchnaged per day
NO3D=20;              % Deep nitrate concentration
SiOH4D=25;            % Deep Silico concentration

xdot=zeros(15,1);

% Annual sinusoidal TEMPREATURE variation
TMP=5+(9*0.5*(1-cos(2*pi*(t-90)/365)));      % varies from 5 to 14

% Day/night and annual sinusoidal variation
annual=0.5*(1-cos(2*pi*t/365));              % varies from 0 to 1
LIGHT=0.2+0.6*annual;
daynight=max(0,cos(2*pi*t));
LIGHT=daynight*LIGHT;

% Small Phytoplankton N = x(1)

GppPSn=VmaxS*((x(6)/(x(6)+KNO3S)*exp(-PsiS*x(7))+x(7)/(x(7)+KNH4S)))
    *exp(KGppS*TMP)*LIGHT*x(1);
ResPSn=ResPS0*exp(KResPS*TMP)*x(1);
% Second order (quadratic) natural mortality
%MorPSn=MorPS0*exp(KMorPS*TMP)*x(1)*x(1);
% First order natural mortality
MorPSn=MorPS0*exp(KMorPS*TMP)*x(1);
ExcPSn=GammaS*GppPSn;
GraPS2ZSn=max(0,GRmaxSps*exp(KGraSps*TMP)*(1-exp(LamSps*(PS2ZSstar-x(1)))))*x(3);
GraPS2ZLn=max(0,GRmaxLps*exp(KGraL*TMP)*(1-exp(LamL*(PS2ZLstar-x(1)))))*x(4);
xdot(1)=GppPSn-ResPSn-MorPSn-ExcPSn-GraPS2ZSn-GraPS2ZLn;

% Large Phytoplankton N = x(2)

GppPLn=VmaxL*min(...
    (x(6)/(x(6)+KNO3L)*exp(-PsiL*x(7))+x(7)/(x(7)+KNH4L)),
    (x(13)/(x(13)+KSiL)*RSiNPL))
```

```
      *exp(KGppL*TMP)*LIGHT*x(2);
ResPLn=ResPL0*exp(KResPL*TMP)*x(2);
% Second order (quadratic) natural mortality
%MorPLn=MorPL0*exp(KMorPL*TMP)*x(2)*x(2);
% First order natural mortality
MorPLn=MorPL0*exp(KMorPL*TMP)*x(2);
ExcPLn=GammaL*GppPLn;
GraPL2ZSn=max(0,GRmaxSpl*exp(KGraSpl*TMP)*(1-exp(LamSpl*(PL2ZSstar-x(2))))*x(3));
GraPL2ZLn=max(0,GRmaxLpl*exp(KGraL*TMP)*(1-exp(LamL*(PL2ZLstar-x(2))))*x(4));
GraPL2ZPn=max(0,GRmaxPpl*exp(KGraP*TMP)*(1-exp(LamP*(PL2ZPstar-x(2))))*...
          exp(-PsiPL*(x(4)+x(3)))*x(5));
xdot(2)=GppPLn-ResPLn-MorPLn-ExcPLn-GraPL2ZSn-GraPL2ZLn-GraPL2ZPn;


% Small Zooplankton N = x(3)

GraZS2ZLn=max(0,GRmaxLzs*exp(KGraL*TMP)*(1-exp(LamL*(ZS2ZLstar-x(3))))*x(4));
GraZS2ZPn=max(0,GRmaxPzs*exp(KGraP*TMP)*(1-exp(LamP*(ZS2ZPstar-x(3))))*
          exp(-PsiZS*x(4))*x(5));
% Second order (quadratic) natural mortality
%MorZSn=MorZS0*exp(KMorZS*TMP)*x(3)*x(3);
% First order natural mortality
MorZSn=MorZS0*exp(KMorZS*TMP)*x(3);
ExcZSn=(AlphaZS*(1-BetaZS))*(GraPS2ZSn+GraPL2ZSn);
EgeZSn=(1-AlphaZP)*(GraPS2ZSn+GraPL2ZSn);
xdot(3)=GraPS2ZSn+GraPL2ZSn-GraZS2ZLn-GraZS2ZPn-MorZSn-ExcZSn-EgeZSn;

% Large Zooplankton N = x(4)

GraZL2ZPn=max(0,GRmaxPzl*exp(KGraP*TMP)*(1-exp(LamP*(ZL2ZPstar-x(4))))*x(5));
% Second order (quadratic) natural mortality
%MorZLn=MorZL0*exp(KMorZL*TMP)*x(4)*x(4);
% First order natural mortality
MorZLn=MorZL0*exp(KMorZL*TMP)*x(4);
ExcZLn=(AlphaZL*(1-BetaZL))*(GraPL2ZLn+GraZS2ZLn+GraPS2ZLn);
EgeZLn=(1-AlphaZL)*(GraPL2ZLn+GraZS2ZLn+GraPS2ZLn);
xdot(4)=GraPS2ZLn+GraPL2ZLn+GraZS2ZLn-GraZL2ZPn-MorZLn-ExcZLn-EgeZLn;

% Predatory Zooplankton N = x(5)

% Second order (quadratic) natural mortality
%MorZPn=MorZP0*exp(KMorZP*TMP)*x(5)*x(5);
% First order natural mortality
MorZPn=MorZP0*exp(KMorZP*TMP)*x(5);
ExcZPn=(AlphaZP*(1-BetaZP))*(GraPL2ZPn+GraZS2ZPn+GraZL2ZPn);
EgeZPn=(1-AlphaZP)*(GraPL2ZPn+GraZS2ZPn+GraZL2ZPn);
xdot(5)=GraPL2ZPn+GraZS2ZPn+GraZL2ZPn-MorZPn-ExcZPn-EgeZPn;

% NO3 = x(6)

RnewS=(x(6)/(x(6)+KNO3S)*exp(-PsiS*x(7)))/
```

```
    ((x(6)/(x(6)+KNO3S)*exp(-PsiS*x(7)))+x(7)/(x(7)+KNH4S));
RnewL=(x(6)/(x(6)+KNO3L)*exp(-PsiL*x(7)))/...
    ((x(6)/(x(6)+KNO3L)*exp(-PsiL*x(7)))+x(7)/(x(7)+KNH4L));
Nit=Nit0*exp(Knit*TMP)*x(7);
UPWn=ExUP*(NO3D-x(6));     % Upwelling effect
xdot(6)=-(GppPSn-ResPSn)*RnewS-(GppPLn-ResPLn)*RnewL+Nit+UPWn;

% NH4 = x(7)

DecP2Nn=VP2N0*exp(KP2N*TMP)*x(8);
DecD2Nn=VD2N0*exp(KD2N*TMP)*x(9);
xdot(7)=-(GppPSn-ResPSn)*(1-RnewS)-(GppPLn-ResPLn)*(1-RnewL)-Nit+
      DecP2Nn+DecD2Nn+ExcZSn+ExcZLn+ExcZPn;

% PON = x(8)

DecP2Dn=VP2D0*exp(KP2D*TMP)*x(8);
SEDn=Vsedn/H*x(8);
xdot(8)=MorPSn+MorPLn+MorZSn+MorZLn+MorZPn+...
      EgeZSn+EgeZLn+EgeZPn-DecP2Nn-DecP2Dn-SEDn;

% DON = x(9)

xdot(9)=ExcPSn+ExcPLn+DecP2Dn-DecD2Nn;

% Deep NO3 = x(10)

xdot(10)= -UPWn;

% Deep PON = x(11)

xdot(11)= +SEDn;

% Deep dissolved Si pool =x(12)

UPWsi=ExUP*(SiOH4D-x(13));  % Difference between deep pool and surface layer
xdot(12)= -UPWsi;  % Net loss from deep pool

% Si(OH)4 = x(13)

% with surface remineralization
%DecP2si=VP2Si0*exp(KP2Si*TMP)*x(14);
%xdot(13)=(-GppPLn+ResPLn+ExcPLn)*RSiNPL+UPWsi+DecP2si;

% WITHOUT surface remineralization
xdot(13)=(-GppPLn+ResPLn+ExcPLn)*RSiNPL+UPWsi;

% Opal  = =x(14)

SEDsi=Vsedsi/H*x(14);
%Si reimineralization
```

```
%xdot(14)=(MorPLn+GraPL2ZSn+GraPL2ZLn+GraPL2ZPn)*RSiNPL-SEDsi-DecP2si;

%No Si reimineralization
xdot(14)=(MorPLn+GraPL2ZSn+GraPL2ZLn+GraPL2ZPn)*RSiNPL-SEDsi; % No Si remin

%Deep Opal pool = x(15)
xdot(15) = +SEDsi;
```

Appendix 7 Implementation and User's Guide for the *NEMURO*/MATLAB Model.

A description of the implementation of the *NEMURO*/MATLAB model is provided below. The governing equations are described in Table 3 and model parameters are those corresponding to the "Station P base case" run as in Table 4. Two MATLAB programs are needed to run this case:

Nemuro_base.m: this is the MATLAB code containing the model equations detailed in Table 3. The full listing of the MATLAB code is provided in Appendix 6. The model parameters for the base case are included (hardwired) into the code.

Nemuro_base_commands.m: these are the commands to be issued to run the model and to generate the plots. The full listing of the MATLAB is provided in Appendix 5.

These files can also be downloaded from the PICES website http://www.pices.ios.ca/model/.

To run the model, the files should reside in a common directory. Within a MATLAB window, the simplest way to reproduce figures 5 and 6 of the report is to type "**Nemuro_base_commands**" after the MATLAB prompt. The execution of all the commands (initaliaztion, equation set-up, equation solution and plotting) will likely take several minutes on a PC with a Pentium III processor. The base case model is set up for a 20 year run with 2-hour time steps. The standard Runge-Kutta solver "ode45" is used in solving the system of equations. To get more information on the properties of the solver, type "help ode45" from within a MATLAB window.

As written, changes in initial conditions should be made in *Nemuro_base_commands.m* while changes in the form of the governing equations, or in the internal parameters should be made in the *Nemuro_base.m* file.

Appendix 8 FORTRAN code to reformat the *NEMURO*/1-D Yamanaka model biological output file into a format compatible for MATLAB plotting.

```
      parameter(nlayers=50)
      character*80 dateinfo
      real zd(nlayers+1),zl(nlayers)
      open(1,file='Ythist_Bering.dat',status='old')
      open(2,file='YThist_mat.dat',status='unknown')
c
      do il=1,nlayers
        read(1,*)jj,zd(il),zl(il)
      end do
      read(1,*)jj,zd(nlayers+1)
c
      write(*,*)' enter starting year'
      read(*,*)iy
      write(*,*)' enter starting Julian day'
      read(*,*)iday
      write(*,*)' enter interval between data in days'
      read(*,*)incd
c
      do it=1,1000000
        read(1,100,end=10)dateinfo
          do iz=1,nlayers
            read(1,*)i,p1,p2,p3,p4,p5,p6,p7,p8,p9,p10,p11
     &                          ,p12,p13,p14
            write(2,101)iy,iday,zd(iz),p1,p2,p3,p4,p5,p6,p7,p8,p9,p10,p11
     &                          ,p12,p13,p14
          end do
          iday=iday+incd
      end do
   10 continue
  100 format(a)
  101 format(2i6,15(1x,e12.5))
      stop
      end
```

Appendix 9 MATLAB script to plot the *NEMURO*/1-D Yamanaka model biological output.

```
load YThist_mat.dat;
bio=YThist_mat;

nz=50;
z=bio(1:nz,3);

nt=length(bio);

t=bio(1:nz:nt,1)+bio(1:nz:nt,2)/365.;
lt=length(t);
[t,z]=meshgrid(t,z);

%
% first page
%

%fullpage
subplot(411)
psn=reshape(bio(:,4),nz,lt);  % plots all days
colormap(jet)
axis([0 1 -300 0])
h=surface(t,z,psn);
set(h,'EdgeColor','interp','FaceColor','interp','zdata',zeros(size(t)))
%set(gca,'clim',[10 25])
colorbar
%xl=xlabel('Year')
%set(xl,'FontSize',16)
set(gca,'XTick',[])
yl=ylabel('Depth (m)')
set(yl,'FontSize',16)
tl=title('Climatology Bering PS_n')
set(tl,'FontSize',18)
hold on

subplot(412)
zsn=reshape(bio(:,6),nz,lt);
colormap(jet)
axis([0 1 -300 0])
%axis([10 16 -300 0])
colorbar
h=surface(t,z,zsn);
set(h,'EdgeColor','interp','FaceColor','interp','zdata',zeros(size(t)))
%set(gca,'clim',[10 25])
colorbar
%set(gca,'clim',[33.2 33.7])
%colorbar
%xl=xlabel('Year')
%set(xl,'FontSize',16)
```

```
set(gca,'XTick',[])
yl=ylabel('Depth (m)')
set(yl,'FontSize',16)
tl=title('ZS_n')
set(tl,'FontSize',18)
hold on

subplot(413)
pln=reshape(bio(:,5),nz,lt);
colormap(jet)
axis([0 1 -300 0])
%axis([10 16 -300 0])
colorbar
h=surface(t,z,pln);
set(h,'EdgeColor','interp','FaceColor','interp','zdata',zeros(size(t)))
colorbar
%xl=xlabel('Year')
%set(xl,'FontSize',16)
set(gca,'XTick',[])
yl=ylabel('Depth (m)')
set(yl,'FontSize',16)
tl=title('PL_n')
set(tl,'FontSize',18)
hold on

subplot(414)
zln=reshape(bio(:,7),nz,lt);
colormap(jet)
axis([0 1 -300 0])
%axis([10 16 -300 0])
colorbar
h=surface(t,z,zln);
set(h,'EdgeColor','interp','FaceColor','interp','zdata',zeros(size(t)))
colorbar
xl=xlabel('Year')
set(xl,'FontSize',16)
%set(gca,'XTick',[])
yl=ylabel('Depth (m)')
set(yl,'FontSize',16)
tl=title('ZL_n')
set(tl,'FontSize',18)
hold on

%
% second page
%

fullpage
subplot(411)
zpn=reshape(bio(:,8),nz,lt);  % plots all days
colormap(jet)
```

```
axis([0 1 -300 0])
h=surface(t,z,zpn);
set(h,'EdgeColor','interp','FaceColor','interp','zdata',zeros(size(t)))
%set(gca,'clim',[10 25])
colorbar
%xl=xlabel('Year')
%set(xl,'FontSize',16)
set(gca,'XTick',[])
yl=ylabel('Depth (m)')
set(yl,'FontSize',16)
tl=title('Climatology Bering ZP_n')
set(tl,'FontSize',18)
hold on

subplot(412)
pls=reshape(bio(:,13),nz,lt);
colormap(jet)
axis([0 1 -300 0])
%axis([10 16 -300 0])
colorbar
h=surface(t,z,pls);
set(h,'EdgeColor','interp','FaceColor','interp','zdata',zeros(size(t)))
%set(gca,'clim',[10 25])
colorbar
%set(gca,'clim',[33.2 33.7])
%colorbar
%xl=xlabel('Year')
%set(xl,'FontSize',16)
set(gca,'XTick',[])
yl=ylabel('Depth (m)')
set(yl,'FontSize',16)
tl=title('PL_s')
set(tl,'FontSize',18)
hold on

subplot(413)
zls=reshape(bio(:,14),nz,lt);
colormap(jet)
axis([0 1 -300 0])
%axis([10 16 -300 0])
colorbar
h=surface(t,z,zls);
set(h,'EdgeColor','interp','FaceColor','interp','zdata',zeros(size(t)))
colorbar
%xl=xlabel('Year')
%set(xl,'FontSize',16)
set(gca,'XTick',[])
yl=ylabel('Depth (m)')
set(yl,'FontSize',16)
tl=title('ZL_s')
set(tl,'FontSize',18)
```

```
hold on

subplot(414)
zps=reshape(bio(:,15),nz,lt);
colormap(jet)
axis([0 1 -300 0])
%axis([10 16 -300 0])
colorbar
h=surface(t,z,zps);
set(h,'EdgeColor','interp','FaceColor','interp','zdata',zeros(size(t)))
colorbar
xl=xlabel('Year')
set(xl,'FontSize',16)
%set(gca,'XTick',[])
yl=ylabel('Depth (m)')
set(yl,'FontSize',16)
tl=title('ZP_s')
set(tl,'FontSize',18)
hold on

%
% third page
%

fullpage
subplot(511)
no3=reshape(bio(:,9),nz,lt);  % plots all days
colormap(jet)
axis([0 1 -300 0])
h=surface(t,z,no3);
set(h,'EdgeColor','interp','FaceColor','interp','zdata',zeros(size(t)))
%set(gca,'clim',[10 25])
colorbar
%xl=xlabel('Year')
%set(xl,'FontSize',16)
set(gca,'XTick',[])
yl=ylabel('Depth (m)')
set(yl,'FontSize',16)
tl=title('Climatology Bering NO_3')
set(tl,'FontSize',18)
hold on

subplot(512)
nh4=reshape(bio(:,10),nz,lt);
colormap(jet)
axis([0 1 -300 0])
%axis([10 16 -300 0])
colorbar
h=surface(t,z,nh4);
set(h,'EdgeColor','interp','FaceColor','interp','zdata',zeros(size(t)))
%set(gca,'clim',[10 25])
```

```
colorbar
%set(gca,'clim',[33.2 33.7])
%colorbar
%xl=xlabel('Year')
%set(xl,'FontSize',16)
set(gca,'XTick',[])
yl=ylabel('Depth (m)')
set(yl,'FontSize',16)
tl=title('NH_4')
set(tl,'FontSize',18)
hold on

subplot(513)
pon=reshape(bio(:,11),nz,lt);
colormap(jet)
axis([0 1 -300 0])
%axis([10 16 -300 0])
colorbar
h=surface(t,z,pon);
set(h,'EdgeColor','interp','FaceColor','interp','zdata',zeros(size(t)))
colorbar
%xl=xlabel('Year')
%set(xl,'FontSize',16)
set(gca,'XTick',[])
yl=ylabel('Depth (m)')
set(yl,'FontSize',16)
tl=title('PON')
set(tl,'FontSize',18)
hold on

subplot(514)
don=reshape(bio(:,12),nz,lt);
colormap(jet)
axis([0 1 -300 0])
%axis([10 16 -300 0])
colorbar
h=surface(t,z,don);
set(h,'EdgeColor','interp','FaceColor','interp','zdata',zeros(size(t)))
colorbar
%xl=xlabel('Year')
%set(xl,'FontSize',16)
set(gca,'XTick',[])
yl=ylabel('Depth (m)')
set(yl,'FontSize',16)
tl=title('DON')
set(tl,'FontSize',18)
hold on

subplot(515)
sio=reshape(bio(:,16),nz,lt);
colormap(jet)
```

```
axis([0 1 -300 0])
%axis([10 16 -300 0])
colorbar
h=surface(t,z,sio);
set(h,'EdgeColor','interp','FaceColor','interp','zdata',zeros(size(t)))
colorbar
xl=xlabel('Year')
set(xl,'FontSize',16)
%set(gca,'XTick',[])
yl=ylabel('Depth (m)')
set(yl,'FontSize',16)
tl=title('SiO')
set(tl,'FontSize',18)
hold on
```

Appendix 10 FORTRAN code to reformat the *NEMURO*/1-D Yamanaka model physical output file into a format compatible for MATLAB plotting.

```
      parameter(nlayers=50)
      character*80 dateinfo
      real zd(nlayers+1),zl(nlayers)
      open(1,file='Yphist_Bering.dat',status='old')
      open(2,file='YPhist_mat.dat',status='unknown')
c
      do il=1,nlayers
        read(1,*)jj,zd(il),zl(il)
      end do
      read(1,*)jj,zd(nlayers+1)
c
      write(*,*)' enter starting year'
      read(*,*)iy
      write(*,*)' enter starting Julian day'
      read(*,*)iday
      write(*,*)' enter interval between data in days'
      read(*,*)incd
c
      do it=1,1000000
        read(1,100,end=10)dateinfo
          do iz=1,nlayers
            read(1,*)i,p1,p2,p3,p4,p5,p6
            write(2,101)iy,iday,zd(iz),p1,p2,p3,p4,p5,p6
          end do
          iday=iday+incd
      end do
   10 continue
  100 format(a)
  101 format(2i6,7(1x,f12.5))
      stop
      end
```

Appendix 11 MATLAB script to plot *NEMURO*/1-D Yamanaka model physical output.

```
load YPhist_mat.dat;
TSAv=YPhist_mat;

nz=50;
z=TSAv(1:nz,3);

nt=length(TSAv);

t=TSAv(1:nz:nt,1)+TSAv(1:nz:nt,2)/365.;
lt=length(t);
[t,z]=meshgrid(t,z);

%fullpage
subplot(311)
Temp=reshape(TSAv(:,4),nz,lt);  % plots all days
colormap(jet)
axis([0 1 -300 0])
h=surface(t,z,Temp);
set(h,'EdgeColor','interp','FaceColor','interp','zdata',zeros(size(t)))
%set(gca,'clim',[10 25])
colorbar
%xl=xlabel('Year')
%set(xl,'FontSize',16)
set(gca,'XTick',[])
yl=ylabel('Depth (m)')
set(yl,'FontSize',16)
tl=title('Climatology Bering Temperature')
set(tl,'FontSize',18)
hold on
%clear Temp

subplot(312)
%Sal=reshape(TSAv(1:nt,5),nz,length(t));
Sal=reshape(TSAv(:,5),nz,lt);
colormap(jet)
axis([0 1 -300 0])
%axis([10 16 -300 0])
colorbar
h=surface(t,z,Sal);
set(h,'EdgeColor','interp','FaceColor','interp','zdata',zeros(size(t)))
%set(gca,'clim',[10 25])
colorbar
%set(gca,'clim',[33.2 33.7])
%colorbar
%xl=xlabel('Year')
%set(xl,'FontSize',16)
set(gca,'XTick',[])
yl=ylabel('Depth (m)')
```

```
set(yl,'FontSize',16)
tl=title('Salinity')
set(tl,'FontSize',18)
hold on
%clear Sal

subplot(313)
Ahv=reshape(log10(TSAv(:,7)),nz,lt);
colormap(jet)
axis([0 1 -300 0])
%axis([10 16 -300 0])
colorbar
h=surface(t,z,Ahv);
set(h,'EdgeColor','interp','FaceColor','interp','zdata',zeros(size(t)))
colorbar
%xl=xlabel('Year')
%set(xl,'FontSize',16)
%set(gca,'XTick',[])
yl=ylabel('Depth (m)')
set(yl,'FontSize',16)
tl=title('log_{10}Ahv (cm^2/sec)')
set(tl,'FontSize',18)
hold on
```

REPORT OF THE 1999 MONITOR TASK TEAM WORKSHOP

Introduction

Bruce A. Taft, 10580 NE South Beach Drive, Seattle, WA 98110, U.S.A. E-mail: bat65@aol.com
Yasunori Sakurai, Faculty of Fisheries, Hokkaido University, 3-1-1 Minato-cho, Hakodate, Hokkaido, Japan 041. E-mail: sakurai@pop.fish.hokudai.ac.jp

The Task Team met in Vladivostok October 8-10, 1999. The first day was devoted to a workshop on the relationship between planning of a monitoring system for the subarctic N. Pacific within PICES and the international planning activity taking place within the Global Ocean Observing System (GOOS) community. The report is divided into two sections: the first section presents abstracts of papers delivered in the workshop, and the second section summarizes subsequent discussion of issues raised in the workshop and other matters. The second section includes recommendations.

Section I. Workshop Abstracts

Purpose of the MONITOR Workshop on PICES and GOOS

Patricia Livingston
Alaska Fisheries Science Center, National Marine Fisheries Service, NOAA, 7600 Sand Point Way NE, Seattle, WA 98115-0070, U.S.A. E-mail: Pat.Livingston@noaa.gov

The Global Ocean Observing System (GOOS), sponsored by IOC, WMO, UNEP, and ICSU, is a scientifically-based, long-term international program that seeks to provide practical benefits to society through the collection and timely distribution of oceanic data and products, including assessments, assimilation of data into numerical prediction models, the development and transfer of technology, and capacity building. "Operational oceanography" is a term that has been used in international GOOS discussions.

GOOS recently held its first International Agreement Meeting in which there was strong international support for at least some of the GOOS modules, which presently include Climate, Health of the Oceans (HOTO), Living Marine Resources, Coastal, and Services modules. In the North Atlantic, ICES has recently formed a steering group on GOOS that has developed a set of recommendations with regard to their involvement in GOOS activities. PICES nations in the western Pacific are involved in one of the most advanced regional components of GOOS, North-East Asian Regional GOOS. Presently, PICES scientific committees and the CCCC Program are involved in activities that are related to GOOS. We need to begin discussions of how we should move towards advancing a North Pacific GOOS program that meets the needs of PICES member countries. This one-day discussion, held during the PICES CCCC MONITOR Task Team Workshop provided a forum for PICES scientists to learn about GOOS and to develop recommendations for PICES future involvement.

It was certainly appropriate to have held this workshop as part of the PICES GLOBEC CCCC MONITOR Task Team effort. GLOBEC recognizes that some of the monitoring efforts initiated under the GLOBEC umbrella will be considered candidates for long-term monitoring under GOOS. At the regional level, PICES nations are beginning GOOS strategic planning and activities related to the NEAR-GOOS effort, so it is important for us to learn from those efforts but also for us to bring our ecosystem perspective to these programs. There is a great deal of activity and planning going on in the international front and PICES needs to see where these efforts are going. Some of these efforts such as HOTO require that we bring in the expertise and perspectives of our MEQ Committee to discuss their relevance and importance to PICES. The data sharing aspects of GOOS may provide practical benefits to PICES nations as they seek to understand and predict the state of the ocean – a task that requires the sampling efforts and data of more than one nation.

International Global Ocean Observing System Program

Ned Cyr
Ocean Science & Living Resources, Intergovernmental Oceanographic Commission, UNECO, 1 rue Miollis, 75732 Paris Cedex, Fance. E-mail: n.cyr@unesco.org

The Global Ocean Observing System (GOOS) is a sustained coordinated international system for gathering ocean data. GOOS is also a system for processing the data to enable the generation of beneficial products and services as well as the research and development on which such services and products depend for their improvement. Information arising from this long-term, multidisciplinary monitoring will be used to assess present and future states of the oceans in support of their sustainable use, contribute to the prediction of climate change and variability and meet the needs of a wide range of users. GOOS will differ from most present observing systems in the following ways: (1) modeling and forecasting is a part of its mandate as well as data collection; (2) the approach is holistic, integrated and interdisciplinary rather than narrow or sectoral; and (3) it is designed to deliver useful products for both decision-makers and the scientific community.

Planning for GOOS is conducted through four modules: Climate; Living Marine Resources; Coastal and Health of the Oceans. For each module, a strategic design panel has been established to define the requirements of the system in its area. In addition to the observational requirements, the panels also specify the products required by users and the capacity building and data management infrastructure necessary to support the module. The climate and HOTO modules are most advanced with regard to specifying system requirements.

The GOOS Initial Observing System (IOS) is already bringing together relevant international programs under the aegis of GOOS. These ongoing programs are consistent with GOOS design principles. Examples are the TAO array of buoys, the Coral Reef Monitoring Network and the Continuous Plankton Recorder Survey of the Sir Alister Hardy Foundation for Ocean Science. In addition, countries are encouraged to identify national programs which could be considered relevant contributions to GOOS.

Several pilot projects are also being planned to take forward aspects of the GOOS design, including the Global Ocean Data Assimilation Experiment (GODAE) the Array for Real-Time Geostrophic Oceanography (ARGO) and the Pilot Research Array in the Tropical Atlantic

(PIRATA). The main GOOS pilot project, GODAE, is designed to demonstrate the power of integrating satellite and *in situ* data using model data assimilation and the value of a global system capable of working in real time. GODAE is needed for open-ocean analyses and forecasts and to establish boundary forcing for regional models to improve forecasting in coastal systems.

Although the GOOS system is intended to exist indefinitely, the planning phase will be completed by 2010. The strategic design plans should be completed by 2001, during which time a data and information management system also will be developed. From 2000 to 2010 GOOS will be implemented progressively, including the addition of more national and international observing systems and the establishment of additional pilot projects.

There is ample opportunity for closer cooperation between PICES and GOOS. It is suggested that PICES can contribute to GOOS in the following ways: (1) identify existing relevant ocean observations in the subarctic Pacific which could contribute to GOOS; (2) develop an integrated PICES-GOOS plan based on existing routine observations and augmented with new observations as required; and (3) develop a plan to identify and implement transition of relevant North Pacific research activities to routine observations and ultimately data products.

LMR Module of GOOS

Warren S. Wooster
University of Washington, School of Marine Affairs, 3707 Brooklyn Avenue, Seattle, WA 98105-6715, U.S.A. E-mail: Wooster@u.Washington.edu

The LMR Panel met in March of 1998 (Paris) and March 1999 (Montpelier), and is scheduled to meet in Talcahuano, Chile, in December 1999. Initially, the Panel focused on offshore ecosystems, but after the second meeting, coastal fisheries were also assigned to the LMR module (previously they were to be considered by the coastal Panel). Present GOOS plans call for the LMR module to be combined with coastal GOOS and other modules some time in 2000.

Work of the LMR-GOOS Panel is not so advanced as that of other panels because of the relative difficulty of determining which parameters most effectively define the state of a marine ecosystem and which of them can be routinely monitored in a cost-effective way. Monitoring the physical state of the ocean is much easier to conceptualize, development of the technology of the measurements is far advanced, and there are already operational systems in place. In the case of living marine resources, on the other hand, there are few present observing systems on which to build, many of the desired variables are difficult to measure in a routine fashion, and there are few agreed linkages between measured physical and biological variables and desired products such as forecasts of abundance and availability of living marine resources. The latter will depend on improved ecosystem understanding which should result from the work of GLOBEC and other relevant research.

Relevant measurements for LMR range from physics and nutrients up through the various trophic levels to fish, sea birds and marine mammals. A generic table of categories of desired measurements has been developed and is being elaborated to a more specific list in selected regions, for example the Chilean coast. The observing system to determine such parameters must, to the extent possible, depend on remote sensing and on ships of opportunity, since dedicated observing systems will be difficult to fund on a continuing basis.

In the development of the LMR module, some existing monitoring programs have been nominated as components of the Initial Observing System (IOS), and several in the Pacific and Southern Ocean are under consideration. There are also pilot projects, such as the CPR program that is now funded in the northeast Pacific. PICES can help to identify other components of the IOS and other pilot projects in its region, can furnish suggestions for the list of desired measurements and preferred methods of making them, and can otherwise assist in the further development of the Living Marine Resources module.

NEAR-GOOS

Jihui Yan
National Marine Environmental Forecast Center, SOA, 8 Dahuisi Road, Haidian District, Beijing, P.R. China 100081. E-mail: yanjh@axp800.nmefc.gov.cn

NEAR-GOOS is a regional project of GOOS in the western Pacific region that was initiated in 1996. The present participating countries are the People's Republic of China, Japan, the Republic of Korea and the Russian Federation. The aims are to demonstrate the usefulness of a regional observing system in GOOS, to promote free exchange of oceanographic data in real time over the Internet to be used to create daily maps of sea conditions in the marginal seas of the northwestern Pacific and to distribute ocean data to a wide range of marine scientists. At present, the marine environmental data included in the system are physical data such as temperature, salinity, and ocean currents and waves. In the future, biological and chemical variables will be added to the system. Other high priorities are the expansion of the number of contributors and users, development of a uniform data format and improvement of data quality submitted to NEAR-GOOS. NEAR-GOOS collaborates with other relevant programs such as NEAR-HOTO and NOWPAP, and organizations such as PICES.

Status of ICES-GOOS

Robin Brown
Ocean Science and Productivity Division, Institute of Ocean Sciences, P.O. Box 6000, Sidney, B.C., Canada. V8L 4B2. E-mail: brownro@dfo-mpo.gc.ca

ICES has established a Steering Group on the Global Ocean Observing System (SGGOOS). The task of the SGGOOS is to prepare an action plan for how ICES should take an active and leading role in further developments and implementation of GOOS at a North Atlantic regional level with special emphasis on operational fisheries oceanography. In order to help formulate the action plan, a workshop was held in March 1999, in Bergen, Norway. The terms of reference for the workshop were as follows: (1) identify existing ocean observing activities within ICES that are relevant to GOOS; (2) investigate how observations already being made routinely could be combined and enhanced and incorporated within a common plan: (3) propose a possible design for an ICES regional GOOS component; and (4) develop a draft implementation plan for ICES-GOOS. The next steps to be taken by ICES are: (1) to ensure that ICES is represented (formally) at the highest levels in GOOS (I-GOOS and GSC) and to invite

IOS-GOOS representatives to relevant ICES meetings; and (2) to obtain representation on the GOOS Living Marine Resources Panel and thereby influence the planning and in particular to provide assurance that fish are properly incorporated in the panel's activities.

Japan GOOS Program

Takashige Sugimoto
Ocean Research Institute, University of Tokyo, 1-15-1 Minamidai, Nakano-ku, Tokyo, Japan. 164-8639. E-mail: sugimoto@ori.tokyo.ac.jp

The Real-Time Data Base (RTDM) and Delayed-Mode Data Base (DMDB) in Japan are operating successfully. These extensive systems were developed at the Japan Oceanographic Data Center (JODC) prior to GOOS and have a long history of use in Japan. The Japan Meteorological Agency (JMA) produced a Japanese version of the NEAR-GOOS brochure, which will help to promote the development of NEAR-GOOS. A five-year research program is now being implemented by Japanese universities. As part of this study, real-time monitoring of the volume transport and path of the Kuroshio will be carried out, and chemical and biological data in the northwest Pacific will be collected by ships and satellites. The basic goal of this study is to improve understanding of ocean processes through forecasting of temperature, salinity, currents, chemical substances and biological productivity in marginal seas of the western Pacific. It is expected that many of these measurements will become long-term components of GOOS.

Russian GOOS Program

Vyacheslav B. Lobanov
Pacific Oceanological Institute, 43 Baltiyskaya Street, Vladivostok, Russia. 690041. E-mail: pacific@online.marine.su

The Russian national GLOBEC plan is not finally designed and approved. However, GLOBEC-like ecosystem studies of various agencies are included in the list of priority science and development programs adopted by the Ministry of Science and Technologies for the post-perestroika period. One of the major programs among them is the Ecosystem Dynamics project that has been implemented mostly by the institutes of the Russian Academy of Sciences. Other agencies such as the Hydrometeorological Committee, the Committee on Fisheries, the Naval Hydrographic Service and the Ministry of Education (universities) carry on ecosystem studies in accordance with their ministry programs. Because of a lack of funding, the number of monitoring programs were considerably reduced over the last few years, particularly within the last two agencies.

The Hydrometeorological Committee is officially responsible for the monitoring and assessment of environment quality including the marine environment. It maintains a net of meteorological stations and observations along standard hydrographic sections located in the Okhotsk and Japan seas. Data archival and methodological support is provided by the Far Eastern Regional Hydrometeorological Research Institute (FERHRI) (contact: Dr. Yuriy Volkov, Director -

hydromet@online.ru). The Hydrometeorological system provides data on physical forcing related to the oceanic and atmospheric conditions. Observations of temperature, salinity, hydrochemistry at standard levels from the surface down to 1000-1500 m and marine meteorology were obtained along repeated fixed sections since the late 50s; however, by the end of the 90s, a number of operational coastal stations were eliminated and the hydrographic sections program was terminated because of funding cutbacks.

Ecosystem studies by the Committee on Fisheries are focused mostly on higher trophic level organisms and physical forcing. The main organizations dealing with monitoring programs in the North Pacific are the Pacific Research Fisheries Center (TINRO-Center), Sakhalin Research Institute of Fisheries and Oceanography (SakhNIRO) and Kamchatka Research Institute of Fisheries and Oceanography (KamchatNIRO). In the 80s, the TINRO-Center (contact: Dr. Lev Bocharov, Director - root@tinro.marine.su) started regular assessment of demersal/pelagic fishes and invertebrates, zooplankton and ichthyoplankton distribution as well as hydrographic and hydrochemical conditions in the Bering, Okhotsk and Japan seas and Kuril Isl. area. Some cruises also sample nekton, primary production, bacteria and protozoa. CTD measurements are typically done down to 500 m, trawl and acoustic sampling is used to obtain fish distribution data at a typical 30 mi spacing. The surveys cover quite large areas and are repeated annually at particular seasons: March-May - northwestern shelf of the Okhotsk Sea (pollock survey); May-July - western Kamchatka shelf (crab survey); July-September - western Bering Sea (pollock survey); and July-October - Okhotsk Sea (salmon survey). Hydrographic observations are also made along two fixed sections through the Japan Sea (0-200 m) and along a section across the Kamchatka Strait (0-1500 m).

Observations and sampling by SakhNIRO (contact: Dr. Felix Rukhlov, Director - okhotsk@tinro.sakhalin.ru) are very similar to those made by TINRO. Monitoring is principally in a region within 100 mi of Sakhalin Is. in the Okhotsk Sea and Tatar Strait. Hydrography and plankton are observed twice per year along standard sections down to 500-1500 m depth. An annual survey of fishery resources includes juvenile distribution of pollock, herring and cod. Monitoring of salmon is also implemented at fishery plants.

At least three institutes of the Russian Academy of Sciences are engaged in ecosystem monitoring: the Pacific Oceanological Institute (POI), the Institute of Marine Biology (IMB) and the Institute of Automation and Control Processes (IACP). POI (contact: Prof. Victor Akulichev, Director - poi@eastnet.febras.ru) conducts studies of physical forcing and lower trophic levels at various areas of the North Pacific. Long-term monitoring of the water mass and current structure of the western boundary of subarctic gyre (Kuril-Kamchatka area) began in 1990 as the INPOC project, and was then followed by joint surveys with TINRO (1994) and SakhNIRO (1996). The results indicate indicate circulation changes in the area over the 90s which should produce a notable response of higher trophic level organisms. It is expected the survey will be continued on an annual basis. Another area of planned monitoring is the Peter the Great Bay and the adjacent northwestern part of the Japan Sea. Circulation and water exchange in the coastal area, mesoscale eddies and their input to fluxes and ecosystem dynamics are the main topics of the POI studies that are to be conducted as a part of the CREAMS-II program.

The Institute of Marine Biology (contact: Dr. Vladimir Kasiyanov, Director - inmarbio@-mail.primorye.ru) monitors both the lower and the higher trophic levels of the Peter the Great Bay ecosystem. The area of the study is bounded by the Tuman river mouth (Tumangan project) and Amursky Bay.

Inter-Institute Center for Satellite Monitoring of the Environment (contact: Dr. Emil Herbeck herbeck@iapu2.marine.su) has been recently established by IACP, POI and TINRO. This center will maintain monitoring of the Japan and Okhotsk seas based on NOAA AVHRR and

SeaWiFS thermal and ocean color imagery measurements.

In relation to Russian plans for ecosystem monitoring, the following issues should also be discussed: feasibility of implementation, methods of observations and data quality control, and data accessibility. In many cases, even when the project is approved, its implementation depends on funding availability. Even if the allocated funds do not allow full implementation, partial implementation is often possible. Special attention should be given to the methods of measurement, sampling design, analysis and data quality control. This is especially critical in the construction of long time series. Data availability for the international oceanographic community may also be a serious issue. Information on some physical and hydrochemical parameters in some areas of marginal seas may be restricted for international exchange.

Besides national plans, Russia is already involved in international projects related to monitoring of the North Pacific such as NEAR-GOOS and NOWPAP (contact: water@unep.org). The NEAR-GOOS project is the North-East Asian Regional component of the Global Ocean Observing System (GOOS) initiated by the IOC Sub-Commission for Western Pacific (WESTPAC). Participating countries are China, Japan, Korea and Russia. The area of interest covers Japan, and the East-China and Yellow seas. The scope of the project is to facilitate the exchange of marine environmental data through a system of real-time and delayed-mode data base that should provide free internet access for any user. The environmental parameters included in the system are so far focused on physical data in order to ensure the successful initiation of the operation. With the operation of the system well underway and given the requirements of the user community, it is necessary to extend the variables included in the system to include chemical and biological data. At present the Russian contribution to the NEAR-GOOS data exchange system includes marine meteorological data which are being contributed to the Real Time Data Base by FERHRI. POI has made available previously classified data from 13,628 oceanographic stations for international data exchange under the IODE/GODAR project. These data may now be contributed to the NEAR-GOOS Delayed Mode Data Base. For further development of the NEAR-GOOS program in Russia, it is required (a) to determine the regulations for international data exchange for the NEAR-GOOS program at the national level; (b) to provide necessary funds for NEAR-GOOS activities; and (c) to improve the telecommunication system in the country. The last one is extremely important in order to involve more users and contributors to the NEAR-GOOS data base (NEAR-GOOS contact: http://www.unesco.org/ioc/goos/neargoos.htm).

An additional international project which has similar objectives as NEAR-GOOS covers a similar geographic area and involves the same countries, but covers a much wider range of marine, coastal and associated fresh water environments, is the Action Plan for Protection, Management and Development of the Marine and Coastal Environment of the Northwest Pacific Region (Northwest Pacific Action Plan - NOWPAP). It was established in 1994 under the United Nations Environment Program as one of the components of its Regional Seas Program. NOWPAP includes a sub-project focused on the establishment of a collaborative, regional monitoring program that is developing jointly with IOC/WESTPAC. The last Inter-governmental Meeting on NOWPAP suggested the establishment of a regional monitoring center to co-ordinate activity of participating countries (contact - water@unep.org).

In summary, Russia still has plans for large-scale ecosystem monitoring of the Northwest Pacific and marginal seas. Its execution depends on the economic situation in the country and availability of national funds. Russia can offer resources for cooperation with the international marine science community, which includes experienced research groups, individual scientists and a large research fleet.

Contributions to this report by Drs. Yury Zuenko and Gennady Khen of TINRO and Gennady Kantakov of SakhNIRO are highly appreciated.

People's Republic of China GOOS Program

Jihui Yan
National Marine Environmental Forecast Center, SOA. 8 Dahuisi Road, Haidian District, Beijing, P.R. China 100081. E-mail: yanjh@axp800.nmefc.gov.cn

Data are collected at 14 coastal observation stations distributed between Xiaochangshan in the Bohai Sea and Zhelang in the East China Sea. This data base includes waves, SST and marine meteorological parameters. Real-time data can be accessed by all users via the Internet.

USA GOOS Program

Bruce A. Taft
10580 NE South Beach Drive, Seattle, WA 98110, U.S.A. E-mail: bat65@aol.com

The primary focus of the USA GOOS Climate Module Committee has been the execution of program ARGO (Array for Real-time Geostrophic Oceanography). This program was originally proposed by a group of USA scientists and is now in the process of being developed as an international program under the GOOS banner. The plan is to deploy globally a large number of Palace floats to measure profiles of temperature and salinity in the upper 2000 m of the ocean. In addition, measurements of velocity are obtained at the level where the floats drift before they periodically ascend to the surface to broadcast profile data to a satellite receiver. The resulting data set will be used to estimate the geostrophic component of the velocity field.

The Committee is presently working on the following aspects of the program: (1) develop algorithms to calculate salinity from the temperature, conductivity and pressure data; (2) consider development of an improved system for preparing and telemetering the profile for ultimate assimilation into numerical models; and (3) the transports in the narrow western boundary currents will not be measured by the floats and a supplemental system needs to be designed.

The present plan is to obtain 3×3 degree coverage in space with a 10 day time step. Initial deployments would begin in the SE Pacific. On this schedule the Subarctic Pacific would be seeded in 2-3 years. Commitments to the global program are currently 80-85% of what will be needed.

Canada GOOS Program

Robin Brown
Ocean Science and Productivity Division, Institute of Ocean Sciences, P.O. Box 6000, Sidney, B.C., Canada. V8L 4B2. E-mail: brownro@dfo-mpo.gc.ca

GOOS Climate Module

Canada has discussed in some detail potential contributions to the GOOS/GCOS climate module, but recommendations at this point are not matched with funding resources. Highest priority has been given to the following projects: (1) five geocentrically positioned tide gauges (two on the east coast, including one new gauge on the Labrador coast, two on the west coast and a new gauge in the Arctic); (2) continuation of the research-based time series on Line P and at the site of the OWS P in the Pacific, at the site of OWS Bravo, and on an annual section across the Labrador Sea; and (3) a substantial (possibly 5% of the global array) contribution of profiling floats to the ARGO program. Canada would consider providing floats in regions outside areas adjacent to the Canadian coast, should the contributions of other nations provide regional coverage in areas of particular Canadian interest. Slightly lower priority has been given to carrying out one transocean section off both the east and west coasts every eight years for the assessment of the inventories and transports of heat, salt and carbon.

Enhancements to GOOS Climate and Coastal Modules

This contribution involves augmentation of the physical ocean observing system. (1) Seasonal sampling of the water properties on Canada's continental shelves and marginal seas (including the Arctic), using hydrographic sections and time series stations (roughly 12 sections and 8 time series stations on the east coast, 9 sections and a moored climate station on the west coast and an annual hydrographic survey in the Beaufort Sea region of the Arctic Ocean). (2) Enhancement of the tide gauge network, some of which would be geocentrically positioned (roughly 6 gauges on the east coast, 4 gauges on the west coast and 1 in the Arctic). These gauges would be in addition to those designated for the climate module. (3) Direct measurement of the volume transport on the Labrador shelf and through the Canadian archipelago. (4) Observations of sea-ice concentration, extent and velocity both off the coast of Labrador, in the Gulf of St. Lawrence and in the Canadian Arctic. The extent to which these measurements will contribute to the GOOS observing system depends on the final design of the climate module monitoring system.

Living Marine Resources (LMR) and Health of the Ocean (HOTO) Modules

Potential Canadian contributions to the HOTO and LMR modules are less clear than for the case of the Climate module because of the generally less advanced state of both GOOS and Canadian planning in these areas. However, under the "Canada Oceans Act", Canada has placed considerable emphasis in developing coastal zone management strategies and designating various ecologically sensitive areas as "Marine Protected Areas". Furthermore, Canada does have operational programs in these areas, especially as they relate to fisheries, fish habitat and overall marine environmental quality. In an effort to evaluate the effectiveness of current monitoring programs in meeting Canada's ecosystem objectives for integrated ocean management and conservation, a Canadian workshop will be held in the fall of 1999. It is expected that, in addition to addressing Canadian issues, this workshop will clarify Canada's input to the design of the LMR module and better indicate how Canada could most effectively contribute to this aspect of GOOS.

INTERNATIONAL PROGRAMS RELATED TO GOOS

International Data Buoy Cooperation Panel

Robin Brown
Ocean Science and Productivity Division, Institute of Ocean Sciences, P.O. Box 6000, Sidney, B.C., Canada. V8L 4B2. E-mail: brownro@dfo-mpo.gc.ca

The Data Buoy Cooperation Panel (DBCP), which was formally established in 1985, is an official joint body of the World Meteorological Organization (WMO) and the Intergovernmental Oceanographic Commission (IOC). It is a part of the WMO Marine Program and is planned for integration within the Global Ocean Observing System (GOOS) as a GOOS existing system. The Panel members are representatives of all members of WMO or member states of IOC which are interested in participating in its activities (present representatives are from Australia, Canada, France, Greece, Iceland, Ireland, Netherlands, New Zealand, Norway, South Africa, United Kingdom and U.S.A.).

Principal objectives of the DBCP are: (1) review and analyze requirements for buoy data; (2) co-ordinate and facilitate deployment programs to meet requirements; and (3) initiate and support action groups; (4) improve quality and quantity of buoy data distributed on the Global Tele-communication System (GTS); (5) information exchange and technology development; and (6) liaison with relevant bodies and programs.

The next DBCP meeting will be held in Wellington, New Zealand, on October 26-30, 1999. Canada will be hosting a DBCP meeting in Victoria, B.C., on October 16-20, 2000. PICES members involved in oceanographic or meteorological programs, particularly involving drifting or moored buoys, are invited to attend.

PICES CCCC Program, MONITOR Task Team and the CPR Initiative

David W. Welch
Department of Fisheries & Oceans, Pacific Biological Station, 3190 Hammond Bay Road, Nanaimo, B.C., Canada. V9R 5K6. E-mail: WelchD@pac.dfo-mpo.gc.ca

It is well known that there are large changes in the size of commercial fish populations in the subarctic North Pacific on decadal time scales. These changes are associated with changes in the atmospheric forcing (displacement and change of strength of Aleutian and Arctic lows) and sea-surface temperature in the region. In order to understand the dynamics of the responses of the biological populations to large-scale air-sea interaction it is necessary to measure the changes in productivity of the ecosystem. A recent example from the N. Atlantic system illustrates the problem. Studies have shown that there is a strong statistical relationship between the phase of the North Atlantic Oscillation (NAO) and plankton abundance (Fromentin and Plaque, 1996). However, in 1996-97 there was a strong phase shift in the NAO without a concomitant change in the plankton population (Planque and Reid, 1998). Without the data from the N. Atlantic Continuous Plankton Recorder (CPR) survey of zooplankton, it would have been incorrectly presumed that the plankton populations also changed in the previously established way.

In its first meeting, the PICES MONITOR Task Team recommended that systematic, large-scale measurements of interannual variability of N. Pacific zooplankton composition and abundance be initiated. It was pointed out that there was a continuing observational program in the N. Atlantic which had successfully measured large-scale plankton variability that was significantly correlated with physical climate signals. The collection device is the CPR which is towed by ships-of-opportunity on monthly transects of the N. Atlantic. The CPR was first used in 1931 and its sampling characteristics are well documented.

In 2000, a two-year pilot CPR sampling program will be started in the N. Pacific under the leadership of Drs. David Welch (Canada) and Sonia Batten (UK). Two lines of sampling will be run: a north-south run (line A) from Prince William Sound, Alaska, to Long Beach, California; and an east-west run (line B) on a great circle route between Vancouver, British Columbia, and Yokohama, Japan (Fig. 1). Line A (proceeding southward) samples Prince William Sound, the offshore region feeding the shelf downwelling zone, the center of the Gulf of Alaska Gyre, the Subactic Transition Zone and finally crosses the CALCOFI grid off California. Line B (proceeding westward) runs parallel to Canadian Line P, cuts across the shelf at the tip of the Alaska Peninsula and then runs northward of the Aleutians before it returns to the N. Pacific near the dateline. The short-term research objective is to obtain data on the time and spatial structure of the near-surface plankton variability along these tracks. The data set will be used to help in the design of a long-term zooplankton sampling program for the N. Pacific which will be able to monitor climate change variability. Of course, there will be advances over time in the technology of estimating plankton abundance. Future plankton monitoring schemes will incorporate these improvements.

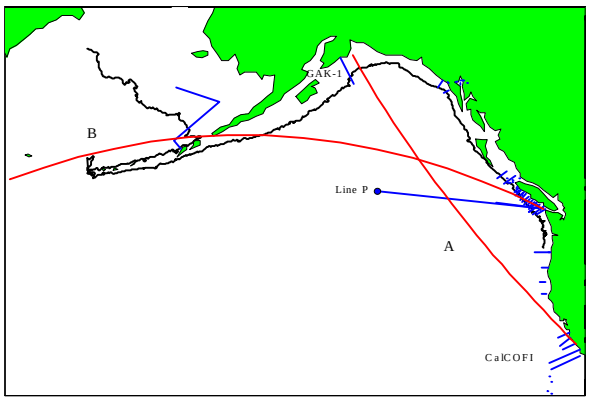

Fig. 1 Funded CPR transects. Line A is an oil tanker route, and Line B is a container ship route. Line A will be run 5 times in 2000 and again in 2001. Line B will be run once each year.

The CPR measurements represent the present best choice to collect a time series that will provide insights into the statistical characteristics of basin-scale climate change variability. PICES investigators would like to see this program imbedded in the initial GOOS plan and expect to work with GOOS to develop a long-term strategy to develop a climate change plankton data base for the subarctic N. Pacific.

Responsibility for the CPR program resides presently with the two leaders and a Scientific Advisory Board. The Board members are Drs. Michael M. Mullin, Charles B. Miller, Jeffrey M. Napp (U.S.A.), David L. Mackas (Canada) and Richard D. Brodeur (U.S.A.).

Section II. Summary of Task Team Discussion and Recommendations

1. Status of shipboard sampling in the subarctic Pacific

David W. Welch
Department of Fisheries & Oceans, Pacific Biological Station, 3190 Hammond Bay Road, Nanaimo, B.C., Canada. V9R 5K6. E-mail: WelchD@pac.dfo-mpo.gc.ca

In order to determine the present subarctic observational programs that are being carried out that contribute to the climate observing system, a survey was undertaken. This study serves two functions: (1) gaps in time and space coverage of the physical, chemical and biological climate variability are clearly identified; and (2) specific efforts can be made to ensure that key elements of present monitoring work are identified and supported within GOOS. The sampling carried out on these ships generally covers physical, chemical and biological variables.

There are significant differences in the east-west coverage and sampling is not uniform among the various ships and surveys because different measurement techniques are employed on different ships (Fig. 2). Nevertheless, the broad outline of Pacific monitoring programs is clear, with the western Pacific near Japan being much more intensely covered than the eastern Pacific, reflecting the long-term programs initiated and carried out by the Japanese. Similar programs occur in the eastern Pacific (California Current survey (CalCOFI, U.S.A.), Ocean Station PAPA line (Canada), and the GAK line south of Seward, Alaska (U.S.A.)) but the overall coverage is lower. The only substantial open ocean monitoring effort is the Canadian Line P program, with most other monitoring work confined to coastal or near-coastal waters.

A significant difference in the level of monitoring is evident when monitoring locations are restricted to locations where sampling occurs at least twice per year (Fig. 3). These observations are particularly important because shifts in seasonality are likely to be detected only when multiple samples are taken. Wintertime observations are less frequent than summer observations because of the difficulties of operating most research vessels in heavy weather. Ship-of-opportunity (SOP) lines are less dependent on weather and may be able to provide more data in winter.

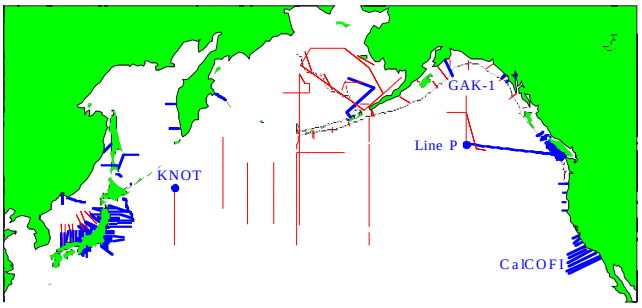

Fig. 2 Summary of on-going monitoring efforts in the PICES arena. The figure shows all locations sampled at least once per year.

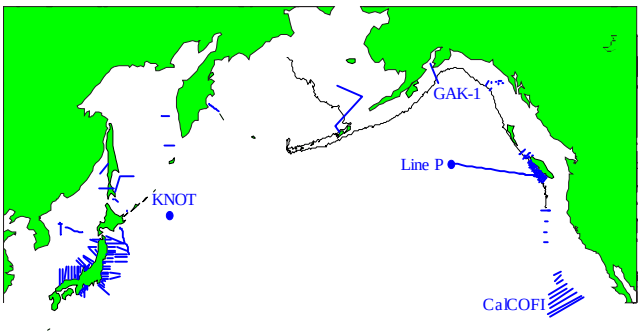

Fig. 3 The same chart as Figure 2, but restricting the definition of monitoring to sampling that occurs two or more times per year. Very little of the North Pacific is adequately monitored if seasonal variation occurs.

2. Time series stations in the subarctic North Pacific

a. Moored measurements in the eastern subarctic Pacific

Bruce A. Taft
10580 NE South Beach Drive, Seattle, WA 98110, U.S.A. E-mail: bat65@aol.com

There are a number of ecological problems that require high time-resolution measurements of physical and biophysical variables. Because the time scales of many biological processes are relatively short, it is necessary to resolve the high-frequency fluctuations in order to accurately represent the longer time-scale variability. Moored instruments are required to obtain the needed data sets. Shipboard sampling is too coarse in time and satellite measurements do not represent the vertical structure of the variability. In the subarctic the conditions are harsh and new mooring designs are required to withstand the extreme environmental stresses. In addition, new sensors need to be designed and evaluated to measure biophysical and chemical variables. Some prototype instruments capable of being moored do exist (pCO_2, nitrate, transmissometer, and fluorometer).

The Task Team was supportive of the pilot studies which have been initiated to moor suites of meteorological and oceanographic instruments in the subarctic. The measurements are relayed to satellite daily. A two-year program has been undertaken by the Pacific Marine Environmental Laboratory of NOAA near OCEAN Station PAPA (50°N 145°W). The first mooring was deployed in September 1998, and replaced with another in September 1999. In 1999 a second mooring was placed to the south in a more benign region in the subtropical gyre at 35°N 165°W. The subsurface measurements were successful on the first mooring but the surface instruments (largely meteorological) were lost in a severe storm after six months.

The Task Team concludes that there will be a large scientific payoff for these efforts and recommends that these scientific and engineering studies be continued until the engineering problems are solved. Mooring time series are necessary to successfully diagnose the relationships between meteorological forcing and physical and biological response in the ocean. Moorings are expensive and vast arrays are not possible. The best use of the technique is to measure the vertical distribution of the variables in a region where the horizontal currents and advection are weak, under these conditions the pattern of time evolution of events below the surface can be documented and the processes surmised.

b. Time series measurements in the western subarctic Pacific

Yukihiro Nojiri
Global Warming Research Laboratory, National Institute for Environmental Studies, 16-2 Onogawa, Tsukuba, Ibaraki, Japan. 305-0053. E-mail: nojiri@nies.go.jp

A new Japanese time series was begun by NIES/JST (Japan Science and Technology Corporation) in June 1998. The station is referred to as KNOT (Kyodo North Pacific Ocean Time Series). The station is located at 44°N 155°E in the western region of the eastward-flowing Subarctic Current. The time series is maintained by Japanese research ships-of-

opportunity occupying the KNOT station when passing near the site. The suite of physical, chemical and biological measurements made depends on the capability of the scientific party aboard the vessel. The station was occupied by 13 visits from June to December 1998, and 10 visits from May to October 1999. In the future, sediment traps will be deployed at KNOT.

3. Measurement of temperature/salinity profiles with PALACE floats

Robin Brown
Ocean Science and Productivity Division, Institute of Ocean Sciences, P.O. Box 6000, Sidney, B.C., Canada. V8L 4B2. E-mail: brownro@dfo-mpo.gc.ca

Planning for a global program to measure the distributions of temperature and salinity in the upper 2000 m is now underway. The technique is to deploy an array of PALACE (profiling ALACE) floats on a 300×300 km grid. The Palace float is designed to sink to a depth of 2000 m where it will drift with the current until its buoyancy is internally modified so the float will rise to the surface; a CTD is mounted on the float which measures the profiles of temperature and salinity on the ascent. At the surface, the float is programmed to send the temperature and salinity data to a satellite. The position of the float at the time of transmission is determined so that an estimate of the current at 2000 m can be determined from the displacement of the float over the time interval of submersion. After the data has been transmitted, the float sinks to 2000 m to begin another cycle. With these data, the geostrophic current can be calculated. The time between ascents will probably be 10 days. The measurement system is termed APEX (Autonomous Profiling Explorer). The array is referred to as ARGO (Array for Real-time Geostrophic Oceanography).

These data will be assimilated into a general circulation numerical model in support of the GODAE (Global Ocean Data Assimilation Experiment) which is a component of the global climate observing system now being planned. The goal of GODAE is to demonstrate the feasibility of routine, real-time global ocean data assimilation and prediction.

The present communication system uses System Argos; new improved satellite systems are under consideration. Transmissions are lost if weather is poor (40% data loss occurs in rough weather). Since the data are transmitted many times, the chance of successful transmission is high. Deployment from high speed commercial ships-of-opportunity is straightforward. System Argos positions are accurate to 150 m. The accuracy of the deep velocity measurement depends on the rate of the rise of the instrument and the parking time of the float at depth. If the float is left at the surface for one inertial period, useful measurements of surface current can be made. Cost of the instrumented floats is about $14K. In the early days salinity measurements were of poor quality because of fouling of the conductivity cell by biological organisms. The use of anti-fouling paint appears to have alleviated this problem for periods up to 3 years.

Commitments to fund ARGO have been forthcoming. At present countries expected to supply floats are U.S.A., Canada, Japan, Australia, United Kingdom, France and Germany. The deployment strategy and the development of a tracking and data distribution facility are presently being worked out.

PICES will benefit greatly from the existence of an ARGO array in the subarctic Pacific. In particular, the availability of a well-measured salinity field will make it possible to look at a large number of scientific questions that at present cannot be addressed because of the lack

of knowledge of the vertical density structure. The Task Team recommends that PICES volunteers to assist in the deployment of the float by offering platforms from which the floats can be launched. PICES is in a unique position to help this program because its member nations operate a number of research vessels in remote parts of the subarctic region.

4. Calibration studies of sampling gear

Stewart M. McKinnell
PICES Secretariat, c/o Institute of Ocean Sciences, P.O. Box 6000, Sidney, B.C. Canada. V8L 4B2. E-mail: mckinnell@ios.bc.ca

A wide variety of sampling gear has been used historically to measure zooplankton abundance. In order to create high-quality climate time series of zooplankton abundance, systematic errors that arise by combining measurements made with different sets of gear must be addressed. Calibration of various systems must be undertaken to resolve this source of error. The Task Team is undertaking a survey of the scope of the problem. At the 1999, meeting results of a comparison of the performance of the NORPAC and SCOR plankton sampling nets (differing mouth size and same mesh size) were presented. Results of this study show that on the order of 40 pairs of measurements were needed to estimate quantitatively the difference in sampling characteristics of the two systems. It is clear that significant ship-time resources will be required to deal with the multiplicity of systems that have been used historically to collect zooplankton samples in the North Pacific. The Task Team will facilitate further critical comparison studies.

5. Revising of MONITOR Task Team Terms of Reference

Patricia Livingston
Alaska Fisheries Science Center, National Marine Fisheries Service, NOAA, 7600 Sand Point Way NE, Seattle, WA 98115-0070, U.S.A. E-mail: Pat.Livingston@noaa.gov

Discussions at the PICES GOOS workshop held October 8-9, 1999, led to the following recommendation to modify the terms of reference of the MONITOR Task Team. The new activities of MONITOR will focus on developing an action plan that will assist in the implementation of GOOS at a North Pacific level and will assist in the transition of PICES GLOBEC monitoring activities to long-term monitoring activities of PICES-GOOS. It was also decided that the action plan would: (1) identify existing ocean observations in the coastal and open N. Pacific that are relevant to GOOS; (2) develop a PICES-GOOS implementation plan based on existing routine observations and augmented by new observations as appropriate; and (3) provide a structured plan on how to move relevant CCCC Program activities to a PICES-GOOS program.

TERMS OF REFERENCE

1. Review existing activities of PICES member nations and to suggest improvements in the monitoring of the Subarctic Pacific to further the goals of the CCCC Program;

2. Consult with REX, BASS and MODEL Task Teams and TCODE on the scientific basis for designing the PICES monitoring system. Questions of standardization and inter-calibration of measurements, particularly in the area of biological collections, should be addressed;

3. Assist in the development of a coordinated monitoring program to detect and describe events, such as El Niño, that strongly affect the Subarctic;

4. Develop a PICES-GOOS action plan for how PICES should take an active and leading role in the further development and implementation of GOOS at a North Pacific level. The action plan would:

   i. identify existing ocean observations in the coastal and open North Pacific that are relevant to GOOS;
   ii. develop a PICES-GOOS implementation plan based on existing routine observations and augmented by new observations as appropriate;
   iii. provide a structured plan on how to move relevant CCCC Program activities to a PICES-GOOS program.

5. Advise and support the CCCC Implementation Panel and Science Board on GOOS-related matters, including representing PICES at key GOOS planning meetings.

REPORT OF THE 1999 REX TASK TEAM WORKSHOP

Herring and Euphausiid population dynamics

Spatial, temporal and life-stage variation in herring diets in British Columbia

Douglas E. Hay and Bruce McCarter
Pacific Biological Station, 3190 Hammond Bay Road, Nanaimo, B.C., Canada. V9R 5K6
E-mail: hayd@pac.dfo-mpo.gc.ca

Over the last 70 years in British Columbia (B.C.), herring stomachs have been examined by different people, in different years, at different places and at different herring life history stages. This brief report summarizes this information and attempts to provide some general conclusions.

Wailes (1935) summarized the food of young herring mainly in the first summer of life. At very young stages, eggs (ova) and nauplii from various invertebrates are most important. Copepod nauplii seem to dominate the food. Wailes noted that food varies with location and concluded that young herring fed on whatever food source was available. A more recent project (1990-1994) gathered data on juvenile herring stomach contents in Georgia Strait, B.C. The juveniles were distinguished by size and age as age 0+ (3-6 months), 1+ (15-18 months) and 2+ (29-32 months). The youngest juveniles (age 0+) fed mainly on copepods. The older and larger juveniles took various zooplankton, with euphausiids being common in the largest fish. The data indicate that diets and juvenile growth varied among areas. There are a number of reports commenting on the diets of herring off the southwestern coast of B.C., and many comment on the frequency of euphausiids (mainly *Euphausia pacifica*, in herring guts. This euphausiid species also is known to be a major component in the diets of other species, such as hake (*Merluccius productus*). One example of the intensity of feeding was made by examination of stomach weights of herring feeding on *E. pacifica* during the fall of 1979. Most guts examined contained *E. pacifica*. In some individuals the gut weight was approximately 20% of their total body weight. In contrast to the apparently high incidence of euphausiids in southern BC herring adults, northern BC herring appear to rely more on copepods. Adult herring guts, from Hecate Strait in northern BC were sampled in the summer and winter of 1985 and 1987 (Tables 1 and 2). The data indicates that copepods were dominant in the diets of herring in 1985 and that euphausiids and amphipods were more common in 1987. In general, the composition of food appeared to be more varied than that of herring found in southern B.C.

Some general conclusions from this brief review are that herring diets vary with: (1) life history stage (compared in the same time and place, herring food varies with size and age); (2) space (compared among herring of same size and age, there are different food items among different locations), (3) time (food varies among seasons but within the same place and among years, compared at the same place).

In general, larval herring rely mainly on copepods with the main diet consisting of copepod eggs and nauplii. Juvenile herring ($<$ 1 year) eat mainly copepods (in BC) but older juvenile herring ($>$ 1 year) eat many items. The incidence of euphausiids increases with juvenile size. Adult herring diets vary: euphausiids are important, but so are copepods in some areas.

This review does not address the major issues

regarding the relationship between zooplankton and herring. Perhaps the major question concerns the relationship(s) between plankton abundance and herring, and how it affects herring growth, population size and recruitment? One may ask: after more than a century of research in this area, why do we not understand it better? A partial answer is that we have lack suitable time-series data on plankton abundance. Further, we know enough to understand that the relationships may be complex and affected by factors that we are only beginning to realize are important.

Reference:

Wailes, G.H. 1936. Food of *Clupea pallasii* in southern British Columbia. J. Biol. Bd. Can. 1: 477-486.

Table 1 Prey species found in herring stomachs from Hecate Strait in 1985.

Fishing date				*Total*		PREY SPECIES
Jul-Aug 1985		*Nov-Dec 1985*				
Wgt (*g*)	%	Wgt(*g*)	%	Wgt (*g*)	%	
328.379	64.5	0.019	0.1	328.398	61.0	*Calanus pacificus*
94.231	18.5	0.983	3.4	95.214	17.7	*Thysanoessa spinifera*
23.432	4.6	1.088	3.8	24.520	4.6	Arthropoda
23.680	4.6	0.218	0.8	23.898	4.4	*Parathemisto spp.*
0.016	0.0	16.914	58.7	16.930	3.1	*Euphausia pacifica*
11.759	2.3	1.644	5.7	13.403	2.5	Copepoda calanoida
1.023	0.2	7.243	25.1	8.266	1.5	Monstrilloidae
6.644	1.3	0.000	0.0	6.644	1.2	*Calanus cristatus*
4.233	0.8	0.000	0.0	4.233	0.8	*Metridia okhotensis*
3.975	0.8	0.003	0.0	3.978	0.7	*Euchaeta elongata*
3.609	0.7	0.000	0.0	3.609	0.7	*Calanus plumchrus*
2.734	0.5	0.000	0.0	2.734	0.5	*Cancer spp.* zoea & megalops
1.994	0.4	0.000	0.0	1.994	0.4	*Hyperia spp.*
1.141	0.2	0.000	0.0	1.141	0.2	Chaetognatha
0.364	0.1	0.271	0.9	0.635	0.1	Euphausiid remains
0.041	0.0	0.272	0.9	0.313	0.1	*Cyphocaris challengeri*
0.293	0.1	0.015	0.1	0.308	0.1	Fish
0.253	0.0	0.000	0.0	0.253	0.0	*Natantia* (shrimp) zoea
0.225	0.0	0.015	0.1	0.240	0.0	*Calanus spp.*
0.230	0.0	0.000	0.0	0.230	0.0	*Primno spp.*
0.212	0.0	0.000	0.0	0.212	0.0	*Gaidius pungens*
0.136	0.0	0.000	0.0	0.136	0.0	Ostracoda
0.117	0.0	0.000	0.0	0.117	0.0	*Candacia columbiae*
0.082	0.0	0.026	0.1	0.108	0.0	Mysidaceae
0.000	0.0	0.070	0.2	0.070	0.0	Fossaridae
0.070	0.0	0.000	0.0	0.070	0.0	*Pleuromamma quadrungulata*
200		*150*		*350*		Number of stomachs examined

Table 2 Prey species found in herring stomachs from Hecate Strait in 1987 (prey counts converted to weights using 1985 average weight/species).

Fishing date				*Total*		
July 1987		*Nov. 1987*				PREY SPECIES
Wgt (*g*)	%	Wgt (*g*)	%	Wgt (*g*)	%	
1.829	2.6	65.243	48.0	67.073	32.7	*Parathemisto spp.*
41.452	59.7	21.747	16.0	63.199	30.8	Euphausiidae
14.113	20.3	16.388	12.1	30.501	14.9	*Euphausia spp.*
1.840	2.6	23.238	17.1	25.078	12.2	Copepoda calanoida
7.778	11.2	6.364	4.7	14.142	6.9	*Thysanoessa spp.*
0.006	0.0	1.272	0.9	1.278	0.6	*Oikopleura*
0.721	1.0	0.203	0.1	0.924	0.5	*Metridia spp*
0.867	1.2	0.000	0.0	0.867	0.4	*Cancer spp*
0.147	0.2	0.499	0.4	0.646	0.3	Hyperiidae
0.215	0.3	0.088	0.1	0.303	0.1	*Cyphocaris spp.*
0.000	0.0	0.285	0.2	0.285	0.1	*Mesocalanus spp.*
0.177	0.3	0.077	0.1	0.254	0.1	*Calanus spp.*
0.116	0.2	0.007	0.0	0.123	0.1	*Neocalanus spp.*
0.114	0.2	0.006	0.0	0.120	0.1	*Euchaeta spp.*
0.000	0.0	0.118	0.1	0.118	0.1	*Corycaeus spp.*
0.009	0.0	0.081	0.1	0.090	0.0	*Pseudocalanus spp.*
0.000	0.0	0.058	0.0	0.058	0.0	*Acartia spp.*
0.009	0.0	0.046	0.0	0.055	0.0	*Primno spp.*
0.034	0.0	0.002	0.0	0.037	0.0	Paguridae
0.013	0.0	0.022	0.0	0.036	0.0	*Epilabidocera spp.*
0.013	0.0	0.022	0.0	0.036	0.0	Amphipoda
0.000	0.0	0.014	0.0	0.014	0.0	*Scolecithricella spp.*
0.002	0.0	0.011	0.0	0.014	0.0	*Limacina helicina*
101		*350*		*451*		Number of stomachs examined

Over winter energy changes in herring from Prince William Sound, Alaska

Augustus J. Paul and J. M. Paul
University of Alaska, Institute of Marine Science, Seward Marine Centre Laboratory, Seward, AK 99664, U.S.A. E-mail: ffajp@aurora.alaska.edu

During the fall of 1995 and spring of 1996, the whole body energy content (WBEC) of *Clupea pallasi* from Prince William Sound (PWS), was examined. Somatic energy exhibited a wide range of values relative to length (SL). In the fall age 0 recruits had an average of 5.7 $kJ \cdot g^{-1}$ wet wt for whole body samples vs 8.0 for age 1 and 0.4-10.2 $kJ \cdot g^{-1}$ for fish of ages 2 to 7. The following spring the 1995 year class, which had just survived their first winter, averaged 4.4 $kJ \cdot g^{-1}$ wet wt for somatic samples, and age 1 fish had similar values, while herring ages 2 to 7 had WBEC > 5 $kJ \cdot g^{-1}$. The fall measures of WBEC showed the young-of-year and age 1 fish stored markedly less energy for overwintering than older herring.

In PWS many sea birds prey on juvenile herring. During the spring and summer, we examined WBEC of herring $\leq$ 165 mm SL.

From May to October, somatic energy ($kJ \cdot g^{-1}$ wet wt) exhibited a wide range of values relative to SL. Young of the year recruits appeared in July and had WBEC of 2-3 $kJ \cdot g^{-1}$ wet wt after metamorphosis and older fish had WBEC of 4-6 $kJ \cdot g^{-1}$ wet wt. By October the WBEC of juvenile herring was typically 4-6 $kJ \cdot g^{-1}$ wet wt.

Age 0 Pacific herring were surveyed in October of 4 years. There were distinct regional and interannual variations in SL and WBEC for individual groups of herring. Likewise within each collection there was typically a large range of size and WBEC values.

Changes in WBEC of captive age 0 herring forced to fast during winter was measured and compared to cohorts collected in the field. Somatic energy content of fasting captives declined at a rate of 23 $kJ \cdot g^{-1}$ wet $wt \cdot d^{-1}$ from 1 December 1995 to 25 January 1996 at mean temperature of 6.6°C. In another observation, fish captured on 1 December 1995 and held without feeding until 1 April 1996 had an average WBEC that changed from 5.2 to 3.2 $kJ \cdot g^{-1}$ wet wt during captivity at ≈5.2°C. Fish that died during fasts had WBEC values ranging from 2.8 to 3.6 $kJ \cdot g^{-1}$ wet wt. During March 1996 the WBEC of field collected age 0 herring averaged 3.8 $kJ \cdot g^{-1}$, with ≈40% having WBEC ≤ 3.6 $kJ \cdot g^{-1}$ wet wt. Thus, by March the average recruit had used most of its stored energy.

These observations on WBEC of Pacific herring determined that in PWS, storing enough energy to survive the first winter is an important hurdle in the recruitment process. Energetically, the recruiting year class, and those entering their second winter, are the most at risk of nutritionally related overwinter mortality. When modelling the transfer of energy from herring to predators fish age, time of collection, site of collection, SL, body wt all modify WBEC. Even within age groups or schools there is a wide range in WBEC values which must be taken into account when producing consumption models.

References

Paul, A. J. and J. M. Paul. 1999. Interannual and regional variations in body length, weight and energy content of age 0 Pacific herring from Prince William Sound, Alaska, *J. Fish Biol.* 54(5): 996-1001.

Paul, A. J. and J. M. Paul. 1998. Spring and summer whole body energy content of Alaskan juvenile Pacific herring. *Alaska Fishery Res. Bulletin*. 5(2): 131-136.

Paul, A. J. and J. M. Paul. 1998. Comparisons of whole body energy content of captive fasting age zero Alaska Pacific herring (*Clupea pallasi Valenciennes*) and cohorts over-wintering in nature. *J. Exp. Mar. Biol. Ecol.* 226: 75-86.

Paul, A. J., J. M. Paul and E. D. Brown. 1998. Fall and Spring somatic energy content for Alaskan Pacific (*Clupea pallasi*) relative to age, size and sex. *J. Exp. Mar. Biol. Ecol.* 223: 133-142.

Foy, R. J. and A. J. Paul. Winter feeding and changes in somatic energy content for age 0 Pacific herring in Prince William Sound, Alaska. *Trans. Amer. Fish. Soc., in press.*

Qualitative texture characteristic of herring (*Clupea pallasi pallasi*) pre-larvae developed from the natural and artificial spawning-grounds in Severnaya Bay (Peter the Great Bay)

N. G. Chupisheva
Pacific Research Institute of Fisheries & Oceanography (TINRO-Centre), 4 Shevchenko Alley, Vladivostok, Russia 690600. E-mail: root@tinro.marine.su

Some authors consider the frequency of morphologically deformed herring larvae to be indicative of the quality of spawning substrate. The relative frequency of normal and deformed larvae in recently hatched herring eggs from natural and artificial spawning grounds has been determined in Severnaya Bay. The maximal quantity (94%) of well-developed larvae hatched from roe was from artificial spawning substrate but was only 25% or less from the natural seagrass substrate (*Zostera marina*). The deformed larvae from natural substrates included the absence of a yolk sac (4.2%) or high water content (16.6%). The principal deformities of larvae from artificial substrates were curvature of the spine (8%) and irregular head and tail parts (5% and 10%). Approximately 50% of larvae with spinal curvature recovered about one day after hatching.

Pacific Herring: Common Factors Have Opposite Impacts in Adjacent Ecosystems

Gordon A. McFarlane, Richard J. Beamish and Jake Schweigert
Pacific Biological Station, 3190 Hammond Bay Road, Nanaimo, B.C., Canada V9R 5J6. E-mail: McfarlaneS@pac.dfo-mpo.gc.ca

Pacific hake are the dominant resident species in the Strait of Georgia (Beamish and McFarlane, 1999) and off the west coast of Vancouver Island in summer (Ware and McFarlane, 1995) – Figure 1. In the La Perouse Bank area, Pacific hake are a large migratory population. During the 1960s, 1970s and 1980s, they spawned off Baja, California during the winter and migrated north to summer feeding grounds (Francis, 1983). Prior to 1990, approximately 25 to 30% of the mature biomass moved into Canadian waters. Since the early 1990s a much larger percentage of the stock (approximately 40%) was present in the Canadian zone.

The fishery for Pacific herring dominated catches in the Strait of Georgia and off the west coast of Vancouver Island from the early 1950s until the mid-1960s (Schweigert and Fort, 1999). The fishery collapsed in the mid-1960s and was closed from 1967 to 1971. It re-opened in 1972 and has been largely regulated by market demands.

Herring are now abundant in the Strait of Georgia and at low levels off the west coast of Vancouver Island (Fig. 2). Predation on herring by hake off the west coast of Vancouver Island increased in direct relation to the increased northward migration of Pacific hake (Ware and McFarlane, 1995). However, hake in the Strait of Georgia reduced their predation on herring despite having a high biomass (Table 1). After 1989, there was a shift to higher mean sea surface temperatures in both areas (Fig. 3) that was part of a large scale shift in climate/ocean conditions as seen in the change in the pattern of the Aleutian Low. Off the west coast of Vancouver Island the high percentage of herring in the diet of hake (approximately 37% annually) is clear evidence of the preference of hake for herring as a prey (Table 2). This preference for herring and the large

biomass of hake has been shown to be the principle cause of the low abundance of herring in this area (Ware and McFarlane, 1995).

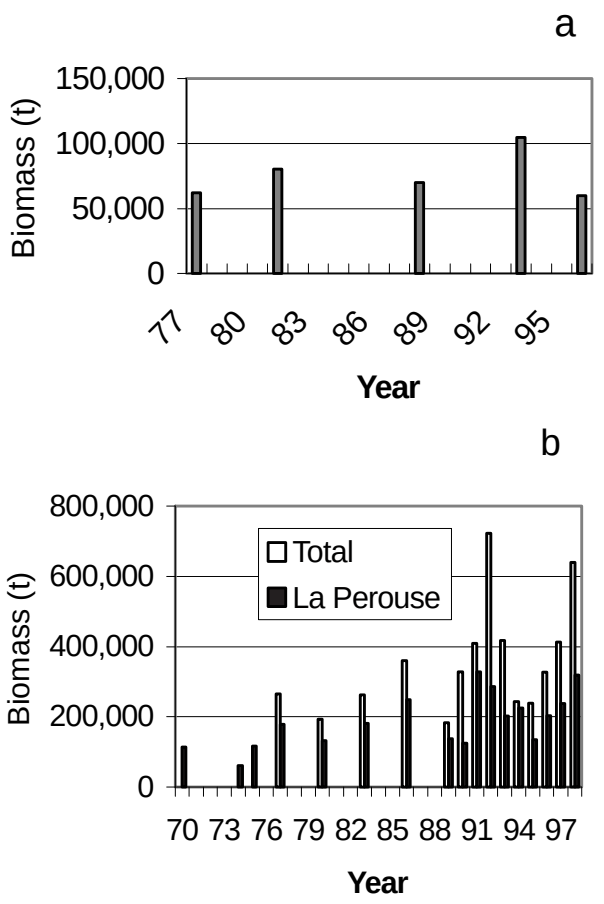

Fig. 1 Biomass estimates (t) of Pacific hake in a) the Strait of Georgia and b) the La Perouse area.

In the Strait of Georgia, hake preference for herring as a prey declined as a consequence of smaller individual size. Our observations of the elimination of herring in the diet of hake in the 1990s is consistent with observations of Tanasichuk et al. (1991), that hake smaller than 40 cm prey almost exclusively on euphausiids and not on herring.

Table 1 Percentage of herring (volume) in the diet of hake from the Strait of Georgia.

Year	Month	Number sampled	% herring in diet
1974	February	601	10.0
1975	Jan-May	3293	23.3
1976	Jan-May	2552	9.9
1981	Feb-May	2072	5.7
1983	Feb and April	2597	30.3
1985	March	607	2.1
1995	Feb-April	572	0.0
1996	Feb-Mar; Oct-Nov	570	0.0
1997	February; Sept-Oct	447	0.0
1998	Feb-March; Sept	307	0.0

Table 2 Percentage of herring (volume) in the diet of hake from the west coast of Vancouver Island (La Perouse).

Year	Month	Number sampled	% herring in diet
1983	July-August	1377	57.0
1985	A	820	40.0
1986	A	2386	9.2
1987	A	1824	28.0
1988	A	3219	58.7
1989	A	1148	11.8
1990	A	998	30.5
1991	A	1105	25.8
1992	A	1663	36.2
1993	A	953	58.5
1994	A	907	18.6
1995	A	916	39.2
1996	A	836	26.8
1997	A	462	17.3

The temperature increases were measures of the ecosystem change but clearly cannot be directly related to the herring abundance trends in the two areas. Thus, the increased temperature in the Strait of Georgia was not associated with a reduction in herring abundance as reported for the west coast of Vancouver. Instead it was associated with improved survival of hake. It is the improved survival that increased their numbers, reduced individual growth, and eliminated predation on herring.

A lesson from this study is that it is the nature of the "reorganization" of the ecosystem after a regime shift that determines the impacts on the population dynamics of a species. A measure of the change, such as temperature, is only one factor affecting the dynamics of populations. The opposite response of herring in the two ecosystems to the climate changes of 1977 and 1989 in adjacent ecosystems, even though the temperature response was similar, indicates that single physical factors need to be related to the dynamics of ecosystems and not just to the observed effect on a single species. It also means that once we see indications that climate/ocean conditions are changing we need to monitor the direction of the new ecosystem organization and adapt our management strategies to this new reality.

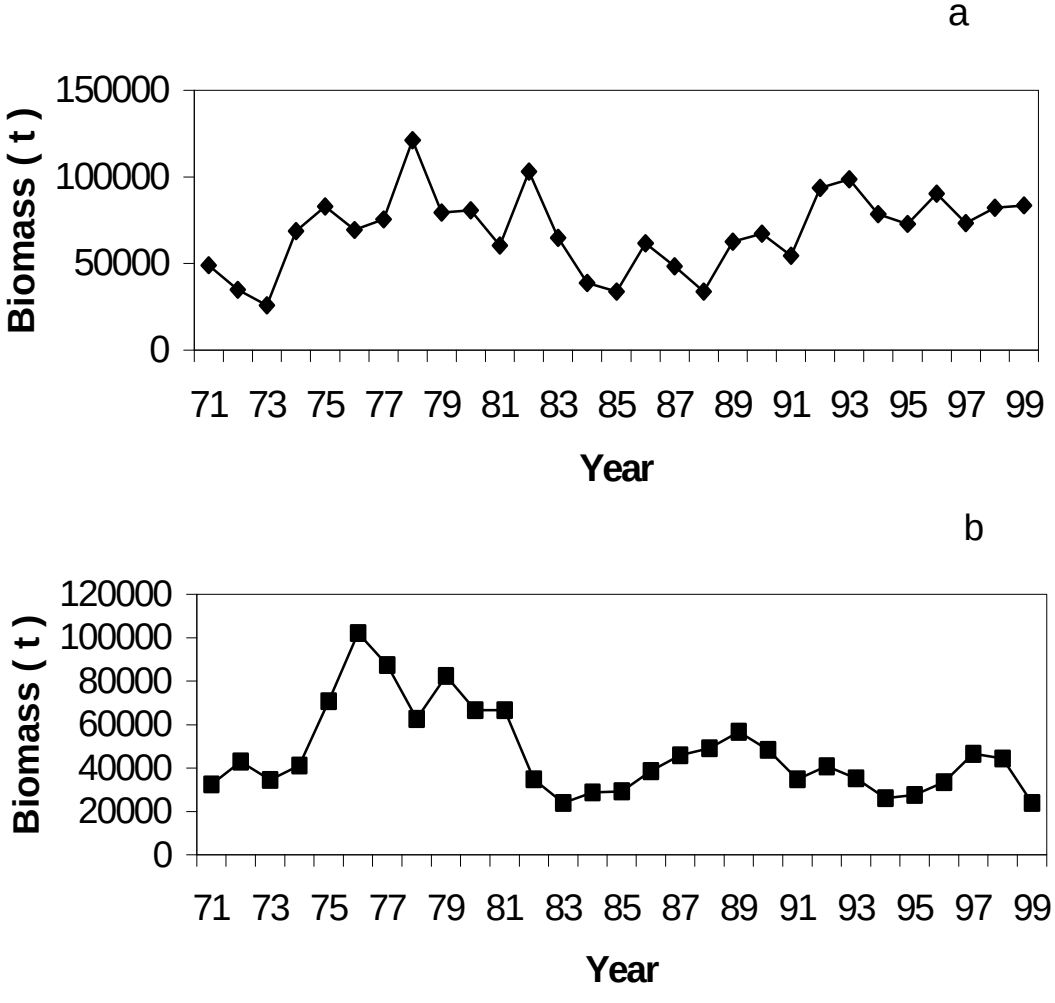

Fig. 2 Biomass estimates (t) of Pacific herring in a) the Strait of Georgia and b) the west coast of Vancouver Island.

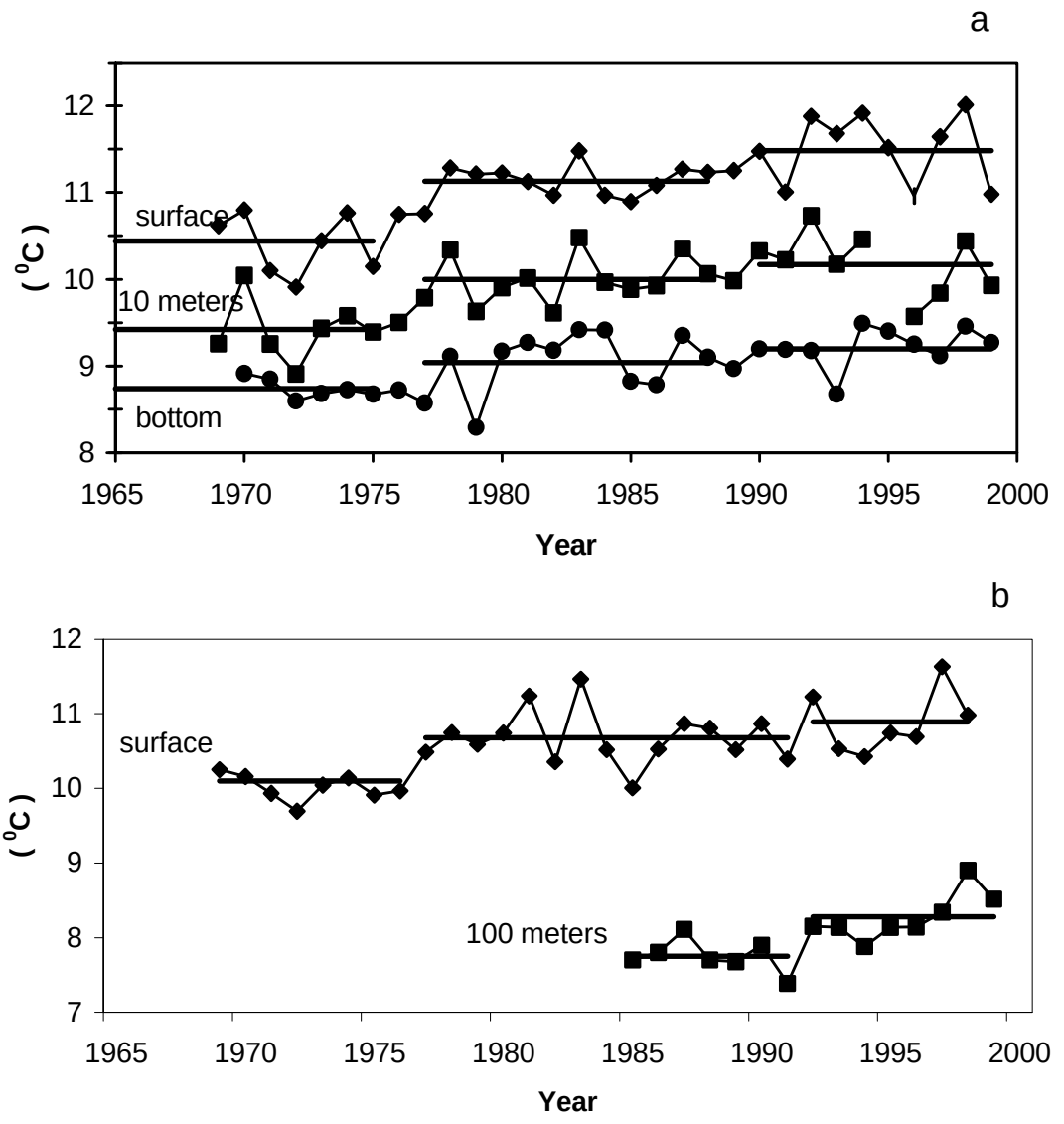

Fig. 3 The average annual sea water temperature at a) surface, 10 m, and bottom in the Strait of Georgia and b) surface and 100 m off the west coast of Vancouver Island. Solid horizontal lines indicate average temperature for regime.

References

Beamish, R. J. and G. A. McFarlane. 1999. Applying ecosystem management to Fisheries in the Strait of Georgia, pp 637-664. *In* Ecosystem approaches for fisheries management. Alaska Sea Grant College Program. AK-SG-99-01, 738 pp.

Beamish, R. J., D. Noakes, G. A. McFarlane, L. Klyashtorin, V. V. Ivonov, and V. Kurashov, 1999a. The regime concept and natural trends in the production of Pacific salmon. Can. J. Fish. Aquatic. Sci. 56: 516-526.

Beamish, R. J., G. A. McFarlane, and R. E. Thomson. 1999b. Recent declines in the recreational catch of coho salmon on the Strait of Georgia are related to climate. Can. J. Fish. Aquat. Sci. 56: 506-515.

Francis, R. C. 1983. Population and trophic dynamics of Pacific hake (Merluccius productus). Can. J. Fish. Aquat. Sci. 40: 1925-1943.

Francis, R. C., and S. R. Hare. 1994. Decadal-scale regime shifts in the large marine ecosystems of the North-east Pacific: a case for historical science. Fish. Oceanogr. 3: 379-391.

McFarlane, G. A., J. R. King and R. J. Beamish. 2000. Have there been recent changes in climate? Ask the fish. Prog. Oceanogr. (*in press*).

Minobe, S.. 1997. A 50-70 year climate oscillation over the North Pacific and North America Geophysical Research Letters, 24(6): 682-686.

Schweigert, J. and C. Fort. 1999. Stock assessment for British Columbia herring in 1999 and forecasts of the potential catch in 2000. Can. St. Ass. Secret. Res. Doc. 99/01, 178 pp.

Tanasichuk, R. W., D. M. Ware, W. Shaw and G.A. McFarlane. 1991. Variations in diet, daily ration, and feeding periodicity of Pacific hake (*Merluccius productus*) and spiny dogfish (*Squalus acanthias*) off the lower west coast of Vancouver Island. Can. J. Fish. Aquat. Sci. 48: 2118-2128.

Ware, D. M. and G. A. McFarlane. 1995. Climate induced changes in hake abundance and pelagic community interactions in the Vancouver Island Upwelling System. *In*: R. J. Beamish (ed.) Climate change and northern fish populations. Can. Spec. Publ. Fish. Aquat. Sci. 121: 590-521.

Long-term fluctuation of the catch of Pacific herring in Northern Japan

Tokimasa Kobayashi[1], Keizou Yabuki[1], Masayoshi Sasaki[2] & Jun-Ichi Kodama[3]

[1] Hokkaido National Fisheries Research Institute, 116 Katsurakoi, Kushiro, Japan. 085-0802. E-mail: tokikoba@hnf.affrc.go.jp

[2] Hokkaido Central Fisheries Experimental Station, 238 Hamanaka-cho, Yoichi, Japan. 046-0021

[3] Miyagi Prefecture, Sendai, Japan. 980-8570

Several spawning grounds of Pacific herring have been observed in the waters of Northern Japan. These spawners are genetically isolated from each other and these populations are classified into the following four types: (I): lagoon-small migration type, (II): oceanic-wide migration type, (III): oceanic-small migration type and (IV): intermediate type between I and II. The Hokkaido-Sakhalin population is one of the oceanic-wide migration type (II) and Mangoku-ura population belongs to type III (Kobayashi, 1993).

Hokkaido-Sakhalin population

Catch and catch at age data for the Hokkaido-Sakhalin population are available since 1878. The annual catch was over 400,000 t from the late 19th century to early in the 20th century, with a historical peak of 970,000 t in 1897 (Fig. 1). However, the population has steadily declined thereafter with continual fluctuation, accompanied with the disappearance of spawning grounds from south to north in the west coast of Hokkaido. In 1955 the spawning ground completely disappeared from the coast of Hokkaido.

Studies of year-class strength, spawner-recruit relationship and observations of oceanographic events led to a hypothesis that the factors controlling the year-class abundance of Hokkaido-Sakhalin population relate to the variations in the spring-summer oceanographic environmental condition. This hypothesis has been tested by examining the data incorporated into a spawner-recruit pattern, for example, sea water temperature and food organism, obtained from spawning-nursery ground. Oceanographic data for the west coast of Hokkaido area is limited, with data from some locations available. Water temperature data for the west coast of

Hokkaido (Fig. 2) were obtained form Kamui, Yoichi, Takashima and Wakkanai and those data were analysed to examine the relationship between year-class strength and sea-water temperature.

As with sea surface temperature there is a large interannual variation. The annual mean seawater temperatures recorded at Takashima showed that an apparent rise in five year running mean after 1910. This tendency was generally seen in all locations off the west coast of Hokkaido. The northerly shift of the spawning area of this population was much accelerated after 1910, though there still remained large extensions of the spawning grounds on the west coast, sufficient to yield a large catch as whole. The records of seawater temperature at Kutsugata rose about 1932 and the amount of catch in Hokkaido and South Sakhalin greatly declined after 1935. There was a remarkable decline in sea surface temperature from 1939-1945 and the temperature rose again after 1946. The catch of herring was maintained to some extent up to 1953, but it declined greatly after 1955. Drastic changes in the marine environment which occurred in about 1955 would have accelerated the decrease in stock size and at the same time caused the changes in biology of the herring (Motoda and Hirano, 1963).

In 1985, there was a sudden appearance of two year old herring (Fig. 3) on the west coast of Hokkaido (1983 year-class). It is assumed that the spawning stock in 1983 was very small so that no information on spawning was obtained from the fishermen in 1983. In 1987 and 1988 eggs spawned on the sea grasses were observed. Thereafter a 1988 year-class also appeared on the west coast but the size of the 1988 year-class was smaller than the 1983 year-class. The decline of the seawater temperature was observed at Wakkanai in spring and early summer season in 1983. The recover of spawning by 1983 year-class of Hokkaido-Sakhalin population was the event after thirty-three years' absence. Interestingly, strong recruitment of the 1983 year-class also appeared in George's Bank herring and Norwegian spring herring. Were these events the result of a coincidental conjunction or a teleconnection? Unfortunately in recent years spawning of Hokkaido-Sakhalin population has not been observed along the coast of Hokkaido.

Mangoku-ura population

Only catch records from recent years are available for Mangoku-ura herring. The catch gradually increased from 1975 and reached >500 t in 1984, declining thereafter to <20 t by 1996. Strong year-classes have appeared every three years since 1975. A significant relationship between the abundance of age 1 fish and the total number of eggs spawned by adult fish was not detected. However it was reported that high survival rates were observed only when the sea temperature near the spawning ground (while herring were in the larval to juvenile stages) was <6°C (Fig. 4. Kodama, 1997).

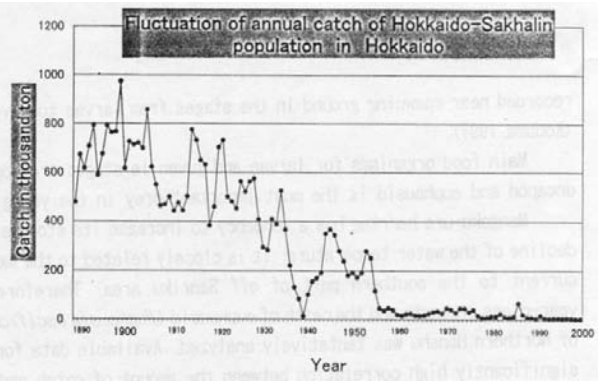

Fig. 1 Hokkaido-Sakhalin herring catch in Hokkaido.

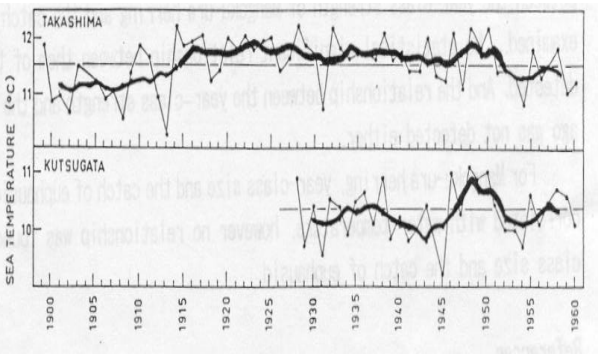

Fig. 2 Secular trends in annual sea temperature and the 5-year sliding means at Takashima and Kutsugata (Yamazaki, 1960).

The diet for larvae and juvenile stages is made up of copepods while the larvae of decapods and euphausiids are the most important prey in the young and adult stages.

The stock size of Mangoku-ura herring tends to increase with the decline of the water temperature (Fig. 5). It is closely related to the extension of Oyashio Cold Current to the southern part of off Sanriku area. Therefore, the relationship between year-class strength and the catch of euphausid (*Euphausia pacificus*) in the Pacific coast of northern Honshu was tentatively analysed. Available data for 1970 to 1977 showed a significantly high correlation between the amount of catch and the extension of cold waters, (<5°C at 100 m) in the area off northeastern Honshu during February through May (Odate, 1979). The abundance of euphausid may affect the survival of juveniles and young herring and the nutritional condition of adult herring. The relationship between the year-class strength of Mangoku-ura herring and the catch of euphausiids was examined and no statistically significant relationship was detected for observations taken during the same year. There was also no significant relationship between year-class strength and the catch of age one herring. For Mangoku-ura herring, year-class size and the catch of euphausiids was positively correlated with water temperature, however no relationship was found between year-class size and the catch of euphausiids.

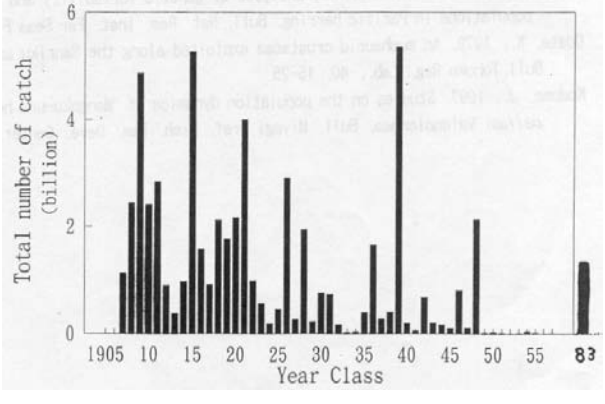

Fig. 3 Year-class strength of Hokkaido-Sakhalin population.

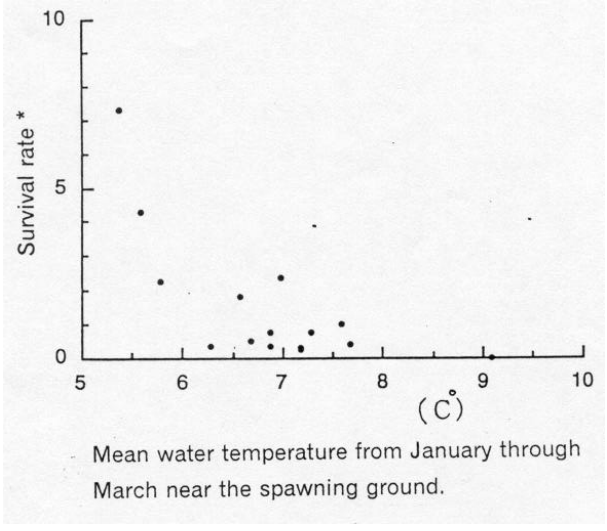

Fig. 4 Relationship between mean water temperature and survival rate (Kodama, 1997).

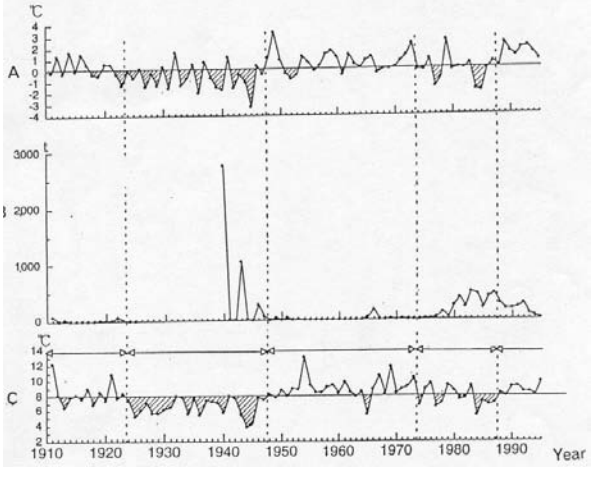

Fig. 5 Long-term fluctuation of catch of Mangoku-ura herring and air and water temperature observed on the coast of Miyagi Prefecture (Kodama, 1997).

A. Mean air tenperarure from Jan. through Feb. at Ishinomaki.

B. Landing of herring in ton.

C. Water temperature in April at Enoshima.

References:

Kobayashi, T., 1993. Biochemical analyses of genetic variability and divergence of

populations in Pacific herring. Bull. Nat. Res. Inst. Far Seas Fish. 30: 1-77.

Kodama, J., 1997. Studies on the population dynamics of "Mangoku-ura herring", *Clupea pallasi* Valenciennes, Bull. Miyagi Pref. Fish. Res. Devel. Center. 15: 1-41.

Motoda, S. and Y. Hirano, 1963. Review of Japanese herring investigations. Rapp. P. – v. Reun. Cons. Int. Explor. Mer. 154: 249-261.

Odate, K., 1979. An euphausid crustacea exploited along the Sanriku and Joban coast. Bull. Tohoku Reg. Lab. 40: 15-25.

Holocene fish remains from Saanich Inlet, British Columbia, Canada

Jacqueline M. O'Connell
Earth and Ocean Sciences - Oceanography Unit, University of British Columbia, Vancouver, B.C., Canada.

Introduction

For most fish populations, available records are too short to resolve decade or century scale fluctuations. Here, the fine sedimentary fish remains record of Saanich Inlet is examined to infer fluctuations in fish population abundances – especially Pacific herring (*Clupea pallasi*) – through the Holocene.

Saanich Inlet

Saanich Inlet is a temperate marine fjord on Vancouver Island, British Columbia, Canada. The deep water in the inlet is anoxic for most of the year and therefore Saanich Inlet sediments accumulate undisturbed through time.

Methods

1. 5 high-resolution, large volume box cores (1A, 1B, 1C, 2A, 2B):
   - ~1.5 m long, recent sediments = 1883-1991
   - 400cm^2 area, 2-year sampling resolution
   - Detailed Pacific herring and hake population fluctuations are inferred
2. Bone and scales were sieved from sediments, identified and enumerated – the majority of remains are from Pacific herring and hake.
3. Data smoothing (low-frequency robust trends), anomalies (periods of high and low abundance) and spectral analyses (high-frequency) and comparison to physical (ALPI- Aleutian Low Pressure Index), biological (diatoms, hake) and human (herring landings) time series.

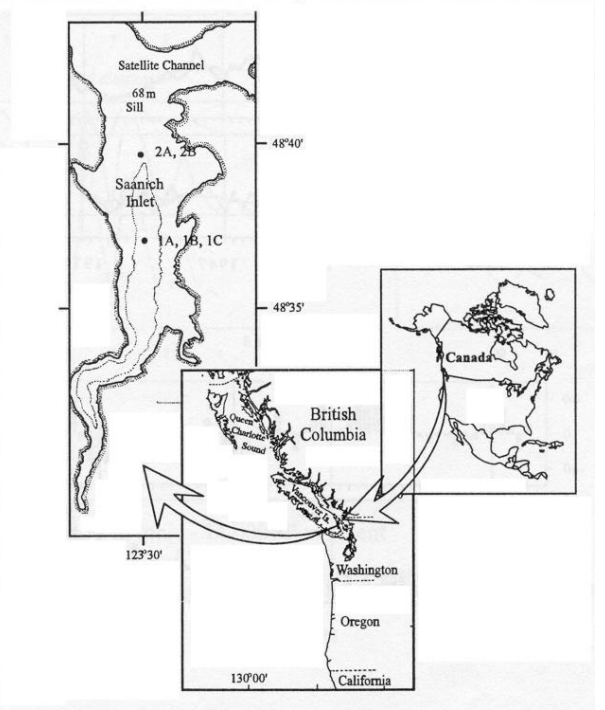

BOX CORE TRENDS: The past 100 years

Smoothing: Well documented crash of herring populations in the late 1960s.

Anomalies: The herring scale record shows major transitions in keeping with the timing of regime shifts in the North Pacific Ocean.

Cross-spectral analyses: coincidental timing of scale deposition and physical/biological datasets and exploitation rates (4-10 year periodicity) does suggest correlation/common mechanisms. These timescales of variation warrant further investigation.

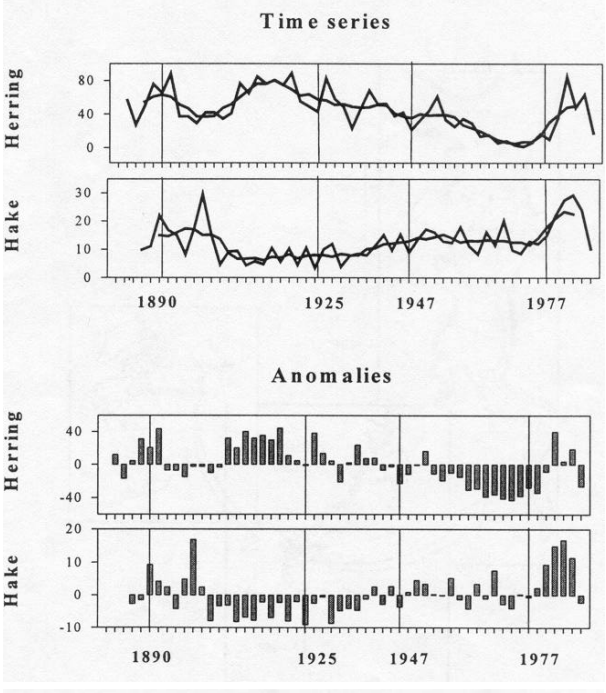

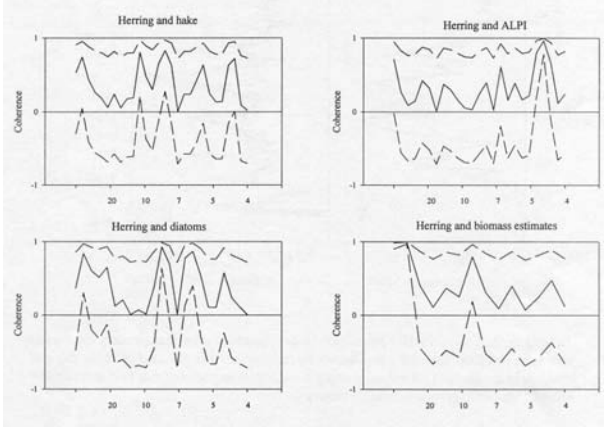

ODP CORES: Holocene record

ODP piston core

- 118m long – 14,000BP to recent
- 8.3cm^2 area, no replicates
- Generalized century to millennia-scale fish story, focussing on herring

Herring depend on secondary production by zooplankton rather than primary production as a source of food however a millennia-scale relationship was detected between fish and diatoms in the Saanich record, suggesting a consistent response of fish to diatom levels OR of both biotic groups to climate factors.

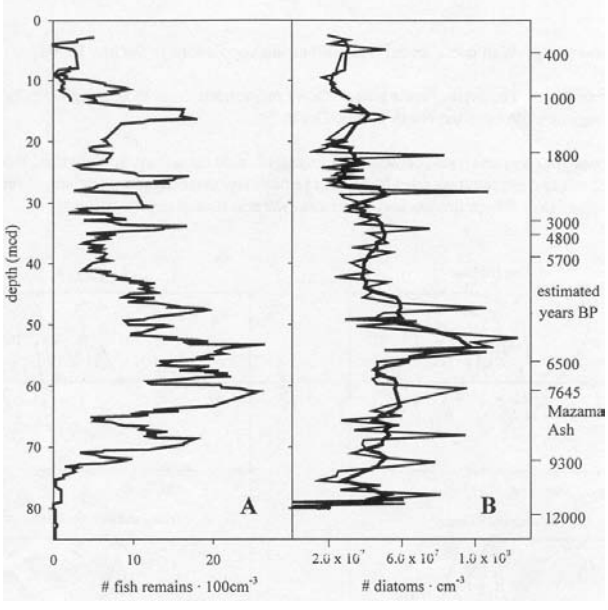

Taxonomic identification was only possible for 37% of the remains in the ODP core but over half of the bone fragments were herring. An interesting qualitative story of first appearances was inferred indicating that herring were early colonizers of the inlet after deglaciation (12,000yBP).

Overall

Detailed, large volume sedimentary records are useful to infer long-term dynamics of herring and their major hake predators.

From the high-resolution, large volume box core samples, some potential factors correlated to fish dynamics were explored. Response to

documented regime shifts and higher-frequency 4-10 year periodicities were detected in the herring data, and in biological (sedimentary hake scale record, diatoms) and physical factors (ALPI), as well as fishing intensity (historical landings).

From the ODP cores, a long-term relationship between primary and tertiary trophic levels does appear to be resolved in the Saanich record. Herring were among the first fish to colonize post-glacial Saanich Inlet.

Further research of this kind may help to provide testable hypotheses about patterns and causes of long-term variability. Data such as these may also prove invaluable to management of herring stocks as a better understanding of the timescales of change may assist in planning for major regulatory changes at periods of low abundance.

References:

O'Connell, J. M. and V. Tunnicliffe. The use of sedimentary fish remains for interpretation of long-term fish population fluctuations. Marine Geology. *In press*.

O'Connell, J. M. A 110-year sedimentary record of Pacific herring (*Clupea pallasi*) and hake (*Merluccius productus*) from Saanich Inlet, British Columbia, Canada. *In prep*.

Tunnicliffe, V., J. M. O'Connell and M. R. McQuid. A Holocene record of marine fish remains from the Northeastern Pacific. Marine Geology. *In press*.

On relationship between crustacean zooplankton (Euphausiidae and Copepods) and Sakhalin-Hokkaido herring (Tatar Strait, Sea of Japan)

Elsa R. Ivshina and Irina Y. Bragina
Sakhalin Research Institute of Fisheries and Oceanography, 196 Komsomolskaya St., Yuzhno-Sakhalinsk, Russia. 693016, E-mail: elsa@tinro.sakhalin.ru

Introduction

Sakhalin-Hokkaido herring is potentially the most abundant among all herring populations in the Far East. During the last several decades, the status of that population has been extremely low. A significant reduction in abundance began in 1940–50s and during the 1980–90s, the population appeared to be in a critical situation. The reasons for the decline were discussed widely (Svetovidov, 1952; Probatov, 1958; Hirano, 1961; Kondo, 1963; Motoda & Hirano, 1963; Birman, 1973; Pushnikova, 1981; 1996; Sokolovsky & Glebova, 1985). A majority of scientists considered that the main reason of this phenomenon was a change in ocean conditions such as the warming in the northern Sea of Japan and adjacent areas. Increasing commercial pressure on the Sakhalin-Hokkaido herring population is considered to be another important reason.

It is well known that the abundance of each generation depends on many factors, both biotic and abiotic. Prey abundance affects them to a considerable extent as well. In the Tatar Strait, the zooplankton community, feeding structure and other problems connected with herring feeding were studied actively. However, a question of the relationship between the biomass of the dominant zooplankton forms, the main components of herring feeding, and the number of Sakhalin-Hokkaido herring were not considered. The aim of our work was to determine the relationship between the biomass of one of the main components of feeding (crustacean zooplankton such as Euphausiidae), the number of Sakhalin-Hokkaido herring generations and the biomass of predatory zooplankton.

Materials and methods

In this work the dependencies between the abundance of Sakhalin-Hokkaido herring year-class at age 1+ (given as calculated data), biomass of small and large fractions of euphausiid, and biomass of the predatory zooplankton forms (*Sagitta elegans* is dominant among them) which feed on herring larvae, and small forms of the prey zooplankton are considered. General zooplankton biomass and copepod biomass data are reported as well. All data are considered for spring and fall during the period 1986-1992.

The abundance of Sakhalin-Hokkaido herring year-classes was estimated from aircraft observations and Pope's cohort analysis. In further analyses, the abundance of year-classes at age 1 was displaced one year forward.

Zooplankton data were collected during the seasonal (spring and fall) hydrobiological surveys carried out at the standard stations. A total of 700 stations was occupied. A Juday net (diameter of input hole – 0.37 m) was used to collect zooplankton samples and an egg and larvae net (diameter of input hole – 0.37 m). The samples were collected by hauling the 0-100 m layer.

The method of zooplankton determination was standard. For Juday samples, a division on fractions was applied and a catching efficiency was used for different systematic and dimensional zooplankton groups. All data given in the report on the condition of zooplankton community are averages for the study area. Temperature was considered on the line of Slepikovsky Cape – the sea at 0-50 and 50-100 m layers averaged for April-May (spring) and September-November (fall).

Results

The main region of Sakhalin-Hokkaido herring inhabitation at present time is the southwestern coast of the Tartar Strait (Sea of Japan). Spawning, embryogenesis, and feeding of fry and fingerlings take place here. Within the Tartar Strait mature herring form the prespawning stocks in March-May, and then feeding stocks in June-October, mainly in the region between 47-49°N near Sakhalin shelf and slope. The most intensive herring eat during the prespawning and after spawning periods in June-July. In August-September the intensity of feeding somewhat falls down. As a rule, the greatest stocks are being formed in places with significant water temperature gradients and high zooplankton biomass.

The base of feeding for herring juveniles near the southwestern Sakhalin is formed by Harpacticoida, Coryphiidae, Calanoida, and Euphausiidae. Adult fish eat mainly *Calanus*, Euphausiidae, *Sagitta*, and Mysidae i.e. the largest and most abundant forms of plankton.

In the area of the southern Tatar Strait, hydrobiological surveys found 4 species of Euphausiidae in the samples. These included the the cold water species *Thysanoessa raschii, T. inermis, T. longipes* and a moderately-cold water species *Euphausia pacifica*. At the end of April to the beginning of May, the eggs, nauplii, calyptopis and furcilia stages were present together with adult specimens. In spring T. inermis was dominant in both frequency and biomass. Its average biomass in the region was 23.76 $mg \cdot m^{-3}$. In autumn, *T. longipes* occurred most often, their density was not high – 7.77 $mg \cdot m^{-3}$. As to biomass of euphausiids on the whole, its value is small and varies from 4 to 58 $mg \cdot m^{-3}$ in spring and from 6 to 40 $mg \cdot m^{-3}$ in autumn, making from 1 to 9.6% of total zooplankton biomass. Table 1 shows that the biomass of euphausiids does not play a leading part and their share does not exceed the average 8.0% in the community.

During the study period extensive stocks of euphausiids with high biomass, like those described in the literature for the 1950–70s, were not found. Euphausiids were not dominant in herring stomach samples as well.

Judging from the results of analysis of stomach contents, the copepods *Neocalanus plumchrus* and

Pseudocalanus minutus are the base of herring diet in recent years. These are the dominant plankton in the zooplankton community structure in the southern Tatar Strait. On a study area copepod prevailed in zooplankton community as in spring, so in autumn (Table 1).

Table 1 Biomass of zooplankton main groups, 1986 – 1992 (%)

Taxa	Spring	Fall
Copepoda	61.6	50.5
Euphausiidae	5.9	8.0
Amphipoda	3.8	10.9
Chaetognatha	16.3	13.5

Comparison of herring abundance with total zooplankton biomass and biomass of copepods has shown that in spring their indices are out of phase. For autumn period a similar tendency was not evident because this season is characterized not only by the active consumption of plankton by herring, walleye pollock, cod juveniles, and capelin, but also the development of a complex community of neritic zooplankton species (Fig. 1).

Despite the fact that the base of the Tatar Strait zooplankton community and the base of herring diet are copepods, we have considered a relationship between a number of herring year-classes and the biomass of euphausiids, so far as this zooplankton group is important in the diet of herring, especially juveniles. For the period between 1986–1992, the most numerous year-class of herring was observed in 1988. The number of 1 year old individuals reached 312.4 million. This was a harvestable generation during a period of generally weak recruitment during the 1980s and early 1990s. Though its abundance was lower than the 1983 generation, it was a harvestable year-class from 1984 –1995.

During the period 1986–1992, a relatively high biomass of euphausiids was recorded in the spring of 1990 and in spring and autumn 1992. Our observations indicated that in 1987, the year before the formation of the harvestable year-class, and in 1988, the biomass of euphausiids was below the interannual level. A small fraction of euphausiids, which in summer-autumn period is one the main dietary components for herring fingerlings was not high as well. Zooplankton predators' biomass in spring was also low (Fig. 2).

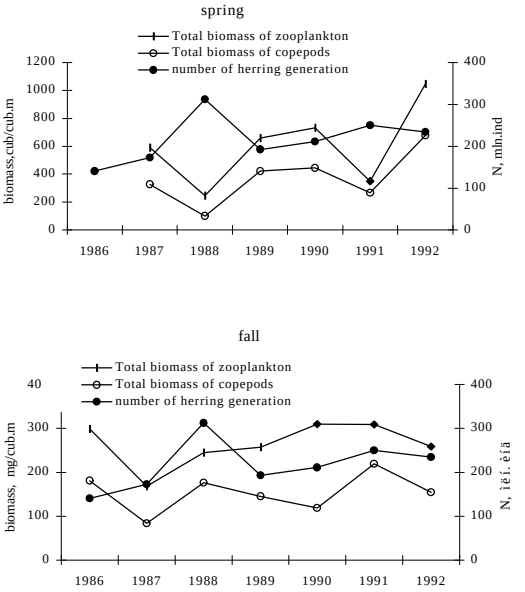

Fig. 1 Total biomass of zooplankton and herring generation

In 1988, a significant negative temperature anomaly in the 0–50 and 50–100 m layers in southern Tatar Strait was registered, and most clearly observed in the spring period (see Figures 4 and 5). In 1989–1990, high values for total euphausiid biomass were distinctive in spring and autumn and high values of zooplankton predators were found as well. Small zooplankton fractions were distinguished by the low biomass, especially in autumn period (Fig. 3). Unlike 1988, these years had positive temperature anomalies (Fig. 3 and 4).

A significant negative correlation was observed only between the number of herring and the biomass of small euphausiids in spring (-0.72) and biomass of predators in spring (-0.87). But

such situation occurs only in the summer period, since the new generation of herring begins to eat small zooplankton in summer, at the same time the predators begin to act.

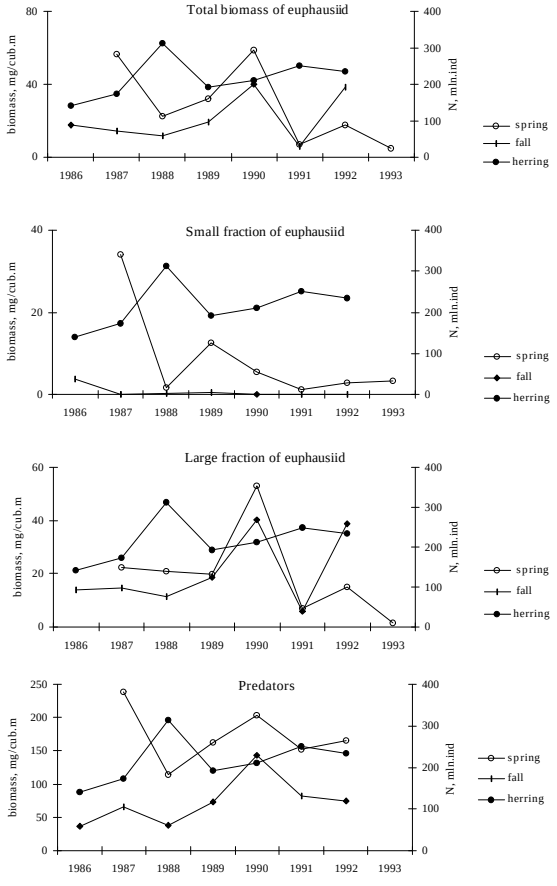

Fig. 2 Biomass of euphausiids, predators and number of herring generations

A relationship between the number of herring, autumn and spring biomass of euphausiids and water temperature was not evident. But for the year in which the 1988 herring year-class was formed, low water temperatures in the upper layer in spring and autumn, and low values of euphausiid biomass occurred as well. In general, a feedback between the number of herring and biomass of euphausiids and predators was observed. However, some clear dependency on interannual scale between the number of herring generations and biomass of euphausiids was not determined for a study period. It is probably caused to the fact that euphausiids are not the main component of the herring feeding, and to the reduction of a total euphasiid biomass coincided with the period of depression of the Sakhalin-Hokkaido herring population.

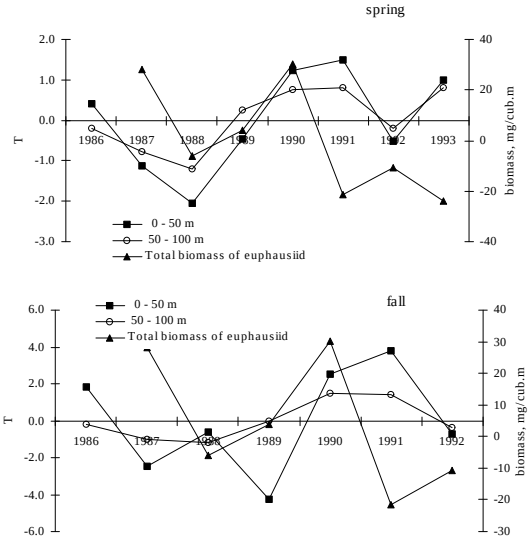

Fig. 3 Total biomass of euphausiid and layer temperature (0-50, 50-100 m), deg C.

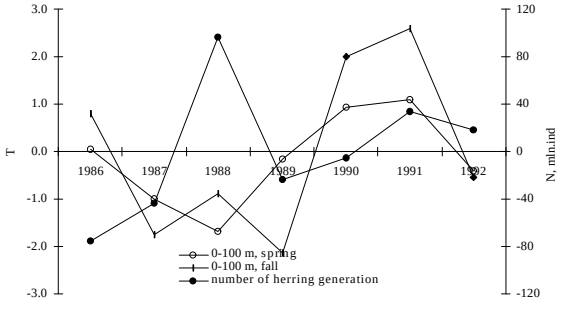

Fig. 4 Number of herring generation and layer temperature (0-100 m), deg C.

Table 2 Correlation between the annual number of herring at age 1 and the biomass of some zooplankton forms.

Total Euphausiid		Small euphausiids		Large euphausiids		Predator biomass	
Spring	Fall	Spring	Fall	Spring	Fall	Spring	Fall
-0.63	-0.14	-0.72	-0.57	-0.25	-0.08	-0.87	-0.03

References

Birman I.B. 1973. Heliohydrobiological ties as the basis for long-term predictions of industrial fish supplies (with salmon and herring as examples). Vopr. Ichthyol. 13: 23-37. (in Russian)

Kondo H. 1963. On the condition of herring (Clupea pallasi C. Et V.) in waters around Hokkaido and Sakhalin during recent years. Hokkaido Fisheries Experimental Station. 3: 1-18 (In Japanese)

Motoda S., Hirano Y., 1963, Review of Japanese Herring Investigation, Rapp. et process verbaux, 154, 249-261

Pokrovskaya, 1954a. Feeding of Pacific herring at south-western coast of Sakhalin . Izv. TINRO, 1954. V.39, p. 351-352. (in Russian)

Pokrovskaya, 1954b. Feeding of Pacific herring at south-eastern part of Tartar Strait (Sea of Japan) . Izv. TINRO, 1954. V.41, p. 309-318. (in Russian)

Probatov A.N. 1958. Fluctuations of Sakhalin-Hokkaido herring abundance due to oceanological conditions. Proceedings of Oceanological Commission. 3: 124-125. (in Russian)

Pushnikova G.M. 1981. On stock condition and the optimal exploitation age of Sakhalin-Hokkaido herring. Izv. TINRO. V.105,: p.79-84. (in Russian)

Pushnikova G.M. 1996. Fishery and stock condition of the Sakhalin waters herring. Scientific proceedings of Far Eastern State Technical Fishery University. 8: 34-43. (in Russian)

Sokolovski A.S., Glebova S.Yu. 1985. Fluctuations over long periods in the numbers of Sakhalin-Hokkaido herring. Herring of North Pacific. Vladivostok. TINRO. 3-12. (in Russian)

Svetovidov A.N. 1952. Fluctuations of the southern Sakhalin herring catches and their reasons. Zoolog.journ.31: 831-842. (in Russian)

Fish predation on krill and krill antipredator behaviour

Stein Kaartvbeedt

Department of Biology, University of Oslo, P.O. Box 1064, Blindern, N-0316 Oslo, Norway. E-mail: stein.kaartvedt@bio.uio.no

Krill constitute a key component in oceanic food webs. They have a diverse diet and are prominent prey for fish. The search strategies of fish foraging on krill differ among species, locations, and time of day and may involve visual search as well as ambush feeding based on hydrodynamic signals created by the swimming prey. This talk addresses the feeding behaviour of herring (*Clupea harengus*), whiting (*Merlangius merlangus*) and Norway pout (*Trisopterus esmarki*) foraging on krill (*Meganyctipahnes norvegica*), mainly based on research carried out in the Oslofjord, Norway.

Herring in the study area school above the krill at day, schools disperse at night and herring then forage on vertically migrating krill. Nocturnal predation is probably visual, and seems to be restricted to the upper 20-30 m. The non-schooling whiting lives deeper than herring, occupying the same depth range, and performing a similar diel migration pattern to that of krill. They forage on krill throughout the diel cycle. Prey search may be visual both day and night, and whiting appears to be able to forage at lower light intensities (i.e. deeper water) than herring. Norway pout is semi-demersal, largely remaining associated with the bottom at day, migrating into the water column at night. They forage on krill by day where the bottom intercepts the krill daytime habitat, otherwise predation is nocturnal by vertically migrating individuals ascending into the water column. Norway pout has large eyes, and may forage visually in relatively deep water at day. Their swimming behaviour, hanging motionless in the water column, does, however, suggest that they may be ambush feeders by night.

Krill antipredator behaviour includes a flexible DVM pattern, apparently responding to the presence of fish. They partly remain below visually foraging pelagic fish at day, but may avoid the near-bottom zone in presence of demersal fish. In waters devoid of nocturnally foraging planktivores, vertically migrating krill ascend all the way to the surface. while they modify their DVM pattern and largely avoids the upper 20-30 m at night in waters with abundance of nocturnally foraging fish. Antipredator behaviour also constitutes instantaneous escape responses upon encounters with fish. The talk also addresses how more subtle mechanisms like modification of feeding and swimming behaviour in response to mortality risks may be studied in the field. I argue that acoustic studies, comprising acoustic target tracking of individual plankters and fish, hold yet unexploited opportunities for studies of fish-krill interactions and for understanding of both krill and fish behaviour.

Euphausiids and western Bering Sea herring feeding

Nikolai I. Naumenko
Kamchatka Research Institute of Fisheries and Oceanography (KamchatNIRO), 18 Naberezhanya Street, Petrapavlovsk, Russia 683602. E-mail: mail@kamniro.kamchatka.su

The paper is based on long-term information (1939-1998) from weight method examination of 2997 stomach content from 117 coastal stations in Karaginsky Bay, Olyutorsky Bay, Olyutorsky-Navarin area, and 1486 stomach examinations at 9 daily stations. Rations were calculated in three ways: (1) using daily station data; (2) a physiological method using the well-known Vinberg equation; and (3) our identification of a strong dependence between daily ration, body weight, stomach fullness index, and water temperature.

Food composition and trophic activity by Korfo-Karaginsky herring are very labile among years, seasons, areas, age cohorts. The herring diet (excluding the larval stages) contains 70 species of marine animals from 13 classes. The dominant prey is copepods which make up more than a half (51.7%) of the annual ration. The portion of euphausiids in the diet fluctuates annually from 9.8% to 70.7% with average value 42.1%. In May – September the herring feed mainly on copepods – from 49.9% in September to 88.4% in July. During other months, euphausiids contribute 68-88% of the stomach contents.

The variability of the herring diet is related to age composition. Through summer and autumn, age

0+ to age 2+ individuals are found mainly in Karaginsky Bay; age 3+ in Olyutorksy Bay, and age 4+ to age 7+ are adjacent to the Koryak Coast/Elder. Herring reach Far Eastern areas and during periods of high abundance, they inhabit offshore waters. Diet composition is in high conformity with habitat: 4-year-old and older individuals feed more on euphausiids while the younger fish feed on copepods.

The annual consumption of euphausiids by the population is from 1.3 (depressed condition) to 8.7 (high stock abundance) million tonnes. On average, each individual feeds from 0.39 kg (32,000 individuals) to 0.54 kg (45,000 individuals) of these class organisms.

Interactions Between Fish and Euphausiids and Potential Relations to Climate and Recruitment

David M. Checkley, Jr.
Marine Life Research Group, Scripps Institution of Oceanography, La Jolla, CA 93093-0218, U.S.A. E-mail: dcheckley@ucsd.edu

The interaction of euphausiids and fish is complex. Each at times may be the predator, prey, or competitor of the other. However, certain interactions may be dominant. Here, I present preliminary data consistent with one such interaction, predation by euphausiids on sardine and anchovy eggs in the California Current Region.

High resolution maps of near-surface distributions of euphausiids and the eggs of the Pacific sardine (*Sardinops sagax*) and northern anchovy (*Engraulis mordax*) were made during CalCOFI cruise 9603JD using the Continuous, Underway Fish Egg Sampler, CUFES (Checkley *et al.* 1997, in press). This device collects eggs of fish from 3-m depth continuously during a survey by a ship at full speed. Eggs of the target species are identified live at sea, for near-real-time mapping and adaptive sampling, and all eggs are identified and counted ashore in preserved samples. At sea, simultaneous measurement is made of date, time, location, temperature, salinity, and chlorophyll *a* fluorescence. Euphausiids and other plankters are collected as "by-catch" of the egg sampling.

Sardine and anchovy eggs sampled during CalCOFI cruise 9603JD were distributed in a complementary fashion. Sardine eggs were most abundant along the inner edge of the California Current, north of Point Conception, in waters characteristic of isopycnal shoaling. Anchovy eggs were in water upwelled either recently (cool) or in the past (warmed), mostly south of Pt. Conception. An analogous cruise in March 1997 yielded very similar results.

Despite sampling caveats, including possible avoidance of the near-surface intake of the CUFES pump by euphausiids and diel variation in their surface residence, the patterns of sardine and anchovy eggs and euphausiids were complementary during CalCOFI cruise 9603JD. The figure below shows that sardine eggs were abundant only in the absence of euphausiids and vice versa.

Similar results have been obtained off northern Peru for eggs of the anchoveta (*Engraulis ringens*) and euphausiids. This is work in progress in collaboration with Dra. Guadalupe Sanchez (Instituto del Mar del Peru). In essence, anchoveta eggs and euphausiids, occurred but not together.

The most parsimonious explanation of these patterns is euphausiid predation on sardine eggs. These results and those of others indicated that variation in the abundance and distribution of

euphausiids may significantly affect survival of planktonic eggs and larvae and hence recruitment of sardine and other species of fish.

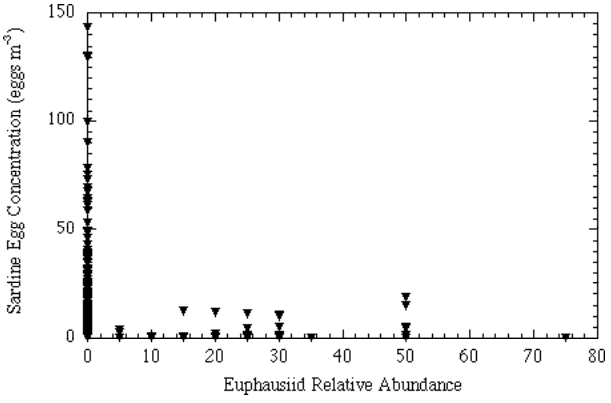

Fig. 1 Concentration of eggs of Pacific sardine (*Sardinops sagax*) in relation to the relative abundance of euphausiids [0(absent), 100(maximal abundance)] in CUFES samples from CalCOFI cruise 9603JD (Checkley *et al*. in press).

Predation and competition require overlap in distributions of species populations, which, in turn, depend on available habitat. Climate variation will affect interactions between fish and euphausiids in part through expansion, contraction, and overlap of such habitats and hence the distributions of the species involved. A high priority should be given to characterizing such habitats and their variation. The use of standardized and coordinated techniques of data collection and analysis is recommended. This is one area in which PICES might take a leadership role. Additional work is also needed on the biology of euphausiids and, in particular, their feeding on fish eggs and larvae. Seminal work was done by Theilacker (1993), but further work is needed in order to quantify the predatory impact of euphausiids on fish eggs and larvae.

References:

Checkley, D.M., Jr., P.B. Ortner, L.R. Settle, and S.R. Cummings. 1997. A continuous, underway fish egg sampler. Fish. Oceanogr. 6: 58-73.

Checkley, D.M., Jr., R.C. Dotson, and D.A. Griffith. In press. Continuous, underway sampling of eggs of Pacific sardine (*Sardinops sagax*) and northern anchovy (*Engraulis mordax*) in spring 1996 and 1997 off southern and central California. Deep-Sea Res.

Theilacker, G.H., N.C.H. Lo, and A.W. Townsend. 1993. An immunochemical approach to quantifying predation by euphausiids in the early stages of anchovy. Mar. Ecol. Prog. Ser. 92:35-50.

Shall we expect the Korf-Karaginsky herring migrations into the offshore western Bering Sea?

Vladimir I. Radchenko and Elena P. Dulepova
Pacific Scientific Res. Fish. Center (TINRO-Center), 4 Shevchenko Alley, Vladivostok, Russia 690600. E-mail: root@tinro.marine.su

In the 1990s, Pacific herring became one of the dominant species in the western Bering Sea pelagic fish community, especially in the sea shelf zone. The Korf-Karaginsky herring population has a leading role in total fishery biomass and herring fishery harvest in the western Bering Sea as in 1960s, when the harvest totalled up to 268,000 mt (Kachina, 1981). Whereas, during the 1980s, the harvest did not exceed 32,000 mt. Since the early 1990s, walleye pollock biomass has noticeably declined due to global climate change and reorganizations of the fish community structure. Herring have occupied a leading place in the southwestern Bering Sea

pelagic layer likely since fall of 1994. Dr. N. I. Naumenko (pers. comm.) considers that the total Korf-Karaginsky herring biomass is equal to 1.7 million tonnes now. It is at least three times greater than for other pelagic fish species in the southwestern Bering Sea shelf.

Assessing the possible effects of increasing herring abundance on further reorganization of the community structure in the western Bering Sea is one from objectives of future studies. High abundance gives herring and important role as plankton consumers and as forage fish for upper trophic level predators. The dynamics of herring spatial distribution is of special interest in this aspect as it could determine role and contribution of herring to the organic matter transport through fish community trophic net in the Bering Sea shelf and offshore zones.

Material and methods

The TINRO-Center database of integrated ecosystem studies consists of materials from twelve complex expeditions carried out from 1986 to 1990 by Russian investigators in the western and central Bering Sea (Shuntov and Radchenko, 1999). Surveys in the central Berign Sea occurred only from 1988-1990. From 1991-1995, the survey area was limited to the southwestern part of the Bering Sea. The epipelagic layer (0-200 m) was investigated in all 12 expeditions. Fish sampling was conducted using a pelagic rope trawl, basically 108/528 m. The trawl bag (length 30-40 m) had mesh size of 30 mm and small-mesh insert (6-12 mm) of length 15m in back part. Archival data of 1,914 trawl hauls executed in these expeditions in upper epipelagic layer were analysed on distribution, abundance and feeding habits of fish and squids species to collate them with recently collected materials.

Since 1995 the bottom trawl and hydro-acoustic surveys were conducted in the western Bering Sea only. Walleye pollock stock assessment was the main objective of these expeditions until 1998. Last year, the first integrated expedition was conducted in this region. The set of expeditionary studies included oceanological, planktonic, bottom and trawl-acoustic surveys with accompanying work on data processing. For all common fish and squid species, feeding habits and biology characteristics have been examined. This regional coverage included the continental shelf and upper slope of the western Bering Sea between depths 49 to 509 m and totalled 37,000 square miles (Fig. 1). A bottom trawl survey (36 hauls) was conducted from August 21 to October 4, 1998. The distance between survey transects was 40 miles in the Anadry Gulf, Navarinsky region, and along the Koryak coast, but 20 miles in the Olyutorsky and Karaginsky Bays. The distance between hauls varied from 5 to 20 miles. The survey was executed by bottom trawl of 35/41m model. In October, an acoustic survey was conducted on the same area with several pelagic trawl hauls. These data give us additional data on herring distribution and seasonal migrations.

Herring stomachs and alimentary tracts were collected during biological investigations after trawl survey hauls. Daily diet calculation was conducted using the method of A. Kogan (1963) for fish that had well-expressed diurnal rhythms. Stomacbs from 205 herring specimens have been processed. Daily diet values and composition have been determined for all common pelagic and groundfish species.

Result

Data from 1998 showed that herring aggregations did not occur outside the shelf zone (Fig. 2) despite both direct and indirect evidence of increasing abundance. During the bottom trawl survey, herring accounted for only 1.5% of the total fish biomass. Indeed, it was determined by insignificant vertical opening of of the mouth of bottom trawl, was unable to catch whole schools of migrating herring.

Herring rarely occurred in trawl catches (no more than 5 fish per 30 minute haul) in the Anadry Gulf and northern waters off the Koryak Coast. Relatively high herring catches occurred in the western and central Koryak Coast (westward from 175°E) and in the eastern Olyutorsky Bay.

Maximal herring catch was at 1.5 tons, or about 5,000 fish per 30 minute haul (Fig. 2).

In October, herring was chiefly distributed in the Karaginsky and Olyutorsky bays (Fig. 3). Herring school records occurred in pelagic layer as pile-shaped spots, sometimes from bottom to sea surface. Maximal catch reached 6 mt, or more than 19,000 fish per 30 minutes pelagic haul. Herring aggregations had length of 2 miles and a height of about 25 m in that area.

Herring aggregations were represented by specimens sized 29 – 32 cm and at age 4+ to age 5+ in the Karaginsky and Olyutorsky Bays. This supports a previous understanding of the predominance of two year-classes in the Korf-Karaginsky herring population – 1993 and, to a lesser degree, 1994. These fish had body lengths (FL) 29-34 cm at survey time and contributed 75.5% of the total herring numbers on the Koryak shelf, and in the southwestern Bering Sea bays. However, the portion of older age groups was higher on the Koryak shelf (1991–1992 year-classes). Whereas, the numbers of herring aged 3+ (FL = 23-27 cm) was remarkable in the continental slope area off the Karaginsky and Olyutorsky bays. In near-shore waters, herring of third marine year (1996 year-class, FL = 21-23 cm) were fixed in survey catches. Age distribution of Korf-Karaginsky herring is presented in Figure 4 for the southwestern Bering Sea bays.

Several euphausiid species formed the base of the herring food supply in all survey regions (Table 1). Their contribution varied from 35.6 to 100% of the herring diet in different regions. Copepods contributed from 5 to 20.9% of the daily diet. Chaetognaths, gammarids, hyperiids, and decapods' larvae also occurred in the herring diet. Herring sized 30-35 cm had significant distinction from smaller size groups in the Karaginsky and Olyutorsky Bays. They mainly fed on walleye pollock juveniles which contributed 54.3% of daily diet. Stomach fullness varied from 42.7-151.7‰ for herring sized 25-40 cm. Smaller herring from the southwestern Bering Sea bays fed more intensively with average stomach fullness at 290.8‰. Daily diet value amounted 3.0% of body weight for fish sized 25-30 cm and 2.7% - for fish sized 30 – 35 cm.

Discussion

The annual cycle of the Korf-Karaginsky herring has been adequately studied. After spawning, it is well known that adult herring have an extensive migration route until late September-October. These migrations cover the continental shelf and slope zones from Goven Cape to the Navarin Cape (Panin, 1951; Prokhorov, 1967; Kachina, 1981).

Some relationship has been observed between the direction and intensity of herring migration with the oceanological regime in the area. In late June of 1991, adult herring occurred in the shallowest areas as seasonal heating did not significantly penetrate in the water column. Despite the anomalous high ocean temperature at the surface (7.5 – 9.6°C), it declined rapidly to 0.1 – 0.8°C at a depth of 20 – 25 m, especially in the eastern part of the Olyutorsky Bay. Water inflow from the offshore zone was observed in the central part of the bay. The main herring aggregations were distributed on the periphery of the gradient zone where water flowed onto the shelf (Fig. 5a).

The same situation occurred in July 1992. Weakly transformed Pacific waters have flowed there from the Near Strait region, and the resulting gradient zone formed in the western part of Olyutorsky Bay. Water flow onto the shelf was more intensive in 1992 than in 1991. Consequently, the herring concentration was significantly higher there. Adult herring (24-30 cm, mean 26.8 cm) catches reached 3 t per one-hour haul. Numerous herring schools occurred in the 4 – 25 m stratum (Fig. 5b).

Table 1 Herring diet value and composition in the western Bering Sea, 21 August – 4 October 1998.

	Regions						
	Karaginsky and Olyutorsky Bays			Off Koryak Coast		Anadyr Gulf	
Herring size groups: →	20 - 25	25 - 30	30 - 35	35 - 40	25 - 30	30 - 35	25 - 30
Prey species							
Parasagitta elegans	-	2.1	-	-	-	-	-
Guracoda	-	-	X	-	-	-	-
Pseudocalanus minutus	-	X	-	-	-	-	-
Neocalanus cristatus	5.0	20.9	7.2	15.0	20	6.5	-
N. plumchrus	-	-	2.1	3.0	-	-	-
Eucalanus bungii	-	-	-	-	-	0.1	-
Candacia sp.	-	-	0.0	-	-	-	-
Meridia spacifica	-	-	0.3	-	-	2.4	-
Thysanoessa raschii	18.0	15.2	8.4	-	-	33.2	40
T. hinspinata	-	-	-	-	-	23.1	-
T. hinermis	15.0	20.4	27.2	-	-	-	60
Euphausiacea (unid.)	60.0	23.7	-	80.0	80	-	-
Parathemisto pacifica	2.0	10.2	0.5	2.0	-	34.7	-
Gammaridea	-	-	-	-	X	-	-
Decapoda (larvae)	-	4.9	-	-	-	-	-
Theragra chalcogramma (aged 0+)	-	-	54.3	-	-	-	-
Fish weight (*g*)	141	322	357	547	233	359	256
Stomach numbers (n)	14	70	55	9	9	28	20
Number of empty stomachs	0	19	6	0	6	10	4
Food lump weight (*g*)	4.1	1.4	2.1	8.3	1.4	2.0	0.7
Mean Stomach fullness ()	290.8	42.7	60.1	151.7	60.1	55.4	28.1
Depth (*m*)	223.0	101-223	132-223	223.0	104.0	104-118	166.0

In early July of 1993, water inflow onto the shelf from the offshore zone was limited and did not effect the SST distribution. Slight curvatures of the isohaline contours indicated weak water inflow in the western Olyutorsky Bay (Fig. 5c). Herring were not aggregated in the bay at that time. Most herring schools likely migrated eastward from the Olyutorsky Cape. In trawl catches herring occurred in insignificant quantities (up to 0.23 tons per one-hour haul) in the depth range 60-120m.

In June–July of 1995 the situation occurred again like to 1992. Relatively weak flow was directed along the continental shelf edge from the Olyutorsky Cape to Karaginsky Island. Inflow of weakly transformed Pacific water was blocked by an anticyclonic eddy located 60 miles southwest of Olyutorsky Cape. Herring sized 26-37cm (mean 29.8 cm) occurred sporadically in trawl catches, mainly in the Olyutorsky Bay. The density of herring was in 3.5 times less than in 1993.

In 1991–1995, adult herring fed mainly upon euphausiids (*Thysanoessa inermis*) and copepods (*Eucalanus bungii*) in May – June, the period of the highest feeding intensity. During these two months, zooplankton consumption by herring contributes about 40% from annual food ration or approximately 1.95 kg of food per fish. In July, the herring daily diet is noticeable lower – from

11.7% of body weight during the feeding peak, to 2.9 – 3.0%, then to 1.9 – 2%. In August and September of 1991 – 1995, herring fed upon a wide spectrum of planktonic organisms in the Olyutorsky Bay: pteropod molluscs (25.2% on average, and in some years up to 77.9%), hyperiids (13.8%), pollock and capelin underyearlings (3.7–4%). During the 1980s, fish juveniles contributed 6% of herring diet. Herring annually consumed about 3,700 t of juvenile pollock and 6,400 t of capelin. On the area off Koryak Coast herring chiefly consumed copepods with *Neocalanus cristatus* predominant in August and September. The euphausiid portion has been estimated at 14% of daily diet in these months. In October the euphausiid portion increased and in December it reached 98% (Table 2).

In 1998, the herring diet composition was similar to that of the first half of 1990s. Euphausiids became a predominant food object and the smaller copepod *E. bungii* was replaced by *N. cristatus*. The daily diet value was higher for this season than in previous years of the study. According to our estimation, 1.7 million t of herring consumed about 45,000 t of food daily, mainly zooplankton (39,800 t). Euphausiids contributed about 21,500 t, equal to more than half of the total forage zooplankton biomass. The estimated euphausiid biomass, based on integrated surveys of the area, was 922,000 t on the continental shelf and slope zones off the Koryak Coast and in the southwestern Bering Sea bays. It means that herring are able to consume 64.1% of the total herring biomass during one month.

Table 2 Kort-Karaginsky herring diet composition (%) by different size groups, by seasons in the western Bering Sea, 1986 – 1993.

Food objects	Herring size groups									
	0 + age		1 + -2 + age				3 +-10 + age			
	Fall	Winter	Spring	Summer	Fall	Winter	Spring	Summer*	Fall	Winter
Euphausids	3.2	45.9	10.0	8.0	12.5	75.0	60.0	35.4	53.1	98.0
Copepods	32.9	29.4	70.0	64.4	37.5	10.5	38.0	20.8	5.0	1.2
Hyperiids	34.2	2.3	15.0	22.2	25.0	-	2.0	13.8	1.9	+
Appendicularians	29.7	-	5.0	0.8	-	-	-	25.2	-	-
Pteropods	+	-	-	4.2	17.5	2.0	-	0.7	25.2	-
Chaetognats	-	22.4	-	+	+	-	-	0.4	14.8	0.8
Juvenile fish, eggs, larvae	-	-	+	0.4	1.8	2.8	+	3.8	-	-
Daily diet value (%BW)	4.2	6.8	3.2	2.3			11.7**	1.9	1.3	1.1

Remarks: * - for herring remaining in the Olyutorsky Bay.
** - during after-spawning period of high feeding intensity.

Data by season: Spring – April – May of 1989 and 1990; Summer – July of 1991 and 1992; Fall – September – Octocber of 1986 and 1987; Winter – late November of 1988, December of 1993.

It can be concluded that general pattern of water circulation likely has a greater effect on herring distribution than other features of physical environment. Herring aggregations are chiefly distributed in zones of water inflow onto the shelf from the offshore. Water flow onto the shelf provides a permanent transport of adult zooplankton organisms, which chiefly inhabit the offshore zone in summer season. Large zooplankton organisms predominate in the herring diet after spawning and their portion gradually increases until late fall. If water inflow

has developed by June to early July, herring schools remain within the bay for feeding. Otherwise, the herring move quickly eastwards from Olyutorsky Cape. It should also be noted that herring aggregations have been observed along the Koryak Coast in the gradient zone periphery near the Central Bering Sea Current entrance of shelf and divergence (Prokhorov, 1967). In early August of 1987, herring catches reached there 18 tons per one-hour trawling.

Euphausiids are characterized by high potential production. The annual productivity to biomass ratio (P/B) is approximately 8 (Ponomareva, 1990). Since the main growth in weight of euphausiids takes place in warmer half-year, we can imagine that the euphausiid biomass is doubled every two months. These crustaceans are consumed rather intensively in the ecosystem. Walleye pollock, salmon, and other fishes feed on euphausiids. Some tightness is evident in the corresponding links of the shelf fish community trophic web.

Extpansion of feeding areas is an inherent characteristic of pelagic fishes during high abundance (Blaber, 1991). In the 1980s, abundant walleye pollock migrations were observed in the offshore Bering Sea basins and a large-scale fishery developed there. The total walleye pollock harvest in the Donut Hole reached 1.3 million tons in 1988. Will herring migrate in the offshore western Bering Sea to utilize its food resources or not?

The Korf-Karaginsky herring migrations through western Commander Basin were determined during the 1960s (Kachina, 1981). It is evident from herring distribution maps in this publication that herring were found offshore, although the author did not point out this feature of herring ecology. In 1992, the pollock fishing fleet observed herring migrating in the northern Aleutian Basin of the Bering Sea. Herring schools withdrew from shelf by up to 60 – 100 miles. Observers reported herring catches of 36 t per trawl haul in the offshore. This behaviour is also observed in the Atlantic–Scandianvian herring population, whose feeding area is chiefly situated above 1,000m depth. Therefore, feeding migration route seems possible for herring in the Bering Sea offshore water.

On the contrary, during the 1960s the Korf-Karaginsky herring biomass reached 3.5 million t, twice the present level (Naumenko et al., 1990). Based on the seasonal dynamics of herring daily diet value, annual Korf-Karaginsky population food ration totals at 24.3 million t (at level of herring biomass in 1.7 million tons). It is noticeably lower than larger plankton production in shelf areas, which can be estimated at 63.9 million tons (from annual biomass 6.2 million tons and P/B =10.3). Last year's euphausiid biomass increased in the herring feeding area and reached 309 $mg \cdot m^{-3}$. Besides, the main part of larger zooplankton consumed by herring is likely transported from the offshore sea with the water flow onto the shelf. Total annual euryphagous zooplankton production was estimated at 3.03 billion t for the whole Bering Sea, or 1,343 $t \cdot km^{-2}$ (Shuntov & Dulepova, 1995).

During the 1990s, significant growth of the Korf-Karaginsky herring biomass can be regarded as stable trend (Radchenko, 1998). However, further increase of the Korf-Karaginsky herring population can be prevented by spawning and early development conditions (Puschaeva, 1969). Several small inlets in the northern Karaginsky and Korf Bays can be regarded as favourable for local herring reproduction. Furthermore, natural mortality rates of egg and larvae sharply increase when spawning stocks are abundant (Puschaeva, 1968; Kachina, 1981). In last year, Dr. Naumenko (personal communication) has observed significant pre-spawning mortality of herring in the Anapka Inlet due to super-abundant herring spawner approach and inability to leave the inlet before reflux.

Thereby, a herring feeding strategy involves consumption of abundant and less motile organisms. During spring and summer feeding route herring aggregations are distributed in zones of permanent plankton transport and accumulation. In early summer, copepods predominate among planktonic crustaceans in

Olyutorsky Bay and it is reflected in herring diet composition. In May – June, in the shelf area off Koryak coast, the peak of herring feeding is related to euphausiids spawning, when euphausiids migrate into shallow areas and remain near the surface even during daytime (Ponomareva, 1990). "Grazing" as feeding strategy is not inherent for herring in the same degree as for pollock. This is indicated by the character of feeding migrations of these fish species: dense, quickly moving schools for herring and dispersion from dense spawning aggregations for pollock.

There are no "ecological limitations" (Blaber, 1991) for herring to migrate into deeper water and feed upon offshore resources. Nevertheless, herring ecology and feeding habits characterize this species as a typical shelf species. At the present level of herring biomass, there is a remote possibility of abundant herring migrations in the offshore Bering Sea. It means that the fish community in the deep-sea regions will have a predator deficit in its trophic structure.

References:

Blaber, N. J. M. 1991. Deep sea, estuarine and freshwater fishes: Life history strategies and ecological boundaries. Sth. Afr. J. Aquat. Sci., 17(1-2); 2-11.

Kachina, T. F. 1981. Herring of the western Bering Sea. Moscow, Legpischeprom. 121p (in Russian)

Naumenko N. I., Balykin P. A., Naumenko E. A., Shaginyan E. R. 1990. Long-term changes in pelagic fish community in the western Bering Sea. Izvestiya TINRO (TINRO Transactions). 111: 49-57 (in Russian)

Panin, K. I., 1951. Feeding herring distribution at the eastern Kamchatka coast. Izvestiya TINRO (TINRO Transactions). 34: 257-259 (in Russian).

Prokhorov V. G., 1968. On seasonal cycles in adult herring biology in the western Bering Sea. Izvestiya TINRO (TINRO Transactions). 61: 216-223 (in Russian).

Puschaeva, A. Ya. 1968. Spring zooplankton and herring larvae feeding in the Anapka Inlet. Izvestiya TINRO (TINRO Transactions). 64: 309-314 (in Russian).

Radchenko V. I. 1998. Scale and causes of growth of the Pacific herring abundance in the western Bering Sea in 1990s. Abstracts of Seventh PICES Annual Meeting, October 14-25, 1998. Fairbanks, USA, P. 102-103.

Shuntov, V. P., Dulepova, E. P. 1995. Present state, bio-and fish productivity of the Bering Sea ecosystem. Complex investigation of the Bering Sea ecosystem. Moscow, VNIRO. P.358-388 (in Russian).

Shuntov, V. P., Radchenko, V. L., 1999. Summary of TINRO ecosystem investigations in the Bering Sea. *In* T.R. Loughlin and K. Ohtani [eds.] The Dynamics of the Bering Sea. University of Alaska Sea Grant, AK-SG-99-03, Fairbanks, 838pp.

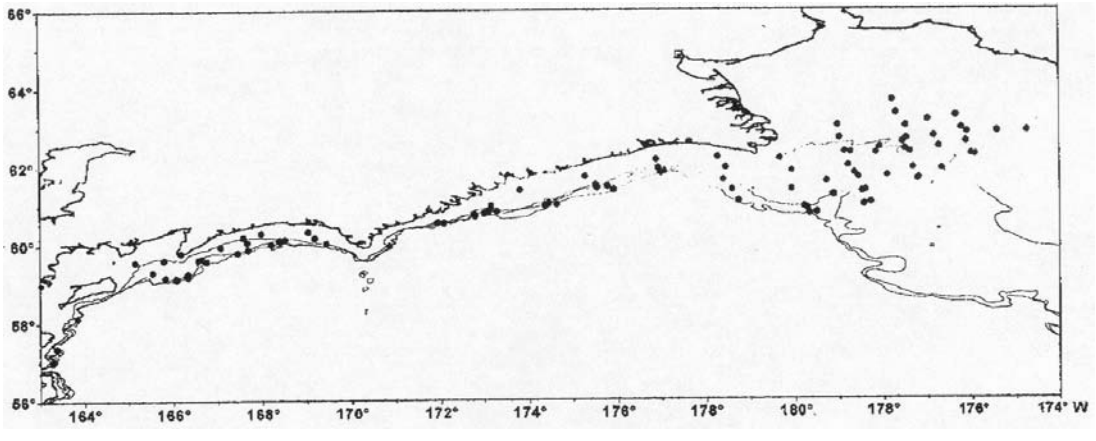

Fig. 1 Scheme of the trawl survey.

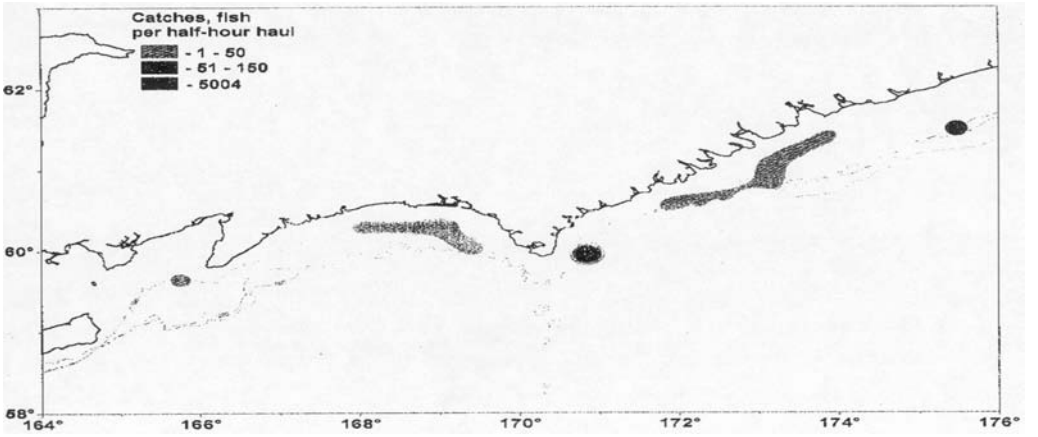

Fig. 2 Pacific herring catch distribution according to *R/V "Professor Kaganovsky"* cruise data in the western Bering Sea, bottom trawl survey, August-September of 1998.

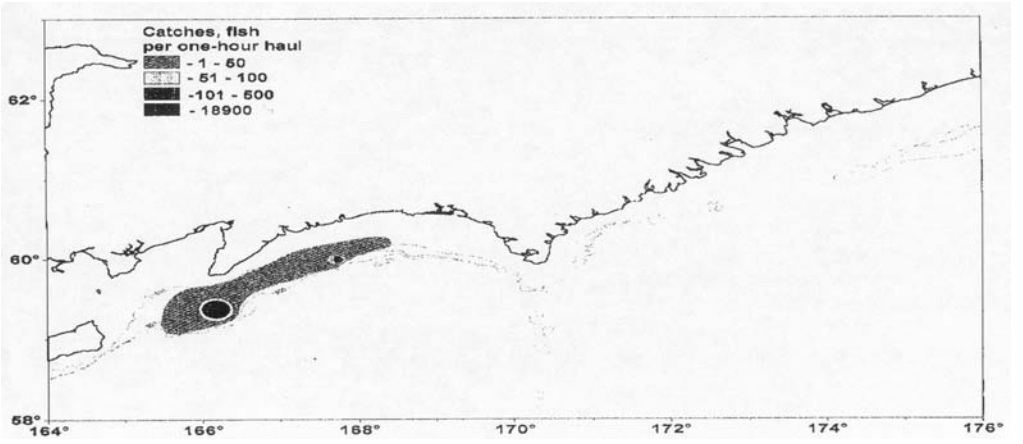

Fig. 3 Pacific herring catch distribution according to *R/V "Professor Kaganovsky"* cruise data in the western Bering Sea, trawl-acoustic survey, October of 1998.

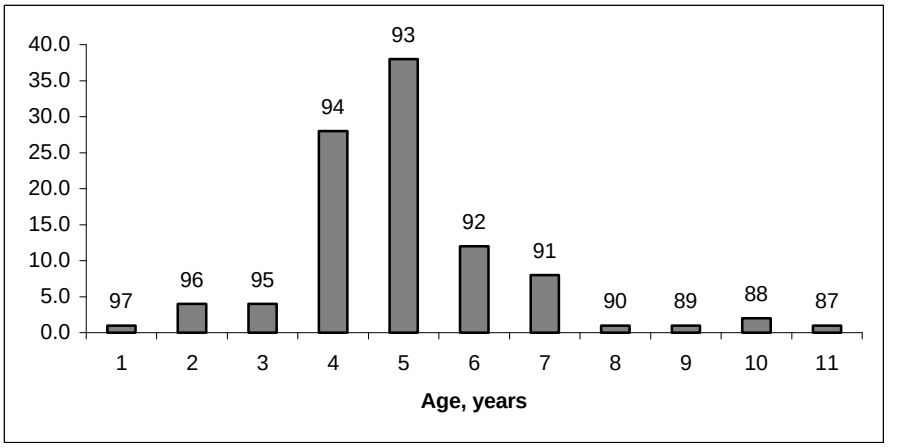

Fig. 4 Herring age distribution in the Karaginsky and Olyutorsky Bays in the western Bering Sea, October 1998.

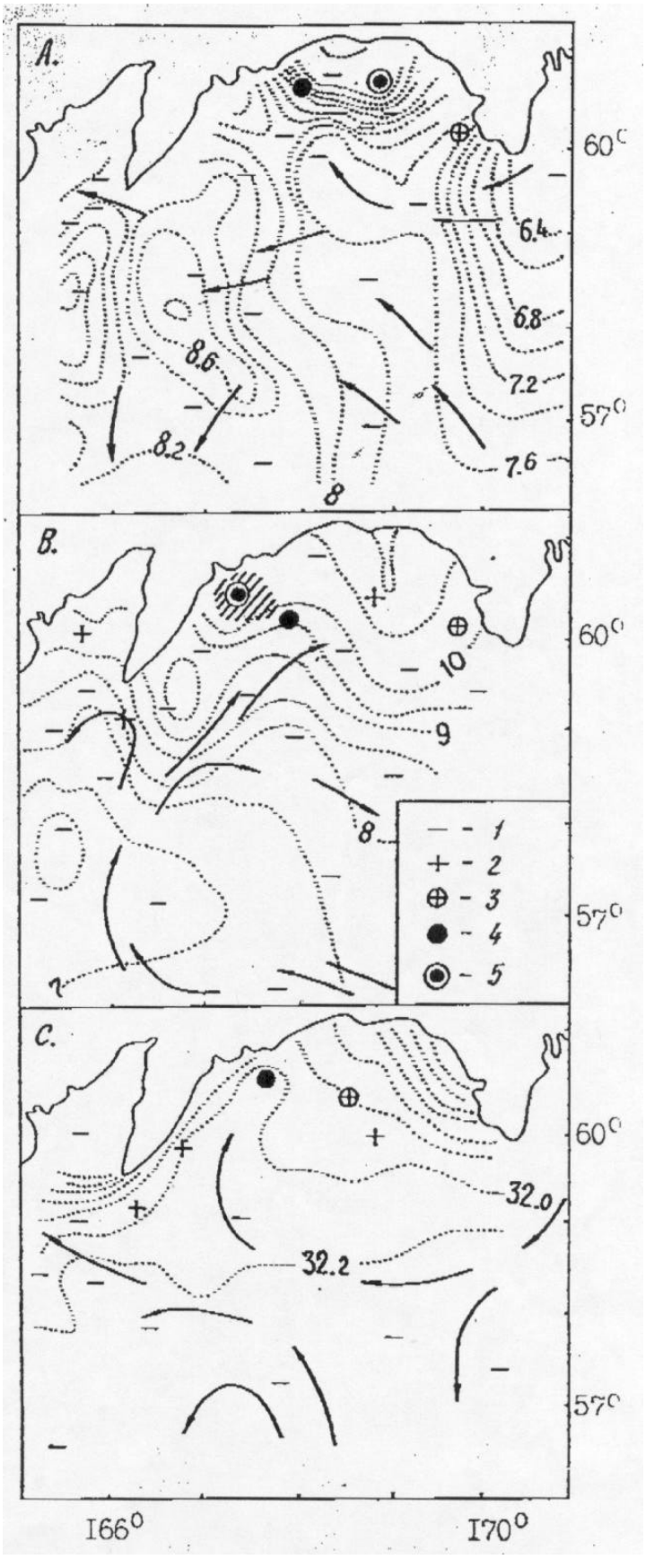

Fig. 5 Herring Catch distribution in the Olyutorsky Bay in the western Bering Sea in Summer of 1991-1993. A) 6/22–7/5/1991; B) 7/3– 7/13/1992; C) 6/15–7/7/ 1993.

Legends:

1 – no catch;
2 – below 10;
3 – 10-100;
4 – 100-1000;
5 – above 1000 kg per one-hour haul.

Area with herring schools acoustic records is shadowed. SST (°C), Figure A, Figure B, and sea surface salinity (‰), Figure C, are presented.

Euphausiids in the Korean waters and its relationship with major fish resources

Young Shil Kang
National Fisheries Research and Development Institute, Pusan, Korea 619-900. E-mail: yskang@nfrda.re.kr

Euphausiids are very important food resources for major fish resources, squid, mackerel, whales and so on in Korean waters. Euphausiids have recently shown an increasing trend in composition of major zooplankton groups, and 10 species were identified from the Korean waters. Until recently, little work has been done in long-term change in abundance of euphausiids in related to climate change and the importance of fish resources in the Korean waters. This study is focus on general distributional pattern, the regional patterns of long-term changes in abundance and the relationship between euphausiid and fish abundance in Korean waters.

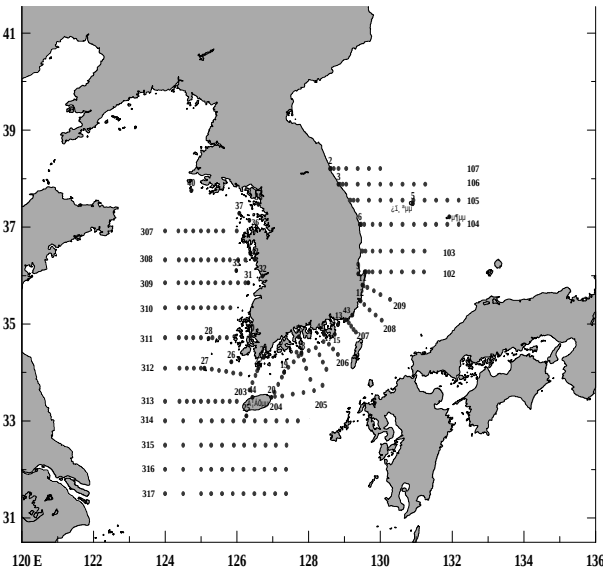

Fig. 1 Map showing the study area and stations; date indicate oceanographic survey stations.

The National Fisheries Research and Development Institute has conducted regular oceanographic surveys 6 times annually (February, April, June, August, October and December) since 1965 in the Korean waters (Fig. 1). From this survey, euphausiids were collected by NORPAC net (0.45 m mouth and 0.33 mm mesh size) with vertical tow from bottom (or 100 m depth) to surface. For this study, data on euphausiid abundance and surface water temperature during 1978-1998 were used. Catches of squid, mackerel and anchovy were analyzed during 1978-1998 in comparison with abundance of euphausiid.

The following 10 species were identified from the Korean waters: *Euphausia recurva*, *E. mutica, E. pacifica, E. nana, E. tenera, E. similis, Pseudeuphausia latifrons, Stylocheiron affine, S. carinatum,* and *Thysanoessa longipes*. Of these species, *E. pacifica, E. nana* and *P. latifrons* were numerically dominant. Seven other species were associated with the influx of the Tsushima Warm Current. *E. pacifica* had a discontinuous distributional pattern. It was found in the Sea of Japan and the northern part of the Korea Strait, and the Yellow Sea. *E. nana* occurred in the intervening area, with some overlap with *E. pacifica* in the east and west.

From distribution of mean abundance of euphausiids during 1978-1998 in the Korean waters it is recognized that euphausiids were densely populated in the coastal area and the western area of Cheju Island in April and June. Although their abundance was very low, they usually aggregated in the coastal area in February, August and October.

Comparing among three separated subareas, east, west and south areas, the south area showed the highest abundance, while the east area was low.

There was a conspicuous seasonal change with the regional variation. In Korean waters a large peak appeared in spring, April and June, and a

small peak occurred in autumn, October. In the south area this pattern is very clear, while in the west and east areas it was not clear.

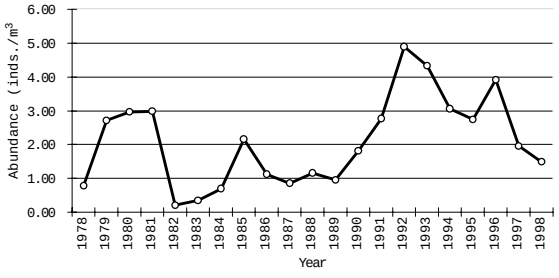

Fig. 2 Year-to-year changes in euphausiids abundance in the Korean waters during 1978-1998.

The annual average abundance from 1978-1998 was 2.52 ind.•m^{-3}. The euphausiids showed an increasing trend since the early 1990s with two increasing periods (Fig. 2). The first occurred from the late 1970s to the early 1980s and the second occurred after 1990. The increase after 1990 was closely associated with the increase of surface water temperature in winter, February and December.

Year-to-year changes in catches of major fish resources, *Engraulis japonica, Scomber japonicus* and *Todarodes pacificus* were compared to euphausiid abundance. *Engraulis japonica* and *Scomber japonicus* are major fish resources in the South Sea, while *Todarodes pacificus* is in the East Sea of Korea. *Engraulis japonica* and *Scomber japonicus* began to increase since 1992 with extraordinary increase in 1993 and 1996, respectively. It did not coincide with euphausiid abundance, but there was a possibility that the increasing trend after 1990 in euphausiids abundance accompanied with increases of *Engraulis japonica* and *Scomber japonicus* after 1992.

Todarodes pacificus increased continuously after 1990. It was closely related to the increase of euphausiid abundance in the East Sea of Korea.

Ecological Zonation of euphausiids off central Oregon

William T. Peterson[1], Leah Feinberg[2] and Julie Keister[2]

[1] National Marine Fisheries Service. E-mail: bill.peterson@noaa.gov

[2] Cooperative Institute for Marine Resource Studies, Hatfield Marine Science Center, 2030 S. Marine Science Drive, Newport, OR 97365, U.S.A.

Introduction

The euphausiids *Euphausia pacifica* and *Thysanoessa spinifera* dominate the euphausiid assemblage along the west coast of North America from Baja California to the Gulf of Alaska. Research in the northeast Pacific has shown that the two species share a common latitudinal range but that *T. spinifera* is a coastal species, restricted to shelf waters while *E. pacifica* is an oceanic species. For example, off southwestern Vancouver Island, Mackas (1992) showed that *T. spinifera* is the dominant euphausiid species in shelf waters and is the only euphausiid common in water depths shallower than about 150 m whereas *E. pacifica* is dominant along and seaward of the shelf break. Off Newport, OR, Smiles and Pearcy (1971) found that *Euphausia pacifica* was far more abundant near the shelf-break than offshore, peaking at a station 25 miles from shore (250 m water depth). In the same data set, *T. spinifera* was found chiefly at a station 15 miles from shore (90 m water depth) but not farther offshore (Smiles, unpublished data). Peterson and Miller (1976), who worked off Newport in 1971 and 1972, did not find *E. pacifica* closer to shore than 20 miles (150 m depth), nor *T. spinifera* further from shore than 20 miles. Thus, off central Oregon the two species have their maxima in abundance at stations within a few miles of each other, with

little or no overlap in their zonal distributions, but how they are maintained in separate ecological zones remains a puzzle. The two species do co-occur in Barkley Sound, a deep fjord that penetrates southwest Vancouver Island (Tanasichuk, 1998a, b). Curiously, in Puget Sound, Dabob Bay, Saanich Inlet and the Straits of Georgia only *Euphausia pacifica* is present (and abundant) whereas *Thysanoessa spinifera* is either uncommon or absent (Ross et al. 1982; Bollens et al. 1992).

The patterns observed off the Oregon coast are not as clear-cut in California waters. CalCOFI Atlas No. 5 shows that *T. spinifera* inhabit both shelf and oceanic waters off northern and central California (Brinton 1967); *E. pacifica* is chiefly an offshore species but has a biomass maxima at the shelf break (Brinton 1962). *T. spinifera* has been found far to sea off northern and central California when associated with mesoscale eddies, filaments and jets -- Mackas et al. (1991) reported high concentration of this species along the shoreward edge of an upwelling filament. Also, Peterson (unpublished data from a survey of the jet/eddy complex off Monterey, July 1991) found large concentrations of *T. spinifera* (40-150 juveniles + adults m^{-3}) in the cool waters of an upwelling filament, 120 miles from shore. On the other hand, Huntley et al. (1995) did not report the presence of *T. spinifera* in their survey of a large eddy off Monterey in June 1993. Mackas et al., Huntley et al. and Peterson all found enhanced concentrations of *E. pacifica* within these mesoscale features. Based on analysis of acoustics data, Swartzman (personal communication) found that the pronounced zonation patterns observed off central Oregon begin to break down south of Cape Blanco.

We have been sampling euphausiid larvae in the coastal zone off Newport, OR during biweekly cruises since 1996 at stations 5 and 15 miles from shore (9 and 28 km respectively). *Thysanoessa spinifera* larvae were always most abundant at the nearshore station whereas *Euphausia pacifica* were usually most abundant at the offshore station. Table 1 compares the densities at each station, where we show data averaged over the growth season of March of one year to February of the next (following Tanasichuk 1998). During the 1997-98 El Niño, both species had their highest overall abundances, probably due to strong onshore advection during this period. With the onset of the 1999-00 La Niña (a period of cool water and high upwelling), densities of *Euphausia pacifica* declined markdly (possibly due to transport offshore).

We also compared our larval density numbers to those from a similar study conducted about 300 miles to the north of Newport, Oregon, in Barkley Sound, Vancouver Island, British Columbia, by Tanasichuk (1998a,b). Large differences in larval densities are seen, with Barkley Sound densities up to 10 fold greater than off Newport (Table 2). However, the ratio of densities of the two species (density of *E. pacifica* divided by density of *T. spinifera*) was very similar when NH 5 is compared to Barkeley Sound (but not NH 15), suggesting that despite differences in production, Barkeley Sound resembles our nearshore station but not our offshore station.

Some very unusual euphausiid species were found off Oregon during the El Niño, *Euphausia recurva* and *E. mutica*. These two species are ordinarily found only in Pacific Central water but occurred shelf waters off Oregon during winter 1997-98. This is the first record of these species off Oregon. Another unusual species was *Nyctiphanes simplex*, a coastal species that is normally most common off Baja California and in the southern California Bight (Brinton 1962, 1967). The meaning of this is that northward transport of coastal water carried *N. simplex* to Oregon (as noted previously by Brodeur et al. 1985. To account for the occurrence of *E. recurva* and *E. mutica*, there must also have been some northward and onshore transport of surface waters from the Central Gyre, due to intense southwesterly storms in winter 1997/98.

Table 1 Interannual variation in euphausiid abundance at inshore (NH5) and offshore (NH15) stations off Newport, Oregon from 1996-2000.

	Euphausia pacifica		*Thysanoessa spinifera*	
	NH 5	NH 15	NH 5	NH 15
1996 - 97	118 m^{-2}	366 m^{-2}	258 m^{-2}	112 m^{-2}
1997 - 98	569	1,077	577	337
1998 - 99	534	510	93	50
1999 - 00	38	59	373	102

Table 2 Euphausiid larval densities in Barkley Sound, Vancouver Island (Tanasichuk 1998) and the ratio of two species (*E. pacifica* : *T. spinifera*) abundance in Barkley Sound and Newport, Oregon.

	Barkley Sound		Ratio	Ratio	Ratio
	E.pacifica	*T.spinifera*	[Bark]	[NH 5]	[NH 15]
1991 - 92	479 m^{-2}	1,168 m^{-2}	0.41		
1992 - 93	2,723	2,742	0.99		
1993 - 94	1,205	669	1.8		
1994 - 95	537	450	1.19		
1995 - 96	1,303	7,372	0.18		
1996 - 97	1,286	2,222	0.57	0.46	3.3
1997 - 98	757	1,039	0.73	0.99	5.2
1998 - 99	4,555	889	5.12	5.74	10.2

References

Bollens, S.M., B.W. Frost, and T.S. Lin. 1992. Recruitment, growth, and diel vertical migration of *Euphausia pacifica* in a temperate fjord. Mar. Biol. 114: 219-228.

Brinton, E. 1962. The distribution of euphausiids. Bull. Scripps Inst. Oceanogr. 8: 51-269.

Brinton, E. 1967. Distributional atlas of Euphausiacea (Crustacea) in the California Current region, Part 1. CalCOFI Atlas #5, 275 pp.

Brodeur, R. D. 1986. Northward displacement of the euphausiid *Nyctiphanes simplex* Hansen to Oregon and Washington waters following the El Niño event of 1982-83. J. Crustacean Biol. 6:686-692.

Huntley, M., M. Zhou and W. Nordhausen. 1995. Mesoscale distribution of zooplankton in the California Current in late spring, observed by optical plankton counter. J. Mar. Res., 53: 647-661.

Mackas, D. L., L. Washburn and S. L. Smith. 1991. Zooplankton community pattern associated with a California Current cold filament. J. Geophys. Res., 96(8): 781-797.

Mackas, D. L. 1992. Seasonal cycle of zooplankton off southwestern British Columbia: 1979-1989. Can. J. Fish. Aquat. Sci., 49: 903-921.

Peterson, W. T. and C. B. Miller. 1976. Zooplankton along the continental shelf off Newport Oregon, 1969-1972: distribution, abundance, seasonal cycle and year-to-year variations. Oregon State Univ. Sea Grant College Program Pub., No. ORESU-T-76-002, 111 p.

Ross, R. M., K. L. Daly and T. Saunders. 1982. Reproductive cycle and fecundity of *Euphausia pacifica* in Puget Sound, Washington. Limnol. Oceanogr. 27: 304-314.

Smiles, M. C. and W. G. Pearcy. 1971. Size structure and growth rate of *Euphausia*

pacifica off the Oregon coast. Fish. Bull. U.S., 69: 79-86.

Tanasichuk, R. W. 1998a. Interannual variations in the population biology and productivity of *Thysanoessa spinifera* in Barkley Sound, Canada, with special reference to the 1992 and 1993 warm ocean years. Mar. Ecol. Prog.. Ser. 173: 181-195.

Tanasichuk, R. W. 1998b. Interannual variations in the population biology and productivity of *Euphausia pacifica* in Barkley Sound, Canada, with special reference to the 1992 and 1993 warm ocean years. Mar. Ecol. Prog., Ser. 173: 163-180.

Environmentally forced variability in larval development and stage-structure: Implications for the recruitment of Euphausia pacifica (Hansen) in the Southern California Bight

Scott M. Rumsey
US Geological Survey, Forest and Rangeland Ecosystem Science Center, 3200 SW Jefferson Way, Corvallis, OR 97331. U.S.A. E-mail: Scott_Rumsey@usgs.gov

Summary
The intent of this field work was to provide empirical evidence in observed larval distributions, stage-structure, and inferred developmental pathways of whether the developmental regime affects the development and abundance of particularly elastic larval stages. Armed with the insights from life-history modelling and demographic analyses (Rumsey and Franks, 1999), I sought to address particular aspects of the *Euphausia pacifica* life-history. First, how are the larval stages distributed vertically in the field with respect to each other and the developmental environment? Second, as indicated by the vertical distribution of calyptopis I stage larvae, is there evidence that females restrict the depth-range of spawning to enhance the profitability of the initial developmental environment? Third, I investigated whether there was variability in furcilia I-II developmental pathways over short (mesoscale) spatial scales, and if found, with what oceanographic conditions particular pathways are associated. Fourth, I described the spatial variability of larval stage-frequency distributions, and the environmental conditions and/or developmental processes with which such variability was associated.

Oceanographic and Demographic Data
Two cruises were conducted in the Southern California Bight, south of the Santa Barbara Channel and Channel Islands, in the winters of 1996 (cruise S9602) and 1997 (J9701). Samples of *Euphausia pacifica* larvae were obtained by MOCNESS transects across mesoscale oceanographic features (Fig. 1). CTD-fluorometer profiles accompanied each station (Fig. 2). *E. pacifica* larvae were identified to stage using morphological criteria (Boden, 1955). The developmental instar of pleopod development was noted for furcilia I-II stage larvae, and the dominant furcilia I-II pleopod developmental pathways determined for each station (after Knight, 1984; Lavaniegos-Espejo, 1994).

Spawning Distribution
Despite differences in the vertical distribution of *E.* pacifica larval stages between cruises, the majority (>95%) of larval stages were found in the upper 100 m (Fig. 3). Eggs were not sampled during either cruise, nonetheless, the presence/absence of the initial larval stages (being weakly swimming, e.g. calyptopis I) with depth is indicative of the depth range of spawning by gravid females. Although the vertical distribution of post-larvae in the night-time samples of both cruises was predominantly in the upper 150 m, their daily ambit spanned 0-300 m depth

(observed in J9701 day samples; Mauchline and Fisher, 1969; Brinton, 1976). The distribution of CI larvae is evidence that the depth range of egg release by *E. pacifica* is restricted relative to that of gravid females. Restricting the depth range of egg release to < 100 m would ensure warmer temperatures (and thus shorter developmental times) as well as enhanced availability of phytoplankton-food for first-feeding larvae.

Furcilia I-II Developmental Pathways

Prolonged developmental times, associated with indirect furcilia I-II pleopod developmental pathways, represent morphogenic plasticity that is likely an adaptive trait in neritic euphausiids inhabiting inherently variable environments. A predominance of indirect pleopod developmental pathways was associated only with the "cool" stations of cruise J9701 (Fig. 4). The proximate developmental temperatures for these larvae were 1-3 °C cooler (0-100 m) relative to temperature profiles for the other J9701 stations and the S9602 stations (Fig. 2). Furcilia I-II developmental pathways were predominantly direct at all S9602 stations (Fig. 4), and the cyclonic eddy with which they were associated was a persistent feature, comparable to the time scale of *E. pacifica* larval development. It is surprising, given the comparatively low chlorophyll conditions for cruise S9602 (Fig. 2), that furcilia development was so direct. Despite > 4-fold difference in chlorophyll fluorescence between cruises (Fig. 2) the proportion of S9602 indirect developmental pathways was indistinguishable from the J9701 "warm" stations, suggesting that temperature regime has a greater impact on early furcilia development than does ambient chlorophyll.

Winter and spring euphausiid abundances (*E. pacifica* included) have increased over the last 40 years in the Southern California Bight (Brinton, 1996), concurrent with a 1.5°C increase in surface temperatures and an 80% decrease in overall macrozooplankton biomass (Roemmich and McGowan, 1995). In contrast to overall macrozooplankton, one might expect diminished euphausiid recruitment success and indirect developmental pathways to be correlated with cooler developmental temperatures. The results of elasticity analyses (Rumsey and Franks, 1999) and the association of indirect furcilia I-II developmental pathways with cooler temperatures during cruise J9701 are in accordance with this notion. Observations of direct furcilia development associated with locally cooler temperatures over a broad geographic range (Puget Sound, Ross et al., 1982; Baja California, Lavaniegos, 1994; Southern California Bight, Knight, 1984), however, are difficult to reconcile with the observations of cruise J9701 and Brinton (1996). Furthermore, it is difficult to reconcile the impaired development observed in association with 10-12 °C conditions given that viable populations farther north in *E. pacifica*'s range certainly endure much colder developmental temperatures yet are not necessarily characterized by indirect furcilia development and diminished recruitment success. The response and tolerance of larval development to temperature heterogeneity may be determined by the temperature conditions during oogenesis and/or at egg release. Thus, variability in *E. pacifica* larval development may be in response to temperature anomalies rather than absolute conditions. Alternatively, the inconsistent relationship between development and temperature among regional populations could result from different physiological "races", each adapted to a distinct temperature range.

Larval Stage-Frequency Distributions

The high proportion of calyptopis I (CI) larvae in the stage-frequency distributions of cruise S9602 (Fig. 5A), suggest that spawning was ongoing or had only recently ceased. The greater proportion of CI larvae at the "green" stations may reflect differences in recent egg release or differences in egg through CI mortality among stations. Although small-scale ($\sim$1 km) differences in egg-inputs remains a possible contributing factor, associated differences among stations in chlorophyll conditions suggest the importance of differences in CI mortality. The CI stage is the first-feeding euphausiid larval stage. Several investigators have asserted that mortality during the CI stage is especially sensitive to environmental conditions (Brinton, 1976; Ross et

al., 1988; Paul et al., 1990), in particularly conditions of food-availability (Hofmann et al., 1992). The greater proportion of CI larvae at the green stations, with significantly greater chlorophyll (0-25 m), may reflect lower mortality at these stations due to more favorable food conditions. Additionally, the proportion of post-larvae (predominantly juveniles and non-mature adults) present at the green stations was greater than at those stations with lower surface chlorophyll. The proportion of post-larvae at a given station provides a rough index of local recruitment success (as most of the post-larvae sampled were juveniles, presumably having recently completed larval development). Although the chlorophyll regime appeared to have little impact on observed furcilia development (previous section), food availability during early larval development in *E. pacifica* may affect CI survivorship and subsequent larval recruitment. Lavaniegos-Espejo (1992) found that laboratory survivorship of *N. simplex* larvae was most affected by state of calyptopis development at the time of collection. The increased survivorship of larvae that started out as CIII vs. CII larvae in her experiments suggests that the food history of calyptopis phase larvae can impact the survivorship of later stages.

Differences in larval stage-frequencies during cruise J9701 (Fig. 5B) were driven mostly by variability in the proportion of the later furcilia stages (furcilia III-VI). FIII-FVI larvae at the "warm" stations exhibited direct pathways of pleopod development, relative to the cooler stations. Accelerated FIII-FVI developmental times associated with warmer temperatures could result in earlier recruitment and result in fewer larvae of these stages sampled. The higher proportion of post-larvae associated with the warm stations further supports this notion of earlier recruitment.

References

Boden, B. P., 1950. The post-naupliar stages of the crustacean *Euphausia pacifica*. Transactions American Microscopy Society 69: 373-386.

Brinton, E., 1976. Population biology of *Euphausia pacifica* off Southern California. Fishery Bulletin U.S. 74(4): 733-762.

Brinton, E., 1996. Will the '96 krill drill head on up the hill, and spill like jill? Or: the '93-'96 krill increases have reached levels which, in the past, have preceded abrupt declines off southern California. California Cooperative Fisherish Investigation Annual Conference, Pacific Grove, CA, Abstracts: V-7.

Hofmann, E. E., Capella, J. E., Ross, R. M., Quetin, L. B., 1992. Models of the early life history of *Euphausia superba*- Part I. Time and temperature dependence during the descent-ascent cycle. Deep-Sea Research 39(7/8): 1177-1200.

Knight, M. D., 1984. Variation in larval morphogenesis within the southern California Bight population of *Euphausia pacifica* from winter through summer, 1977-1978. CalCOFI Reports 25: 87-99.

Lavaniegos-Espejo, B., 1994. Dispersion and development patterns in larvae of *Nyctiphanes simplex* (Euphausiacea) in the upwelling region off Baja California. Marine Ecology Progress Series 106: 207-225.

Mauchline, J., Fischer, L. B., 1969. The biolgoy of euphausiids. Advances in Marine Biology. 7: 1-454.

Paul, A. J., Coyle, K. O., Ziemann, D. A., 1990. Timing of spawning of *Thysanoessa raschii* (Euphausiacea) and occurrence of their feeding stage larvae in an Alaskan Bay. J. Crustacean Biology 10 (1): 69-78.

Roemmich, D. and J. McGowan, 1995. Climatic warming and the decline of zooplankton in the California current. Science 267: 1324-1326.

Ross, R. M., L. B. Quetin and E. Kirsch, 1988. Effect of temperature on developmental times and survival of early larval stages of *Euphausia superba* Dana. Journal of Experimental Biology and Ecology 121: 66-71.

Ross, R. M., K. L. Daly and T. S. English, 1982. Reproductive cycle and fecundity of *Euphausia pacifica* in Puget Sound, Washington. Limnology Oceanography 27(2): 304-314.

Rumsey, S. and P. Franks, 1999. Influence of variability in larval development on recruitment success in the euphausiid *Euphausia pacifica*: elasticity and sensitivity analyses. Marine Biology. 133: 283-291.

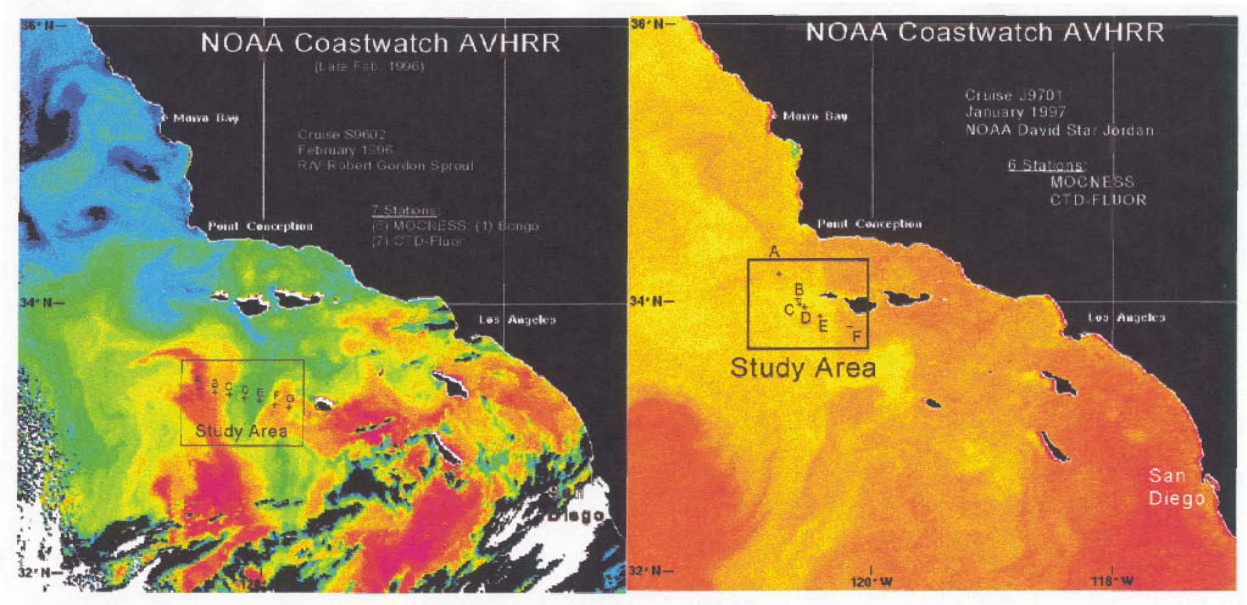

Fig. 1 AVHRR images of sea surface temperature illustrating the study region and station locations for the February 1996 (S9602) and January 1997 (J9701).

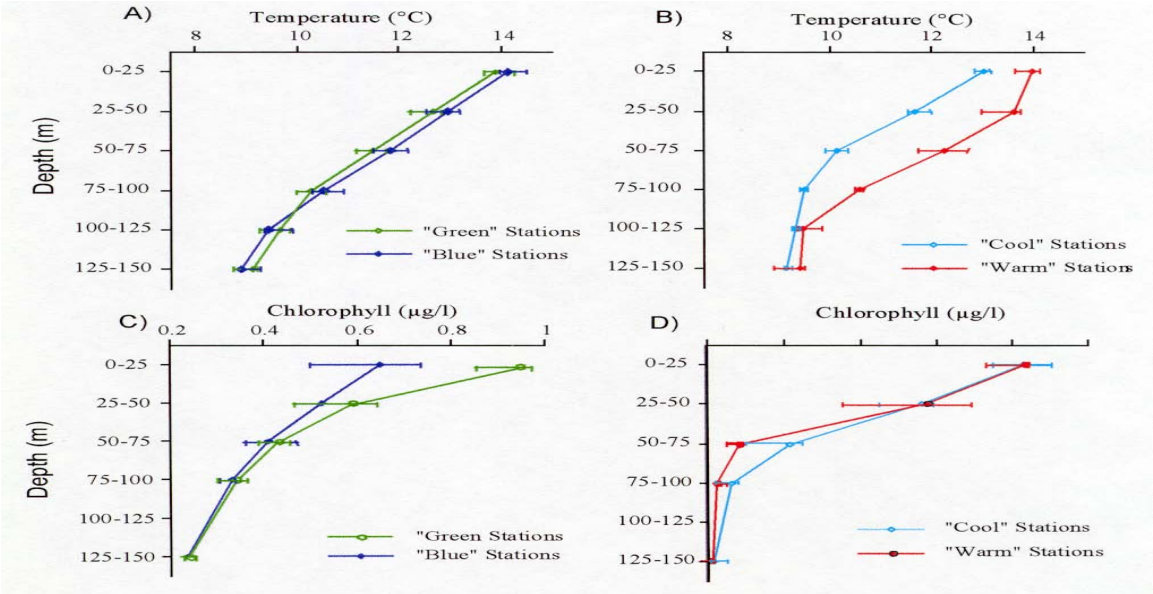

Fig. 2 Temperature and chlorophyll profiles S9602 (A and C) and J9701 (B and D). To facilitate discussion and presentation, high- and low-chlorophyll stations, and warm- and cool-temperature stations are grouped together for the S9602 and the J9701 cruises, respectively.

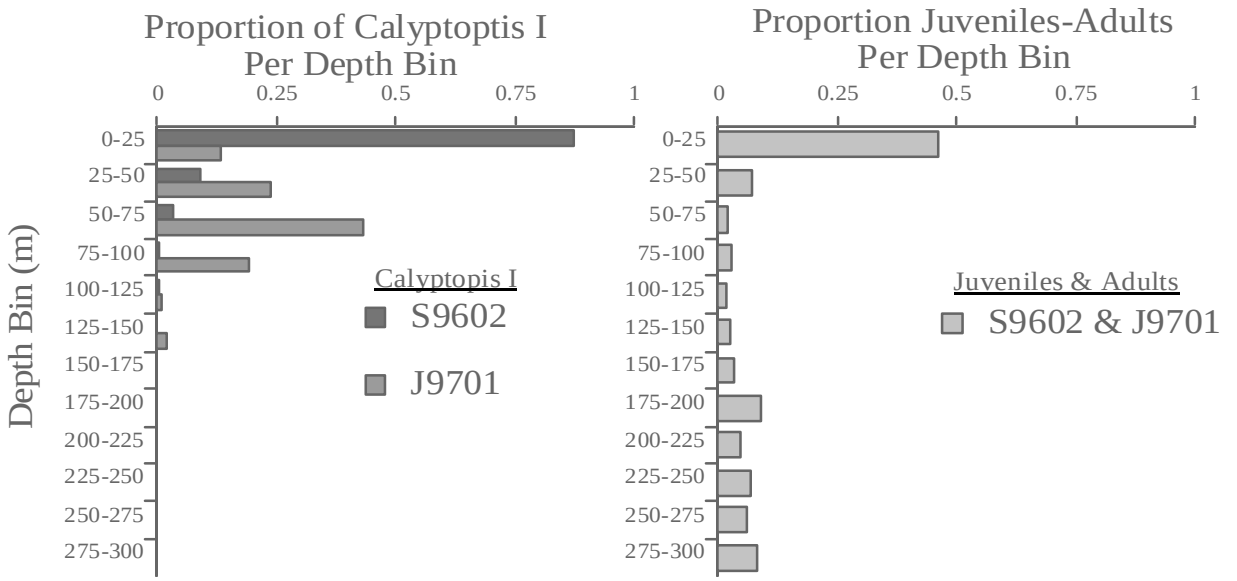

Fig. 3 Inferred depth range of egg release for *Euphausia pacifica* females from the depth distribution of calyptopis I stage larvae. The proportion of calyptopis I stage larvae sampled per 25 m depth bin is presented.

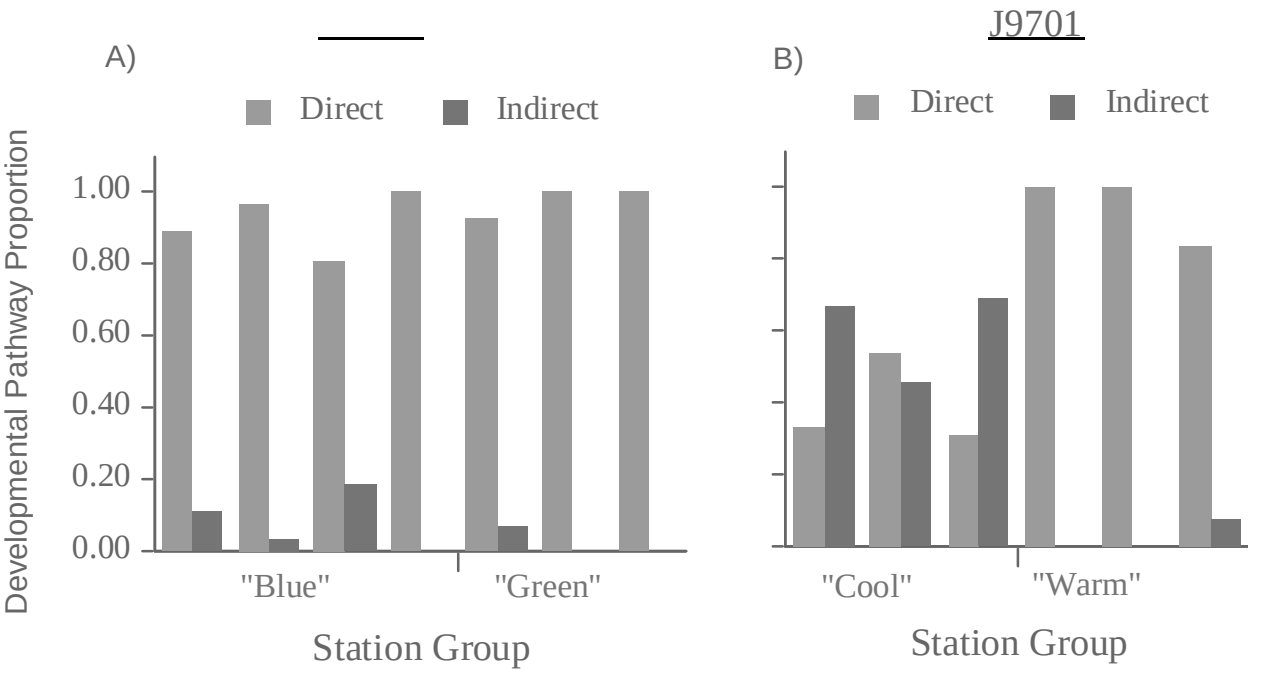

Fig. 4 The proportion of direct vs. indirect developmental pathways, of furcilia I-II stage *Euphausia pacifica* larvae. Data are presented for stations grouped according to chlorophyll regime for cruise S9602 (A), and temperature regime for cruise J9701 (B). ** ($p < 0.001$); * ($p < 0.025$); ns (not significant).

Inverse modelling of developmental parameters in Euphausia pacifica: The relative importance of spawning history and environmental forcing to larval stage-frequency distributions

Scott M. Rumsey
US Geological Survey, Forest and Rangeland Ecosystem Science Center, 3200 SW Jefferson Way, Corvallis, OR 97331. U.S.A. E-mail: Scott_Rumsey@usgs.gov

Factors potentially influencing zooplankton larval population dynamics and recruitment include advection, larval processes, biotic interactions (predation, competition, etc.), and spatial-temporal variability in the magnitude of egg release (Fig. 1). Research has shown that oceanographic conditions can impact larval developmental pathways and demography in *Euphausia pacifica*, thus contributing to variability in recruitment (Brinton, 1976; Knight, 1984). The focus of this paper is to evaluate variability in *E. pacifica* larval stage-frequency distributions observed during two cruises in the Southern California Bight. Relative comparisons of back-calculated (inverse modelled) stage-specific vital parameters (stage duration and specific mortality) and histories of egg input were conducted. The results of the model, in the context of the sampled oceanographic environment and observed larval developmental pathways, were evaluated to determine the relative importance of variability in developmental and specific mortality rates vs. egg-input variability at different scales (within cruises and between cruises).

Within-Cruise Comparisons

Within-year, among-station, differences in stage-frequency structure are more likely associated with developmental loss (variability in stage duration or specific mortality) than with variability in egg input. Although the larval demography for cruise S9602 generally reflects sampling during the crescendo of a spawning pulse, and that for J9701 suggests sampling toward the end of a pulse (Fig. 2A and 3A, respectively), it is unlikely that differences among stations were forced by *spatial* variability in spawning histories. Back-calculated solutions of S9602 relative egg-input indicate that if station differences in larval stage-frequencies was driven by egg-input alone, as much as a 2000% fluctuation in egg-input among stations is required (Fig. 2B). Variability to such an extent exceeds that observed by Brinton (1976) even between peak-spawning and background-spawning winter months (approximately $<$500%). The differences in relative egg input calculated for J9701 (Fig. 3B) is considerably less than the S9602 solutions, but egg inputs for the "warm" stations would have to have been more than twice those of the cool stations for stages CI-FII (a period representing about a month and approximately 50% of the total larval developmental time at ambient temperatures; Ross, 1981). Such extreme differences in the magnitude of egg release during a spawning peak, persisting over 1 km spatial scales (station spacing for S9602) and month time scales, is unlikely.

Due to the exponential nature of larval mortality in the model, the difference in stage duration or specific mortality necessary to explain observed station larval demographics is considerably less than that for egg inputs. The back-calculated solutions of relative developmental loss (stage duration and specific mortality) for the "blue" S9602 stations were more positive than those for the higher chlorophyll "green" stations (Fig. 2C).

The necessary differences in back-calculated stage duration or specific mortality necessary to explain among-station differences in larval stage-frequencies was considerably less than the egg input solutions for the J9701 station groups as well (Fig. 3C). The back-calculated developmental parameters for the "cool" J9701

stations were more positive than the "warm" station solutions for stages CI-FII. The elevated mortality (approximately 10-50%) for these stages at the cool stations is consistent with prolonged developmental times associated with the 1-3°C cooler temperatures.

Between-Cruise Comparisons

A peak in winter spawning activity in the Southern California Bight typically occurs during the months of January-February (Brinton, 1976), however, between-cruise comparison of back-calculated egg inputs (Fig. 4B) suggests that the cruise stage-frequencies (Fig. 4A) reflect sampling at different times during a spawning pulse. Cruise S9602 appears to have sampled toward the peak of a "normal" January-February spawning pulse, while J9701 indicates sampling when the magnitude of spawning activity had diminished. Alternatively, the predominance of younger larvae in the stage-structures of the S9602 stage-frequencies could be the result of elevated mortality in the later larval stages relative to J9701 (Fig. 4C). Such an increase in mortality might be attributable to increased stage durations or specific mortalities, however, an elevated developmental loss during S9602 contradicts observed temperature-chlorophyll conditions and larval developmental pathways. It is more likely that between-cruise differences in larval age-structure were driven by different histories of egg input than by differences in developmental parameters.

Application of a simple inverse model, and some significant assumptions, has allowed me to evaluate the impact of variability in developmental and specific mortality rates in relation to variability in spawning histories in forcing observed differences in larval stage-frequency distributions. A more rigorous comparison of these factors would require an abundance of shiptime and ancillary larval rearing data at prohibitive cost and effort. Ideally one would obtain a time series of egg release prior to the Lagrangian sampling of the larval population, requiring approximately 145 days of ship time (i.e. twice the duration of larval development). Additionally, shipboard observations of stage durations and specific-mortalities at ambient temperature/food conditions, in concert with a time series of stage-frequency curves, would afford the application of more quantitative techniques of estimating stage-specific mortality rates. The inverse method used, the set of assumptions applied, and the relative comparisons of parameters conducted has afforded the opportunity to address hypotheses that otherwise could only be considered by a large-scale research program.

References

Brinton, E., 1976. Population biology of *Euphausia pacifica* off Southern California. Fishery Bulletin U.S., 74(4): 733-762.

Knight, M. D., 1984. Variation in larval morphogenesis within the southern California Bight population of *Euphausia pacifica* from winter through summer, 1977-1978. CalCOFI Rep. 25: 87-99.

Ross, R. M., 1981. Laboratory culture and development of *Euphausia pacifica*. Limnology and Oceanography 26(2): 235-246.

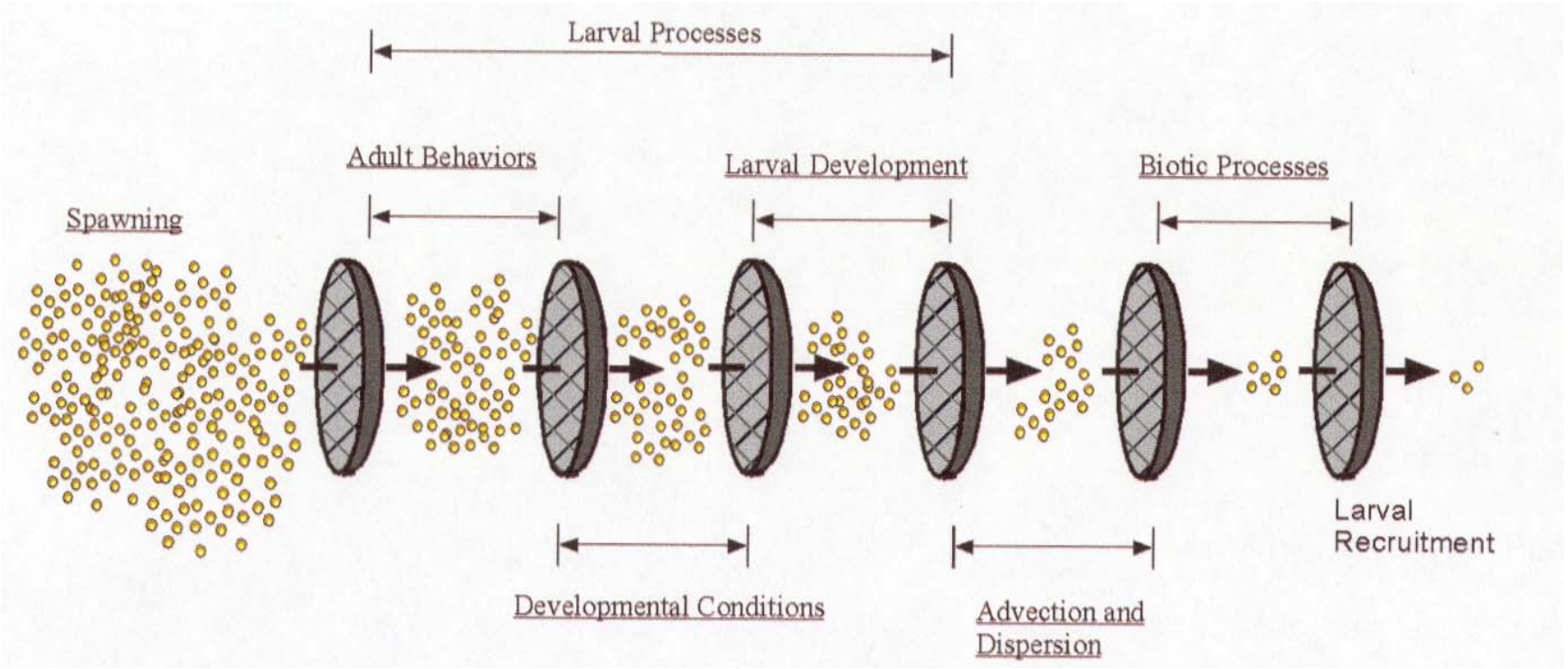

Fig. 1 Schematic representation of processes and behaviours which affect zooplankton recruitment dynamics in general, and *Euphausia pacifica* in particular. The focus of this dissertation includes items grouped under "larval processes".

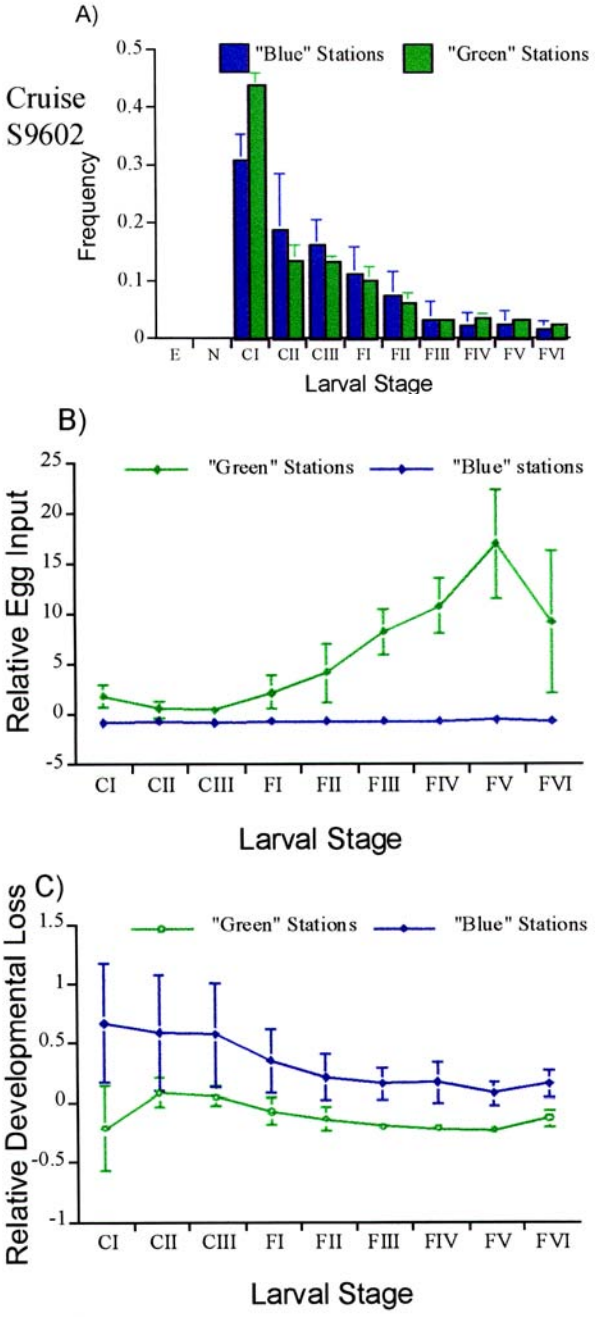

Fig. 2 A) Larval *Euphausia pacifica* stage-frequency distributions for high-and low-chlorphyll station groups during the February 1996 cruise. B) Back-calculated values of relative egg input. C) Back-calculated values of relative developmental loss.

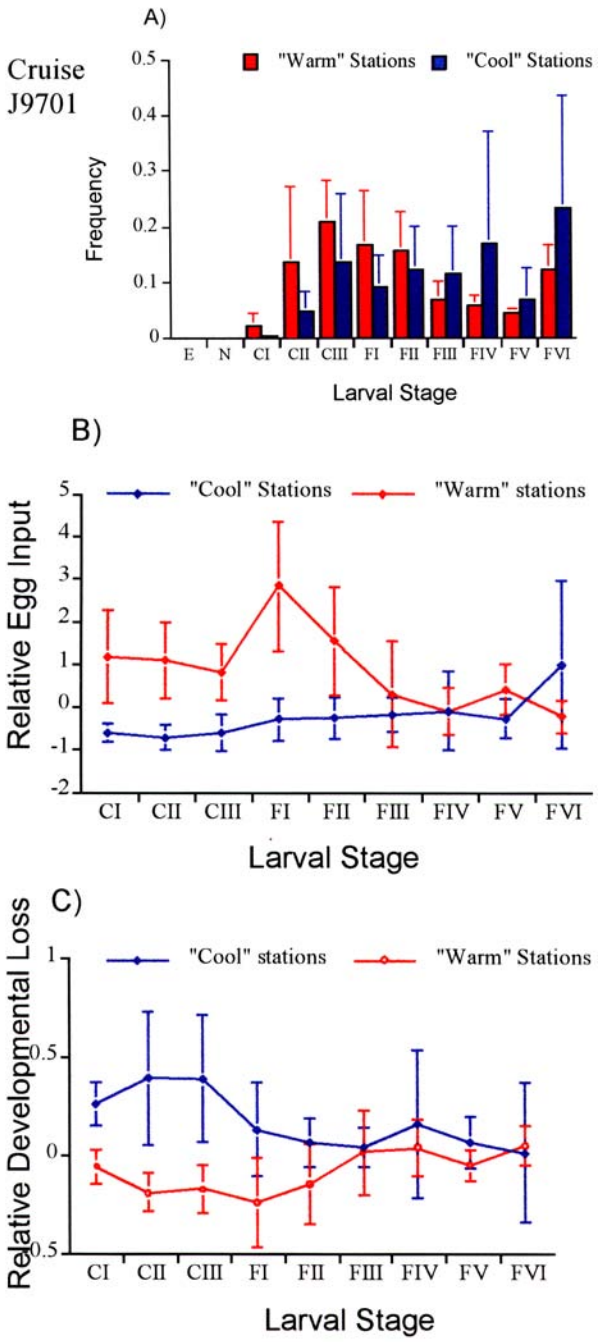

Fig. 3 A) Larval *Euphausia pacifica* stage-frequency distributions for warm- and cool-temperature station groups during the January 1997 cruise. B) Back-calculated values of relative egg input. C) Back-calculated values of relative developmental loss.

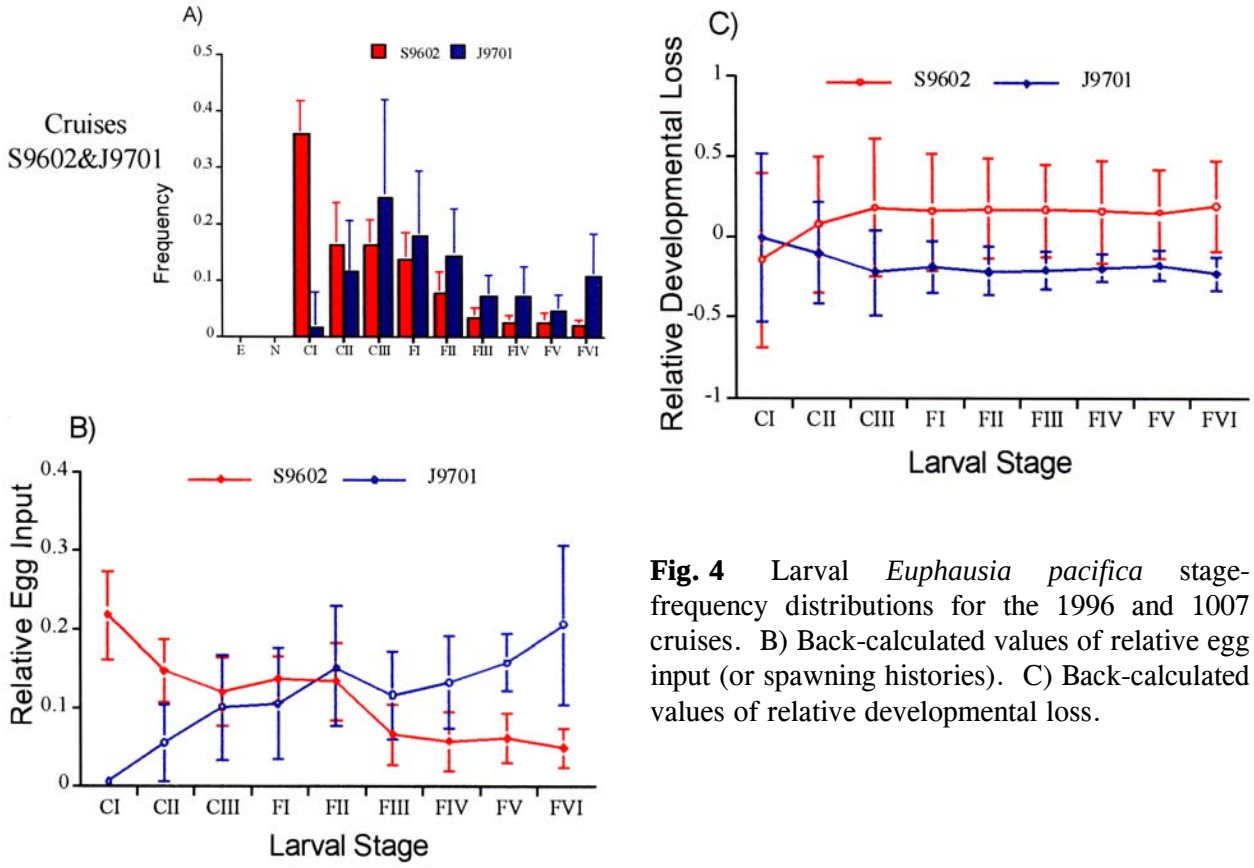

Fig. 4 Larval *Euphausia pacifica* stage-frequency distributions for the 1996 and 1007 cruises. B) Back-calculated values of relative egg input (or spawning histories). C) Back-calculated values of relative developmental loss.

An ecosystem model with zooplankton vertical migration focused on Oyashio region

Michio J. Kishi, Hitoshi Motono & Kohji Asahi
Hokkaido University. E-mail: kishi@salmon.fish.hokudai.ac.jp

An ecosystem model with eight compartments (Fig. 1) was developed in order to describe a Northern Pacific primary and secondary production. This model was made by the request of PICES GLOBEC CCCC Program. Model equations describe the interactions of nitrate, ammonium, two phytoplankton size fractions (tentatively, these are diatom and dinoflagellate), two zooplankton size fractions (tentatively, copepod and microzooplankton), PON, and DON. Formulations for the biological processes are based primarily upon KKYS(Kawamiya et al., 1996, 1997). One dimensional physical-biological coupled model including mixed layer closure model is used to simulate time dependent features of ecosystem off Sanriku district(Fig. 2). Time series of nutrient and plankton distributions obtained from Hokkaido National Institute of Fisheries provide verification of model results. The simulated results were well reproduced the seasonal and interannual change of ecosystems there. Model simulations indicate that vertical migration of copepod is a potentially important factor in determining the trophic structure in the change of phytoplankton species during spring bloom.

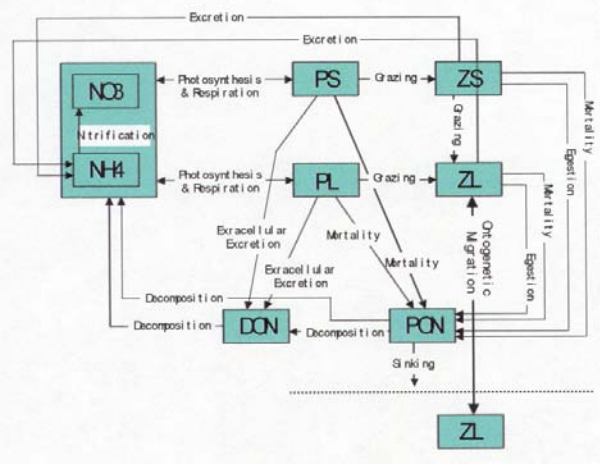

Fig. 1 Six compartment model with vertical migration of large zooplankton (ZL).

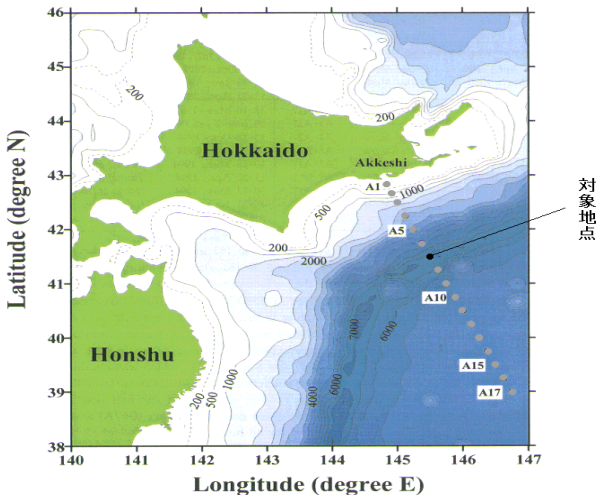

Fig. 2 Applied point of the model (One-D model).

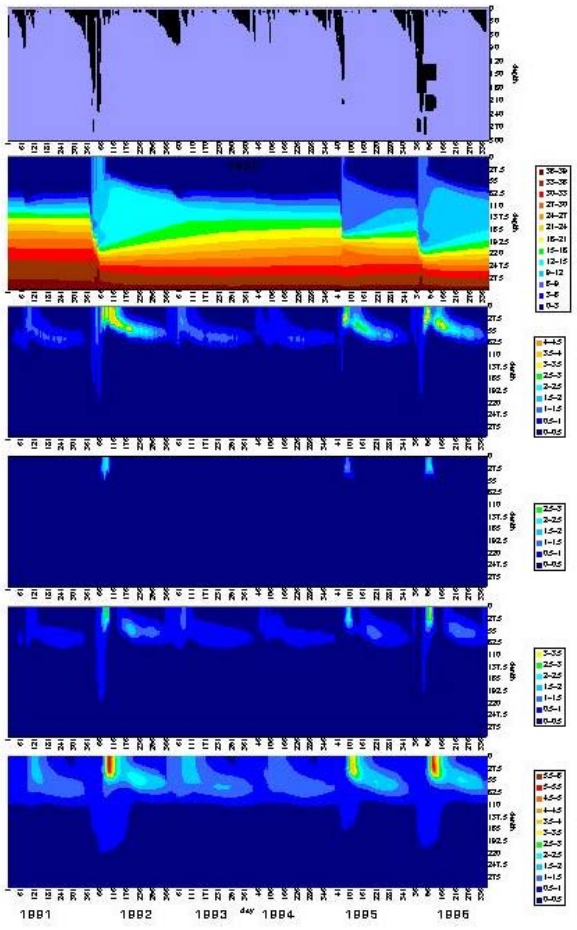

Fig. 3 Calculated results without vertical migration of ZL.

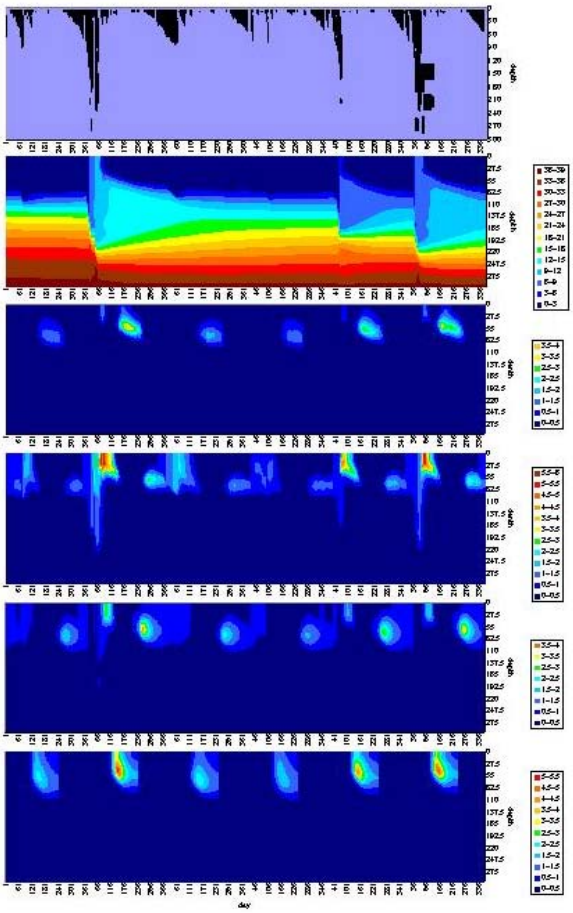

Fig. 4 Calculated results with vertical migration of ZL.

Figure 3 shows in case without vertical migration of copepod. This only shows the spring bloom of small zooplankton (ZS) which causes consequent large zooplankton increase. However as shown in Figure 4, in case with vertical migration of copepods (ZL), in spring large phytoplankton (PL) makes first bloom because small phytoplankton (PS) cannot increase by grazing pressure of small zooplankton and after large zooplankton (ZL) migrate to shallower region small zooplankton decrease by grazing of large one which causes increase of small phytoplankton bloom following large one.

References:

Kawamiya, M., M. J. Kishi, M. D. K. Ahmed and T. Sugimoto, 1996. Causes and consequences of Spring phytoplankton blooms in Otsuchi Bay, Japan. Continental Shelf Res., 16: 1688-1695.

Kawamiya, M., J. J. Kishi, Y. Yamanaka and N. Suginohara, 1997. Obtaining reasonable results in different oceanic regimes with the same ecological physical coupled model. J. Oceanogr., 53: 397-42.

PICES-GLOBEC Implementation Panel on Climate Change and Carrying Capacity Program Executive Committee and Task Team List

Executive Committee:

Dr. Suam Kim (IP Co-chairman) *e-mail: suamkim@pknu.ac.kr*
Dr. David W. Welch (IP Co-chairman) *e-mail: welchd@pac.dfo-mpo.gc.ca*
Dr. Andrei S. Krovnin (BASS Task Team Co-chairman) *e-mail: akrovnin@mx.iki.rssi.ru*
Dr. Gordon A. McFarlane (BASS Task Team Co-chairman) *e-mail: mcfarlanes@pac.dfo-mpo.gc.ca*
Dr. Michio J. Kishi (MODEL Task Team Co-chairman) *e-mail: kishi@salmon.fish.hokudai.ac.jp*
Dr. Bernard A. Megrey (MODEL Task Team Co-chairman) *e-mail: Bern.Megrey@noaa.gov*
Dr. Bruce A. Taft (MONITOR Task Team Co-chairman) *e-mail: bat65@aol.com*
Dr. Yasunori Sakurai (MONITOR Task Team Co-chairman) *e-mail: sakurai@pop.fish.hokudai.ac.jp*
Dr. William T. Peterson (REX Task Team Co-chairman, U.S.A. GLOBEC) *e-mail: Bill.peterson@noaa.gov*
Dr. Vladimir I. Radchenko (REX Task Team Co-chairman) *e-mail: root@tinro.marine.su*
Dr. Tokimasa Kobayashi (REX Task Team Co-chairman) *e-mail: tokikoba@hnf.affrc.go.jp*
Dr. R. Ian Perry (Canada GLOBEC) *e-mail: perryi@pac.dfo-mpo.gc.ca*
Prof. Qi-Sheng Tang (China GLOBEC) *e-mail: ysfri@public.qd.sd.cn*
Dr. Vladimir Karpenko (NPAFC representative) *e-mail: mail@kamniro.kamchatku.su*

**** Task Team Co-chairmen in bold print.***

BASS Task Team:

Canada	Dr. David L. Mackas *mackasd@pac.dfo-mpo.gc.ca* **Dr. Gordon A. McFarlane** *mcfarlanes@pac.dfo-mpo.gc.ca*	China	
Japan	Dr. Makoto Kashiwai *kashiwai@ss.hnf.affrc.go.jp* Prof. Makoto Terazaki *terazaki@ori.u-tokyo.ac.jp* Dr. Akihiko Yatsu *yatsua@ss.nrifs.affrc.go.jp*	Korea	Dr. Suam Kim *suamkim@pknu.ac.kr* Dr. Jang-Uk Lee *julee@haema.nfrda.re.kr*
Russia	Dr. Alexander I. Boltnev *mail@kamniro.kamchatka.su* **Dr. Andrei S. Krovnin** *akrovnin@mx.iki.rssi.ru*	U.S.A.	Dr. Michael L. Dahlberg *Mike.Dahlberg@noaa.gov* Dr. Bruce W. Frost *frost@ocean.washington.edu* Dr. Bruce A. Taft *bat65@aol.com* Prof. Patricia A. Wheeler *pwheeler@oce.orst.edu*

MODEL Task Team:

Canada	Dr. R. Ian Perry *perryi@pac.dfo-mpo.gc.ca* Dr. Daniel M. Ware *ware_mrc@island.net*	China	Dr. Da-Ji Huang *wyxu@ns2.zgb.com.cn*
Japan	Dr. Masahiro Endoh *Endoh@mri-jma.go.jp* **Dr. Michio J. Kishi** *kishi@salmon.fish.hokudai.ac.jp*	Korea	Dr. Jae-Hak Lee *jhlee@sari.kordi.re.kr* Dr. Sinjae Yoo *sjyoo@sari.kordi.re.kr*
Russia	Dr. Vadim V. Navrotsky *navr@online.vladivostok.ru* Dr. Yury Zuenko *root@tinro.marine.su*	U.S.A.	Dr. Linda Jones *Linda.Jones@noaa.gov* Ms. Patricia Livingston *Pat.Livingston@noaa.gov* **Dr. Bernard A. Megrey** *Bern.Megrey@noaa.gov*

MONITOR Task Team:

Canada	Dr. David W. Welch *welchd@pac.dfo-mpo.gc.ca*	China	Dr. Xian-Yong Zhao
Japan	Dr. Kaoru Nakata *may31@nrifs.affrc.go.jp* **Dr. Yasunori Sakurai** *sakurai@pop.fish.hokudai.ac.jp*	Korea	Ms. Young-Jean Choi *yjchoi@iris.metri.re.kr* Prof. Chul Park *chulpark@hanbat.chungnam.ac.kr*
Russia	Dr. Vyacheslav B. Lobanov *pacific@online.marine.su* Dr. Nikolay A. Rykov *hydromet@online.ru* Dr. Mikhail A. Stepanenko *root@tinro.marine.su*	U.S.A.	Dr. Jeffrey M. Napp *Jeff.Napp@noaa.gov* Dr. Thomas C. Royer *royer@ccpo.odu.edu* **Dr. Bruce A. Taft** *bat65@aol.com* Dr. Warren S. Wooster *wooster@u.washington.edu*

REX Task Team:

Canada	Dr. Richard F. Addison *addisonr@pac.dfo-mpo.gc.ca* Dr. N. Brent Hargreaves *hargreavesb@pac.dfo-mpo.gc.ca*	China	Prof. Qi-Sheng Tang *ysfri@public.qd.sd.cn* Prof. Rong Wang *wangrong@ms.qdio.ac.cn*
Japan	Dr. Yasunori Sakurai *sakurai@pop.fish.hokudai.ac.jp* Dr. Yutaka Nagata *nagata@mirc.jha.or.jp* **Dr. Tokimasa Kobayashi** *wadat@s.affrc.go.jp*	Korea	Dr. Jin-Yeong Kim *jiykim@haema.nfrda.re.kr* Dr. Chang-Ik Zhang *cizhang@dolphin.pknu.ac.kr*
Russia	**Dr. Vladimir I. Radchenko** *root@tinro.marine.su*	U.S.A.	Dr. George L. Hunt, Jr. *glhunt@uci.edu* Prof. Brenda L. Norcross *norcross@ims.alaska.edu* **Dr. William T. Peterson** *Bill.peterson@noaa.gov*